Dissertation

Submitted to the
Combined Faculty of Natural Sciences and Mathematics
Heidelberg University, Germany
For the degree of
Doctor of Natural Sciences (Dr. rer. nat.)

Presented by
Girish Karadka Shankara
(M.Sc., M.tech. Chemistry, Polymer Technology)
Born in Koothattukulam, Kerala, India.
Supervisor: Prof. Dr. Michael Grunze and Dr. Pavel A. Levkin
Oral examination: 30th, October 2015

Sulfur containing biologically responsive polymers synthesized via thiol-yne/ene and thiol-epoxide ring opening polymerization

This dissertation was carried out at the
Department of Applied Physical Chemistry
Heidelberg University

Referees:
Prof. Dr. Michael Grunze / Prof. Dr. Michael Zharnikov
Prof. Dr. Hans-Robert Volpp

Acknowledgement

I would like to thank Prof. Dr. Michael Grunze for supervising and reviewing my Ph.D.work. His insightful advices on my thesis and continuous support during my Ph.D. period helped me a lot in performing the Ph.D. thesis. I would like to give my special thanks to Dr. Pavel A Levkin who offered me the opportunity to perform the Ph.D. thesis in his research group. Without his supervision and kind help this thesis would not have been possible. His guidance always helped me to solve the problems I encountered and his great enthusiasm for the research work motivates me to continue and finish my Ph.D. thesis all the time. Many thanks to Prof . Dr. Michael Zharnikov and Prof. (apl.) Dr. Hans-Robert Volpp, for kindly agreeing to be the first and second referee of this work.

I would like to thank all my colleagues: Linxian Li, Shubhangi Kakkar, Yihang Wu, Alexander Efremov, Victoria Nedashkivska, Danuta Kuzmicz, Anna Popova, Junsheng Li, Xin Du, Wenqian Feng, Erica Boles, Florian Geyer, Zewei Bai, Sahil Chabra, Andreas Gast, Isabel Netto, Tina Curz, Konstantin Demir and all other colleagues at APC. It was great to work with these young and brilliant people.

My heartfelt thanks to colleagues from other groups and institutes. Elise Lejeune, Marcel Langer, Silvia Andraschko, Darja Ivannikov, and Geethu Balachandran.

I would also like to thank Dr.Ute Scheppers and Dr. Tim Scharnweber for their valuble suggestions and translation of the abstract.

This work was performed in the group of Dr. Pavel A. Levkin (Group of Chemical Engineering of Biofunctional Materials, Institute of Toxicology and Genetics, Karlsruhe Institute of Technology) and at the department of Applied Physical Chemistry (APC) at the University of Heidelberg. It was funded by the Helmholtz Association's Initiative and Networking Fund (Grant VH-NG-621) and DAAD scholarship.

I sincerely thank my mentors, Dr. T.P Mohandas, Dr. Suresh Bhat, Prof. Sabu Thomas, Prof. K. E. George, Prof. Sunil Narayanankutty and Prof. Rani Thomas.

Many thanks to my friends here and back home who supported throughout the good and bad times. Special mention to Subin Damodaran, Asha Krishnan, Radhika Raveendran, Preetha, Sajna Simon, Sadiq Ali, Hareesh, Vishal, Sammrudhi Kamble, Tina George, Priya Mary, Vimaly, Ditty Dixon, Aishwarya, Sachin Singh, Shyjumon, Monica, Vishnuvardhan, Sunil, Ramu Pradip, Ganesh, Levin and Anek.

I would like to express my sincere gratitude to my family members who have been supporting me all the time. For most I thank my parents, and brother who did their best to help me with everything.

Abbreviations

µM	Micromolar
^{1}HNMR	Proton Nuclear nuclear magnetic resonance
AIBN	2,2-azobis (2-methylpropionitrile)
$CDCl_3$	Deuterated chloroform
CLSM	Confocal laser scanning microscopy
DCM	Dichloromethane
DLS	Dynamic light scattering
DMEM	Dulbecco's Modified Eagle Medium
DMSO	Dimethyl sulfoxide
DMSO-D_6	Deuterated dimethyl sulfoxide-d6
FDA	Food and Drug Administration
FT	Fourier transforms
GPC	Gel permeation chromatography
H_2O_2	Hydrogen peroxide
HUVEC	Human Umbilical Vein Endothelial Cells
mM	Millimolar
MTT	3-(4,5,5-dimethylthiazol-2-yl)-2,5,5-diphenyltetrazolium bromide
PBS	Phosphate buffer solution
PCL	Polycaprolactone
PEG	Polyethylene glycol
PLA	Poly (lactic acid)
PLGA	Poly (lactic-co-glycolic acid)
PPS	Polyphenylne sulfide
PVA	Polyvinyl alcohol
ROS	Reactive oxygen species
SEM	Scanning electron microscopy
TEM	Transmission electron microscopy
THF	Tetrahydrofuran
UV-Vis	Ultraviolet-visible

Abstract

The research work presented in this thesis focuses on the synthesis, characterization and preparation of biologically responsive polymers and their nanoparticles containing sulfur in the main chain. Polymerization using click chemistry is relatively new, simple and easy way for the synthesis of linear polymers. Since the discovery of click reactions a decade ago, researchers were much interested in coupling small molecules but eventually more reports have been published in the recent past were polymers and hyper branched structures were prepared by clicking multifunctional groups. Stimuli responsive linear polymers synthesized by click chemistry is one of the less discussed and interesting fields for polymer chemists due its feasibility and unseen potentials. Three different libraries of polymers, polysulfides, poly (β-hydroxy thioethers) and poly(β-thioesters), were synthesized by thiol-yne reactions, thiol-epoxide ring opening polymerization and thiol-ene reactions.

Intensive research is carried out in the area of biologically responsive nanocarries. Many different approaches and methodologies were adapted in the past years for the development of polymer based drug delivery systems. Stimuli based on enzyme response, chemical, pH or temperature changes are already been thoroughly exploited. Response to oxidation is much less investigated, even though there are few literatures based on oxidation sensitive materials there is still a wide area to be explored and understood. Hydrophobic polymer chains of some of the synthesized polysulfides and poly(β-hydroxy thioethers) can be transformed into more hydrophilic ones by oxidation of sulfur to sulfoxides or sulfones using mild oxidizing agents like hydrogen peroxide. A hydrophobic drug/dye encapsulated in the polymer can be thereby released upon an oxidative trigger. Herein polysulfides and poly(β-hydroxy thioethers) polymers were used to prepare nanoparticles by nanoprecipitation, single emulsion and double emulsion techniques. The nanoparticle morphology, size, zeta potential and stability depend on the method of particle preparation which was optimized to meet the final applications. Oxidation responsive drug/dye release was studied under pathological and physiological concentration of hydrogen peroxide. Cellular uptake and cell viability was studied using Hela cells and HUVEC.

Biodegradable polymers are always a good choice for medical applications. In another approach a new library of poly(β-thioesters) was synthesized via base catalyzed thiol-ene polymerization. The presences of β-thioesters bonds make these polymers liable to hydrolysis and hence biodegradable. Synthesized polymers were further used to prepare surfactant stabilized nanoparticles by nanoprecipitation. Nanoparticle size and surface charge was controlled by changing parameters like polymer and surfactant concentrations. Encapsulated

drug/dye release kinetics was then studied; an accelerated release of the payload was observed in more acidic condition and lesser in neutral pH.

In conclusion, three different libraries of linear polymers were synthesized using thiol-yne/ene and thiol-epoxide ring opening polymerization. Nanoparticles were then prepared using these polymers and oxidative and pH dependent stimuli response was studied. One of the interesting aspects of this kind of polymerization is its simplicity, mild conditions and less work out procedures. Some of these polymeric nanoparticles efficiently respond to the stimuli applied, release kinetics and nanoparticle degradation were also studied. Cellular uptake and cell viability results confirms good uptake of nanoparticles with minimal toxicity.

Zusammenfassung

Der Schwerpunkt dieser Dissertation liegt auf Synthese, Charakterisierung und Herstellung von biologisch aktiven, schwefelhaltigen Polymerketten, sowie auf aus diesen Polymeren erhaltenen Nanopartikeln. Polymerisierungsreaktionen unter Verwendung von Click-Chemie bieten eine relativ neue und einfache Möglichkeit zur Synthese linearer Polymere. Bei der Entdeckung der Click-Reaktionen vor etwa einer Dekade galt das Interesse vor allem Kupplungsreaktionen unter Beteiligung kleiner Moleküle. In jüngster Vergangenheit wurden jedoch in zunehmendem Maße Arbeiten veröffentlich, die sich mit der Herstellung von Polymeren und hyperverzweigter Strukturen durch Click-Reaktionen mit multifunktionellen Gruppen beschäftigen. Durch Click-Chemie synthetisierte stimuliresponsive, lineare Polymere ist eines der weniger diskutierten Forschungsfelder, die für Polymerforscher aufgrund ihrer generellen Darstellbarkeit und des noch nicht realisierten Potentials von Interesse sind. Drei verschiedene Polymerbibliotheken, Polysulfide, Poly(β-hydroxy thioether) und Poly(β-thioester), wurden durch Thiol-Alkin Reaktionen, Thiol-En Reaktionen und Thiol-Epoxid-Ringöffnungspolymerisationen synthetisiert.

Im Bereich biologisch aktiver Nanoträgersysteme wird aktuell intensiv geforscht. Zahlreiche unterschiedliche Herangehensweisen und Methoden wurden in den letzten Jahren für die Entwicklung polymerbasierter Drug-delivery-Systeme adaptiert. Systeme, die eine spezifische Antwort auf Enzymaktivität, chemische Reize, pH- oder Temperaturänderungen zeigen, wurden bereits vielfach beschrieben. Oxidations-sensitive Systeme dagegen wurden bislang wenig untersucht. Obwohl es in der Literatur einige Arbeiten zu oxidationsresponsiven Materialen gibt, sind große Bereiche dieses Forschungsfeld bislang unverstanden und bedürfen weiterer Untersuchungen.

Hydrophobe Polymerketten aus Polysulfiden und Poly(β-hydroxy thioestern) können durch Oxidation von Schwefelatomen zu Sulfoxiden oder Sulfonen unter Verwendung milder Oxidationsmittel wie beispielsweise Wasserstoffperoxid zu hydrophileren Polymeren umgewandelt werden. Ein hydrophober Wirkstoff/Farbstoff, der im Polymerstrang verkapselt ist, kann somit durch ein oxidatives Agens freigesetzt werden.

In dieser Arbeit wurden entsprechende Nanopartikel aus Polysulfiden und Poly (β-hydroxy thioestern) durch Nanopräzipitation bzw. durch einfache oder doppelte Emulsionverfahren hergestellt. Morphologie, Größe, Zeta-Potential und Stabilität der Nanopartikel sind von der jeweiligen Herstellungsmethode abhängig und wurden entsprechend den Anforderungen der letztendlichen Anwendungen optimiert. Experimente zur oxidationsresponsiven Freisetzung

von Wirkstoffen/Farbstoffen wurden mit pathologischen und physiologischen Konzentrationen an Wasserstoffperoxid durchgeführt. Zelluläre Aufnahme von Nanopartikeln und Zellvitalität wurde mit HeLa-Zellen und HUVEC untersucht.

Bioabbaubare Polymere sind stets eine gute Wahl im Hinblick auf medizinische Anwendungen. In einem anderen Ansatz wurde eine neue Bibliothek aus Poly β-thioestern durch basenkatalysierte Thiol-En-Polymerisation synthetisiert. Durch die β-Thioestergruppen neigen die Polymere zur Hydrolyse und sind somit bioabbaubar. Diese Polymere wurden zur Herstellung von Tensid-stabilisierten Nanopartikel mittels Nanopräzipitation eingesetzt. Größe und Oberflächenladung der Nanopartikel wurde hierbei durch Variation der eingesetzten Konzentrationen an Polymer und Tensid gesteuert. Anschließend wurden die Freisetzungskinetiken verkapselter Substanzen untersucht. Im sauren pH-Bereich wurde eine beschleunigte Freisetzung beobachtet im Vergleich zu Messungen bei neutralem pH-Wert.

Kurz lässt sich zusammenfassen: Es wurden drei verschiedene Polymerbibliotheken durch Thiol-Alkin Reaktionen, Thiol-En Reaktionen und Thiol-Epoxid-Ringöffnungspolymerisationen synthetisiert. Daraus wurden oxidations- und pH-responsive Nanopartikel hergestellt und charakterisiert. Interessante Aspekte dieser Art der Polymerisationsreaktion sind deren Einfachheit sowie die milden Reaktionsbedingungen. Einige der Polymer-Nanopartikel reagierten deutlich auf die angewendeten Stimuli. Freisetzungskinetiken und Degradationsverhalten der Nanopartikel wurden ebenfalls experimentell ermittelt. In vitro Zellversuche zeigten, dass die Nanopartikel gut von den Zellen aufgenommen wurden und dabei allenfalls minimal toxisch waren.

Table of Contents

1. Introduction

The production of reactive oxygen species (ROS) as a result of oxidative stress is an example of a response towards a particular stimulus.[1] Other example is the release of insulin to initiate glycogen formation as a result of higher glucose levels in blood.[2] Response to a stimulus is an inevitable natural process to regulate various bodily actions such as fighting of diseases.[3] These examples inspired the researchers and led to the development of "smart" polymers based on biologically active stimuli such as pH, light, temperature, oxidation etc.[4, 5] Stimuli responsive and biodegradable properties of polymers are often exploited in the area of targeted drug delivery systems due to their unique ability to either chemically or physically transform upon induced stimuli.[6, 7] Nanoparticle derived from these "smart" polymers can act as an external matrix to efficiently and site specifically delivers a cargo. Some solid tumor tissues are known to have a slightly acidic pH (~ 6.5) compared to the healthier ones pH (~ 7.4). Target specific delivery of drugs to solid tumors without affecting the healthy tissues was recently achieved using pH sensitive material with sharp physicochemical properties.[4, 8-10] In spite of the existing methodologies, the ability to specifically target therapeutics inside the cells is becoming more important and challenging due to the complexity within the cells and design therapies.[11] Interaction of nanoparticles with cells and the cellular response to physicochemical properties of prepared nanoparticles are the prime factors to optimize for efficient uptake and targeting. However, to achieve the most efficient design and materials are quite challenging because of multiple factors which affects the interaction between nanoparticles and cellular structures.

The design of new smart polymers is always interesting, the main goal of this thesis was to develop new set of polymer libraries which can be used as a matrix to encapsulate molecular cargos and can release site specifically. Stimuli responsive polymers based on pH and temperature have already been thoroughly exploited.[12, 13] Oxidation responsive materials are relatively new area of research, so herein the main focus was in developing new oxidation responsive polymeric systems. To accomplish this, polymer containing molecules which are capable of oxidizing in the presence of mild oxidizing agents such as hydrogen peroxide (H_2O_2) were preferred. Sulfur, like oxygen, is an essential element for life; it displays oxidation states ranging from -2 to +6. The nonmetallic nature and lesser toxicity compared to other chalcogens make them an interesting candidate for designing oxidation sensitive materials.[14] Polymers comprising sulfur are known for their immense and versatile

application for commercial purposes including materials ranging from high end thermoplastics to low oligomers used in lubricants.[15, 16] Sulfur containing polymers are less explored for biomedical applications including target specific drug delivery systems.

The first example on oxidation responsive polymeric vesicles was reported by Tirelli, Hubbell and coworkers in 2004.[17] Polymersome derived from block polymer of PEG-PPS-PEG (poly(ethylene glycol)-poly(propylene sulphide)-poly(ethylene glycol)) was degraded in the presence of 10 % H_2O_2. This led to quest for new polymeric systems with enhanced sensitivity. PPS based polymers and its nanoparticles were further systematically analyzed and optimized by the same authors. This also includes its synthesis, characterization, oxidation response and interaction with cells. Synthesis of poly(alkylene sulfide)s and relevant nanoparticles were mainly achieved via three different strategies, step-growth polymerization, anionic ring-opening polymerization (ROP), and emulsion anionic ROP combined with subsequent crosslinking or functionalization. Drawbacks such as the complexity to perform the polymerization, uncontrollable molecular weight and PDI still prevailed. Interestingly recent findings such as selenium-based responsive polymers and supramolecules, aryl oxalate-containing polymers and phenylboronic ester-containing polymers have improved the efficiency and sensitivity by the order of few millimolar concentrations of H_2O_2. However pathological and physiological concentration of H_2O_2 is much lower.

To overcome the current situation and to address the problems involved in the synthesis such as complexity, the work presented in this thesis also emphasize a simple, easy and efficient click polymerization using thiol-yne/ene and thiol-epoxide reactions. Libraries of linear polymers containing sulfur were prepared using the above mentioned synthetic routes. Three different sets of polymers were produced; polysulfides, poly(β-hydroxy thioethers) and poly(β-thioesters). Further nanoparticles were prepared using these polymers. Even though there exists few reports on oxidation responsive polymeric systems, one of the main concerns and challenge was to design nanoparticles with superior properties and enhanced sensitivity. Herein, libraries of linear polysulfides and poly(β-hydroxy thioethers) were successfully synthesized using thiol-yne and thiol-epoxide reactions.[18] One of the advantages of this click reaction was its feasibility to perform even under ambient conditions. Some of the nanoparticles prepared from these polymers were even sensitive to micromolar concentrations of H_2O_2.

The need for new materials for biomedical applications is widely increasing. Biodegradable and biocompatible materials are interesting choice because of its low side effects on tissues and cells.[19, 20]

Poly(β-thioesters) polymers synthesized using thiol-ene neucleiophilic addition using amine catalysts was reported by Vandenbergh et al.[21] However biodegradability of poly(β-thioesters) nanoparticles was not discussed earlier. Herein biodegradable poly(β-thioesters) was also prepared using thiol-ene neucleiophilic addition. Nanoparticles were prepared form these polymers using surfactant stabilized nanoprecipitation method. The poly(β-thioesters) polymers are hydrolysable due to the presence of β-thioesters bonds present. The degradation and decrease in molecular weight of the poly(β-thioesters) polymers under the influence of NaOH or acetic acid was earlier reported by Vandenbergh et al.[21] This findings motivated to use poly(β-thioesters) polymeric nanoparticles as biodegradable drug delivery systems in this thesis. The study concludes that the release of Nile red dye from poly(β-thioesters) polymeric nanoparticles depends on pH and was observed to be faster under acidic condition (pH 5.01) when compared with neutral pH (pH 7.4).

A brief overview of various sulfur containing molecules, polymers and stimuli responsive polymers are discussed in the following section.

1.1. Sulfur containing organic compounds

Organosulfur compounds play a vital role in many biological functions and hence sulfur is an essential and irreplaceable element for life.[22, 23] Sulfur exists in different forms in many of the naturally occurring compounds such as coal, petroleum and natural gas. Methionine, cysteine, homocysteine, and taurine are the four common amino acids containing sulfur.[24] Important antibiotics derived from fungi, such as penicillin and cephalosporin also contain sulfur.[25] Diallyl disulfide and diallyl sulphide are the major constituents of garlic oil and are responsible for the flavour and fragrance of garlic.[26] Organosulfur compounds are commonly used to prepare artificial food flavoring agents. Food and beverages used in daily life for example: cheese, wine, chocolate etc. also contain organosulfur compounds which are responsible for their unique flavor and odor.[27-31]

1.1.1. Important organosulfur compounds and their application

Thiols: Thiols are compounds with a functional group R-SH (R= alkane, alkene, or other carbon-containing groups). Thiols are sulfur analogues of alcohol, where oxygen is replaced by sulfur. The (–SH) group is also referred to as sulfhydryl group. The lesser difference in

electronegetivity between the sulfur and hydrogen makes it less polar compared to alcohols. When compared with alcohol, thiols are also more acidic and can be easily oxidized. Thiols are usually characterized by strong odor, and easily detectable by human nose even at a concentration of ten parts per billion.[32]

Thiyl radicals are derived from thiols and are well known for their use in vulcanization process. Besides they are also involved in the synthesis of nucleotides.[33] Thiyl radicals are produced as intermediates during the oxidation of antioxidant glutathione.[34] Thiol groups present in the amino acid cysteine are converted to cystine unit having a disulfide bond (S-S) during protein folding.[35]

Thioethers: Functional group with a chemical structure R^1-S-R^2 is known as thioethers; in this case the oxygen atom in ether group is replaced with the sulfur atom. Similar to thiols, thioethers also have a strong or foul odor. Thioethers are less volatile and hydrophilic than the corresponding ethers. Thioethers are also important for their biological role and are found in amino acid methionine and co-factor biotin.

Dimethyl sulfide is the simplest thioether which was found in a marine algae and also the most abundant biological sulfur compound emitted to the atmosphere. Dimethyl sulfoxide (DMSO) is produced by the oxidation of dimethyl sulfide, and is commonly used in the industry as a solvent.[36]

Thioesters: The esterification of carboxylic acid and thiol gives rise to a thioester with the chemical structural formula R^1-S-CO-R^2. Thioester derivatives are well-known for biochemical reactions. Acetyl coenzyme A is an important thioester derivative formed as a result of glycolysis of carbohydrates and oxidation of fatty acids.[37] In recent years, thioester chemistry was used to develop a traceless reversible PEGylation strategy to regulate the activity of protein by Jianwei Chen et al.[38] This technique can be applied in small molecule conjugation, protein cross-linking, and protein−polymer conjugates.[39, 40]

Disulfides: Adjacently bonded sulfur atoms give rise to a disulfide bond or disulfide linkage. They can be represented by the chemical formula R^1-S-S-R^2. In biology the formation of disulfide bond is mainly due to the oxidation of thiols.[41]

Polysulfides: Polysulfides are chemical compounds containing multiple sulfur atoms in the chain and are mainly classified as anions and organic polysulfides. The general formula for the anion polysulfide can be written as S_n^{2-} and for organic ones, RS_nR, where (R = alkyl or

aryl). Organic polysulfides are usually referred to a class of polymers with alternating sulfur atoms in the chain. They can be synthesized by condensation polymerization of organic dihalides and alkali metal salts of polysulfide anions. Organic polysulfides are commercially used as sealants due to their inertness towards solvents, oils and water. The rigidity of elastomers is enhanced by vulcanisation using polysulfide crosslink.[42] The thesis refers to polymers containing multiple sulfur atoms in the chain. A brief literature overview of various polysulfide polymers, its synthesis and application is introduced.

1.1.2. Sulfur containing polymers

Sulfur containing polymers are widely used in many commercial applications due their inherent versatile nature. Depending on the oxidation state of sulfur, it may be highly reactive or an inert substance. Polymers substituted with sulfo groups find numerous applications, for example as emulsifiers, flocculants, thickeners, tanning agents. Sulfonated polymers are also used in ion-exchange membranes for electromembrane processes, such as electrodialysis, polymer electrolyte membrane electrolysis and polymer electrolyte fuel cells.[42-44]

Sulfopolymers are also used in biomedical systems. Much effort has recently been expended to improve blood-contacting biomaterials (e.g., segmented polyurethanes) and develop various polysulfates and polysulfonates as antithrombotic or antiviral agents. Polysulfates have great potential in biomedical applications (e.g., as antithrombotic agents).[45] Polysulfates together with sulfated polysaccharides show activity against a wide variety of enveloped viruses.[46, 47] Sulfated polysaccharide known as carrageenan, are used in ice creams and other food products.[48]

Commercial applications of sulfur containing thermoplastics are mainly focused in the area of polymers with high thermal stability. Poly(thioester)s, poly(thiocarbonate)s, and poly(thiouretane)s are important class of thermoplastics. Poly(thiocarbonate)s are also used as high refractive index materials for optical applications. Thermoplastic elastomers are produced from thiopolyesters and thiopolyurethanes.[49]

Functional polymers based on polysulfoxides can be used as polymeric oxidizing reagents, compatibilizers, and polymer solvents. Polysulfoxides containing chiral sulfonyl groups are used as stationary phases of chiral HPLC column or as polymeric reagents.[50]

1.1.2.1. Biological significance and application of sulfur containing polymers

Sulfur is an equally important element as carbon, nitrogen, oxygen or phosphorous and plays a significant role in many biological functions. Sulfur occurs in biomolecules, such as

proteins, vitamin, cofactors, sugars, nucleic acids, and metabolites, and is an essential component for living organisms. Many of the functional roles and biosynthetic origins of these molecules are yet to be resolved.[51]

Sulfur and oxygen being the part of the same periodic groups, share many characteristic features in their chemical reactivity. However distinct property of sulfur makes it more useful to biological systems. Thiols are more nucleophilic than the respective alcohols and hence better activating groups for thioesters biochemistry; similarly disulfides bonds are more stable than respective peroxides which make it a better choice for protein structures. The higher electronegativity and the number of oxidation states of sulfur compared to oxygen is an advantage to perform versatile functions in biological systems.[52]

1.2.Biodegradable polymeric systems

Biodegradable polymers during the degradation process are transformed into less harmful by-products. For this reason they are extensively researched in the field of drug delivery, bio-implants, tissue engineering etc.[53, 54] Poly(lactic acid) (PLA), poly(lactic-co-glycolic acid), poly(glycolic acid), polycaprolactone (PCL) and their copolymers, have been widely investigated for biomedical application because of their, biocompatibility, biodegradability, and bioresorbability.[55-57] Biodegradable polymeric nanoparticles provide controlled and sustained release propert;.[58] Properties such as low toxicity, nonthrombogenic, nonimmunogenic, noninflammatory, biodegradability make them versatile and the most preferred choice as a drug delivery matrix.[59] Some of the most commonly used synthetic biodegradable polymers are discussed in the following sections.

1.2.1. Polylactide (PLA)

Polylactic acid or polylactide (PLA) are essentially biodegradable polyesters. This type of polymer can be prepared by condensation or ring opening polymerization of biologically derived monomers like starch. The lactic acid monomer is usually obtained via microbial fermentation of agricultural resources or chemical synthesis.[60] PLA generally can exist in three stereochemical forms: poly(L-lactide) (PLLA), poly(D-lactide) (PDLA), and poly (DL-lactide) (PDLLA). Poly lactic acid (PLA) has extensive applications in biomedical fields, including suture, bone fixation material, drug delivery microsphere, and tissue engineering.[61] As a thermoplastic its used in bioplastic, useful for producing loose-fill packaging, compost bags, food packaging, and disposable tableware. The difficulties in

achieving mechanical and barrier properties comparable with conventional synthetic polymers while maintaining biodegradability is one of the major technical challenges.

1.2.2. Polyhydroxyalkanoates (PHAs)

Polyhydroxyalkanoates are prepared from renewable resources by fermentation. Different monomers, and thus (co)polymers obtained by this method depend on the carbon substrates and the metabolism of the microorganism.[62] Poly hydroxybutyrate homopolymer (PHB), is the main biopolymer of the PHA family. Different poly(hydroxybutyrate-cohydroxyalkanoates) copolyesters exist such as poly(hydroxybutyrate-co-hydroxy valerate) (PHBV), poly(hydroxybutyrate-co-hydroxyhexanoate) (PHBHx), poly(hydroxybutyrate-co-hydroxyoctanoate) (PHBO), and poly(hydroxybutyrateco-hydroxyoctadecanoate) (PHBOd). Poly(hydroxybutyrate-co-hydroxy valerate) (PHBV) is used as packing material, due to its toughness. Polyhydroxyalkanoates are used in medical application, for example in the preparation of surgical tools such as surgical mesh, bone plates, ligament and tendon grafts.[63]

1.2.3. Polycaprolactone (PCL)

Polycaprolactone (PCL) was developed by the Carothers group in the early 1930s.[64] PCL can be prepared by either ring opening polymerization of ε-caprolactone using a variety of anionic, cationic and co-ordination catalysts or via free radical ring opening polymerization of 2-methylene-1-3-dioxepane. PCL is widely used in the medical field: in wound dressing, sutures, contraceptive devices, fixation devices,[65] dentistry and tissue engineering.[66-70] PCL degrades slower than polyglycolide (PGA), poly d,l-lactide (PDLA) and its copolymers and therefore was originally used in drug-delivery devices that remain active for over 1 year and in slowly degrading suture materials (Maxon™).[57]

1.2.4. Biodegradable sulfur containing polymeric systems

1.2.4.1.Polythioesters

Synthetic polythioesters, which are analogus to polyesters, were first reported by Marvel and Kotch in 1951.[71] The synthetic approach was the reaction between dithiols and adipoyl chlorides or terephthalyl chlorides. Even though there are many different preparation methods, the application of polythioesters so far was limited due to their complex synthesis. The first biosynthesis of polythioesters were reported by Lutke-Eversloh et al. in 2001.[72]

1.3.Stimuli-responsive polymers

Stimuli responsive polymers are the class of polymers that show response to stimuli such as temperature, pH, light, oxidation-reduction, enzymes etc.[73] The most extensively studied stimuli are temperature and pH, due to their physiological significance.[19] Novel hybrid materials based on multi-responsive systems are hot topics of interest in the area of stimuli-responsive polymers. In recent studies one of the prime criteria in the designing of responsive polymeric systems was the incorporation of dynamic covalent bonds (DCB), referred also as a reversible covalent bond. These bonds are capable of formation or deformation in the presence of an external stimulus.[74] Polymeric nanostructures with inherent and induced reversible properties make them a significant candidate in the area of drug research, tissue engineering, optical systems, biosensors, coatings and textiles.[73, 75] Some of the important drug-polymer conjugates are shown in Table 1.1.[76] This thesis emphasizes on two major stimuli based on oxidation and pH.

Table 1.1 Applications of various stimuli responsive polymeric drug delivery systems.

Drug	Polymer	Application	Ref.
Fibroblast growth factor	Poly(*n*-isopropylacrylamide-*co*-propylacrylic acid-*co*-butylacrylate)	To improve angiogenesis in infracted myocardium	[77]
Ketoprofen	Poly(acrylamide)-*g*-carrageenan and sodium alginate	For colon-targeted delivery	[78]
Dexamethasone	Poly(methoxyl ethylene glycol-caprolactone-*co*-methacrylic acid-*co*-poly(ethylene glycol) methylethylenemethacrylate)	For oral drug delivery	[79]
Protein drug	Alginate and chemically modified carboxymethyl chitosan	For oral delivery	[80]
Docetaxel	Conjugated linoleic acid coupled with pluronic F-127	Peritoneal dissemination of gastric cancer	[81]
Exenatide	PLGA–PEG–PLGA	Treatment of type II diabetes	[82]
Ethosuximide	Chitosan with glycerophosphate	Injectable gels for	[83]

Drug	Polymer	Application	Ref.
	disodium salt and glycerol	depot therapy	
Human mesenchymal stem cells and desferroxamine	Chitosan-beta glycerophosphate	For the treatment of critical limbic ischaemia	[84]
Leuprolide	Polybenzofulvene	For treatment of tumours	[85]

1.3.1. Temperature

Smart materials based on thermoresponsive polymers are widely studied, since the past decade. Polymers exhibit thermoresponsive behavior as a result of their lower critical solution temperature (LCST) and upper critical solution temperature (UCST) nature. Poly(N-isopropylacrylamide) (PNIPAM), and its co-polymers are extensively exploited as a thermoresponsive polymer due to its unique property. [86-88] These materials are having high potential in emerging biomedical and materials fields because of their increased biocompatibility and tunable response. The thermal phase transition of PNIPAM was first observed by Scrapa et al. during late 1960s.[89]

1.3.2. pH

The pH responsive materials can either swell (increase the size) or collapse, depending upon the chemical properties and surrounding pH. There are mainly two types of pH responsive materials. With acidic group (-COOH, -SO_3H) and swelling behaviour in basic pH, like polyacrylic acid or with basic groups (-NH_2) and swelling behaviour in acidic pH (chitosan). These materials are mainly used in controlled drug delivery, personal and home care, industrial coatings, biological and membrane science, viscosity modifiers, colloid stabilization, and water remediation.[90-93]

1.3.3. Enzyme

Enzyme responsive materials are generally restricted to biological applications, like drug-delivery system and injectable scaffolds. Enzyme induced micro- or macroscopic changes in the physical or chemical properties of the material are also more specific in their nature, distingusing them from other stumili responsive materials.[94] In the case of polymeric hydrogels with highly crosslinked three dimensional structure, enzyme responsiveness is

introduced into the crosslinks parts. This causes the swelling or degradation of hydrogel. [95-98]

1.3.4. Redox

Redox-responsive polymeric systems have fascinated researcher due to their immense potential in biomedical applications. The stimuli based on redox is induced by the change in the redox potential in the surrounding environment.[99] Redox responsive polymers are either reduction or oxidation responsive. Polymers with disulfide and diselenide linkages are broadly applied in reduction-responsive polymeric drug delivery systems[99-101]. Besides disulfide and diselenide bonds, there are a few reduction-responsive linkers that were less explored and are based on trimethyl-locked benzoquinone (TMBQ) and 4-*N*-amino- 2,2,6,6-tetramethylpiperidin-1-oxyl-4-yl (TEMPO) compounds.[102, 103]

1.3.5. Oxidation responsive polymeric systems

Reactive oxygen species (ROS), such as superoxide anion (O_2^-), hydrogen peroxide, hydroxyl radical ($OH^{\cdot}$), hypochlorite (OCl^-) and peroxynitrite ($ONOO^-$), are often overproduced locally in diseased cells and tissues and are associated with oxidative stress.[104, 105] Moreover, oxidative stress plays an important role in the development of inflammation,[106] cancer,[107] Alzheimer disease[108, 109] and heart failure.[110, 111] Figure 1.1 shows the possible production of ROS in cells due to different physical and chemical factors.

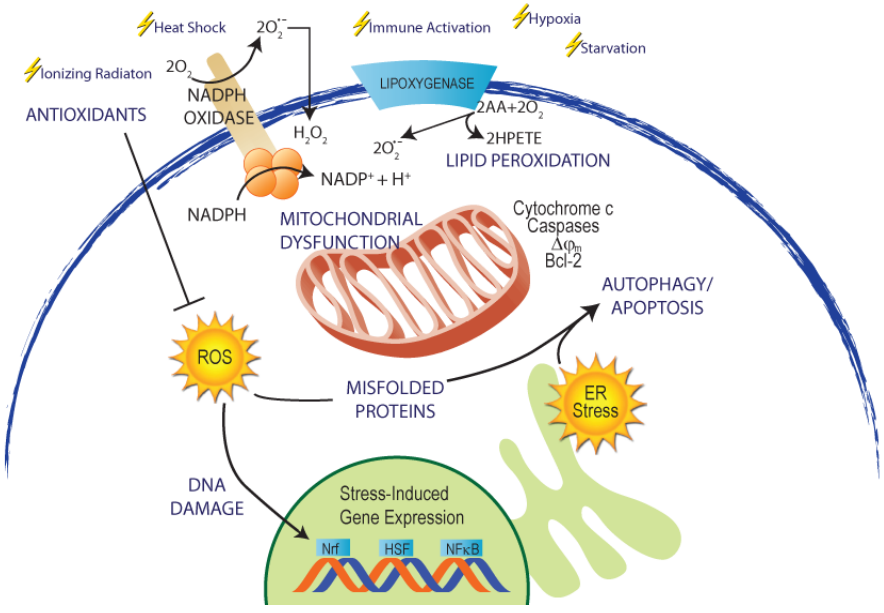

Figure 1.1 Schematic representation of production of ROS in cells.

Accordingly, oxidation-sensitive biomaterials have attracted much attention as nanocarriers of anti-inflammatory drugs, in order to achieve controlled delivery to the inflammation sites.[112] By the same manner, polysulfides,[113, 114] selenium containing polymers,[115, 116] and boronic ester protected polymers[117, 118] have been proposed for the preparation of nanoparticles with ROS-responsive properties. One of the interesting aspects of hydrophobic polysulfides is their ability to oxidise to more polar sulfoxides or sulfones in the presence of oxidizing agents. Furthermore, polysulfides can be synthesized via different polymerization reactions, like ionic ring opening polymerization, "immortal" polymerization or radical-initiated step-growth polymerization.[119-122] The hydrophilicity of the polymer is a crucial factor for achieving fast and efficient oxidation and thus, degradation of nanoparticles. The sensitivity of polysulfides can be improved by adding hydrophilic modules in the polymer backbone or side chains. The advantage of this method is a reduced ratio of sulfide in the polymer, and subsequently a smaller amount of H_2O_2 needed to oxidize the polymer. Although oxidation-sensitive polymers have been widely investigated,[113-118] there are only a few publications where these polymers have shown a response to physiological or pathological concentrations of H_2O_2.[118, 123] The best results were first achieved by Tirelli, Hubbell and co-workers, where the lowest concentration of H_2O_2 to oxidize the polysulfide was 10 vol. %. [113] They also described for the first time the nanoparticles dispersion based on oxidation-responsive polysulfides.

1.3.5.1. Oxidation responsive systems based on polysulfides

One of the first reports on oxidation responsive polymeric system based on poly(ethylene glycol)-poly(propylene sulphide)-poly(ethylene glycol) (PEG–PPS–PEG) block polymers was published in 2004. Napoli et al. described the oxidation response of the polymeric vesicles.[17] The poly(propylene sulphide) (PPS) has a low glass-transition temperature, and most importantly can be oxidized from a hydrophobic to a hydrophilic, poly(propylene sulphoxide) and ultimately poly(propylene sulphone). Oxidative conversion was first introduced to destabilize carriers. Oxidant agent, such as hydrogen peroxide (H_2O_2) was used to transform the polymersome to more hydrophilic form. This publication opened up a new approach for developing a new class of oxidation-responsive polymeric materials. For this reason polysulfide based polymers may find potential applications in the area of nanocarriers in drug delivery, biosensing and biodetection. In following reports, researches used similar mechanism based on oxidation of sulfur. Further, Hubbell et al. investigated the efficiency of polysulfides to encapsulate and release cyclosporine A as a model drug. [124] Both peroxide-

and superoxide-responsiveness of block copolymer were achieved by Hu and Tirelli who also used superoxide dismutase (SOD) in combination.[125]

Later developments included the pH-responsive poly-thioether ketal nanoparticles by Mahmoud et al.[126] Dynamic light scattering (DLS) results showed that these nanoparticles would not degrade completely unless in the buffer solution with both H_2O_2 and acid. The complete release of the cargo can only be attained by using both H_2O_2 and acid; otherwise only partial release was observed when only oxidation stress was used. The minimal toxicity of carriers confirmed their potential in clinical applications. Polysulfide containing oxidation responsive polymers have not been reported extensively. There is a widespread necessity of novel drug delivery systems for anti-inflammatory diseases, and therefore more synthetic methods are required for polymers with various architectures to function in different applications.

1.4. Synthesis of sulfur containing polymers and polysulfides

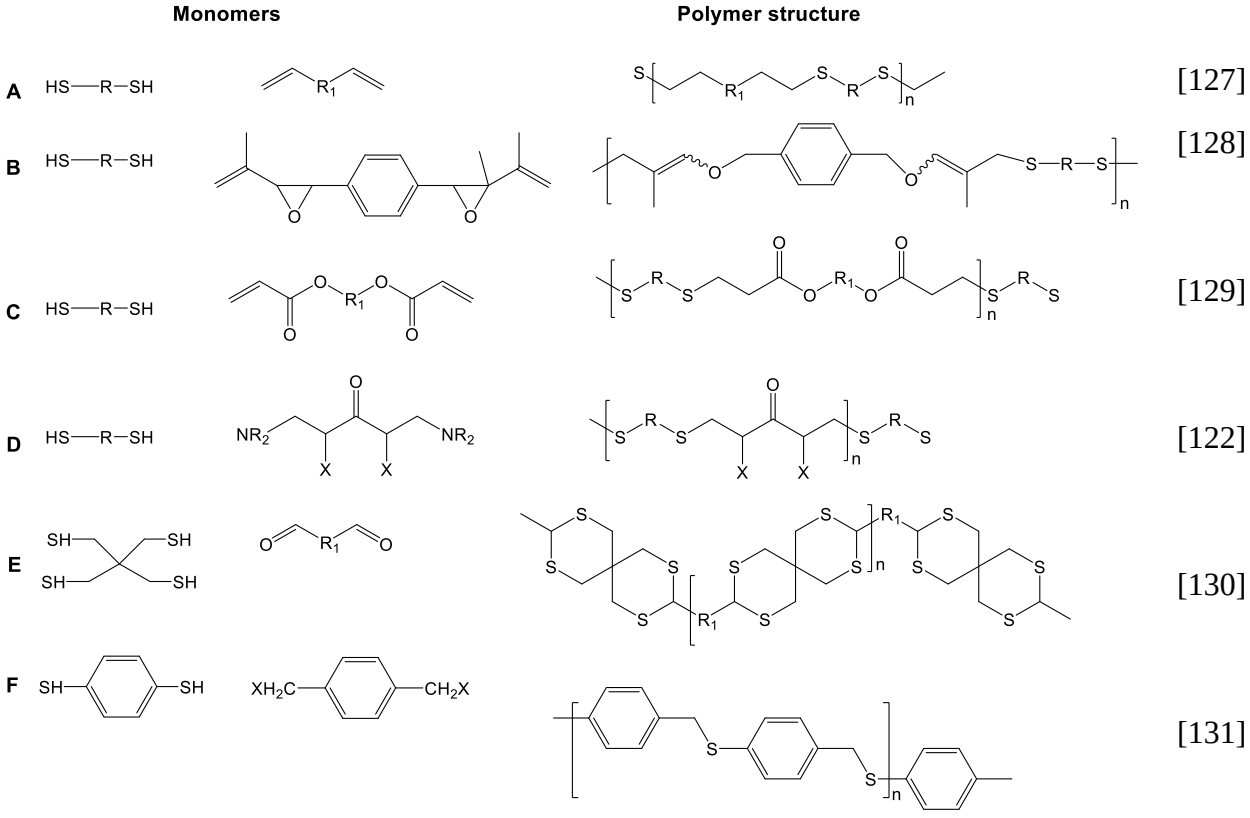

Figure 1.2 Aliphatic polysulfides synthesized by step polymerization.

Polysulfides can either be synthesised using step–growth polymerization or chain polymerization reactions. In a step –growth polymerization, mainly nucleophilic substitution or sometimes nucleophic addition of thiols or alkali metal sulfides with electrophilic halides are involved. Free radical addition of thiols and olefins are also used for the synthesis of polysulfides. Poly(alkylene sulfde) synthesized using diolefins and dimercaptans in the presence of UV light was reported by Marvel in 1948.[127] Similar polyenolthioether was prepared by free radical polyaddition of 1, 3-dimercaptobenze and 1, 5-hexadiyne.[132] Figure 1.2. shows various aliphatic polysulfide synthesized by step polymerization.

1.4.1. Thiol-yne/ene click chemistry

Thiol-yne or thiol-ene click chemistry is a kind of click reaction in which either an alkyne or an alkene reacts with a thiol functional group. Posner in 1950 first reported the addition of thiols to olefin.[133] In 1938 a free radical mechanism was proposed by Kharash et al.[134] The thiol–alkene coupling reactions, whether mediated by a radical[135] or catalyst[136, 137] follows all the necessary conditions for a click reaction, with many advantages. Since the discovery of reversible addition of thiyl radicals onto alkenes, more research work was carried out due to its easiness to perform under mild reaction conditions as well as its versatility on designing materials and even generating polymers via click chemistry approaches. Thiol-alkene addition have been reported for a wide range of alkenyl groups such as haloalkenes,[138-141] enol ethers, fluro enol ethers,[142] vinyl sulphides,[143] vinyl acetates,[144] vinyl phosphonates,[145] acrylates[144] etc.

Radical and photo-initiators including 2,2´-azobis(2-methylpropionitrile) (AIBN), cumyl hydroperoxide and oxygen are commonly used.[146] Photoredox catalysts are also reported in the literature.[147] The radical mediated thiol-ene reaction involves a chain process, Figure 1.3. Thiyl radicals are generated as a result of a photo initiation process during the irradiation of thiols. In the propagation step an intermediate carbon-centred radical is formed due to the addition of thiyl radical across C=C bond, followed by the chain transfer to a second molecule of thiol to give the thiol-ene addition product, which follows the anti-Markovnikov addition, with the generation of a new thiyl radical. Radical–radical coupling results in the termination of the reaction processes. So the radical thiol-ene photo-polymerization processes are also radical step-growth polymerizations. Depending upon the ene and thiol radical thiol-ene reaction can vary considerably.[148]

The Michael addition reaction can be performed under mild reaction conditions, with high conversions and minimal by-product formation. The thiol-ene reactions mediated by a

nucleophilic catalyst such as primary or secondary amines and certain phosphines are also known. The thiol-ene addition in the presence of a phosphine catalyst is shown in Figure 1.4.

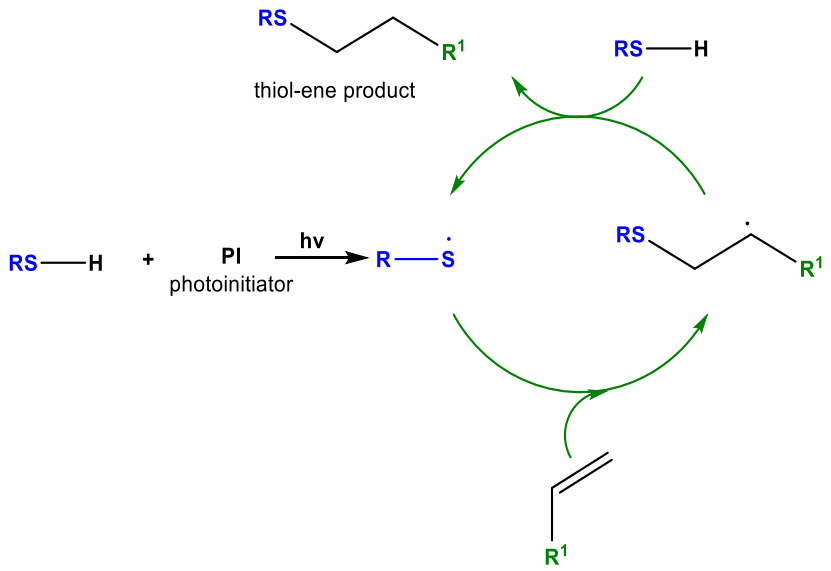

Figure 1.3 Schematic representation of thiol-ene radical click reaction mechanism.

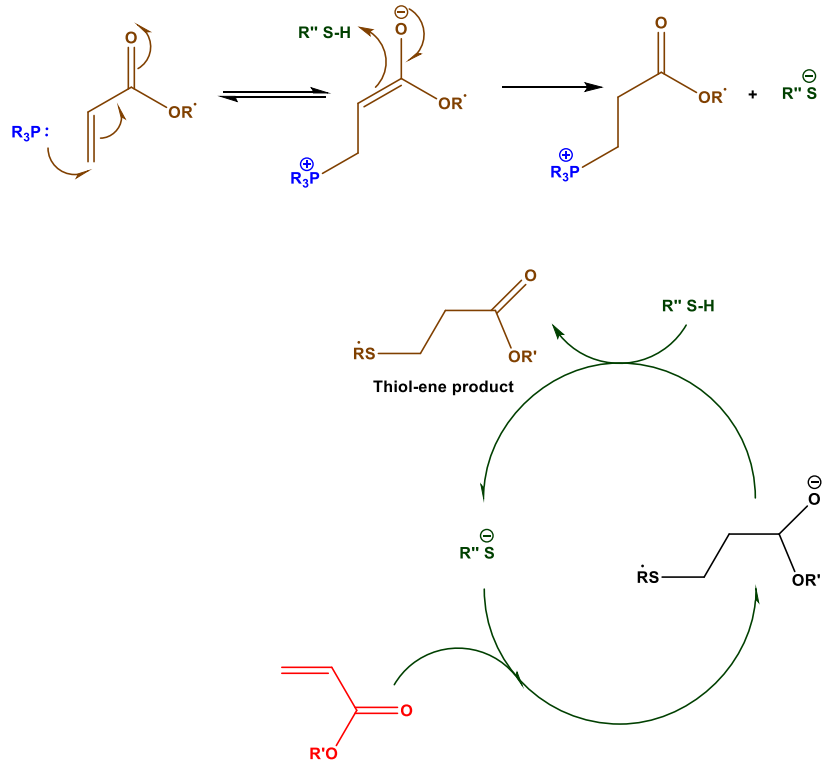

Figure 1.4 Schematic representation of reaction mechanism for nucleophile mediated hydro-thiolation of an acrylic carbon–carbon bond under phosphine catalysis.

Thiol-yne polymerization reaction is similar to the thiol-ene reactions;[149] the addition of thiyl radical to an alkyne group takes place followed by the abstraction of hydrogen from another thiol group by the carbon – centered radical species generated as a result of initial addition. This leads to the formation of a vinyl sulphide moiety and regenerating a thiyl radical. In the case of thiol-ene reaction the thioethers are generated instead of vinyl sulphide. Vinyl sulphides are capable of propagating the reaction further by the addition of a second thiyl radical. A dithoether is finally formed after the completion of reaction between an alkyne and thiols, alkyne act as a difunctional monomer in this step growth polymerization by adding up two thiols to generate a dithioether. The reaction mechanism is shown in Figure 1.5.

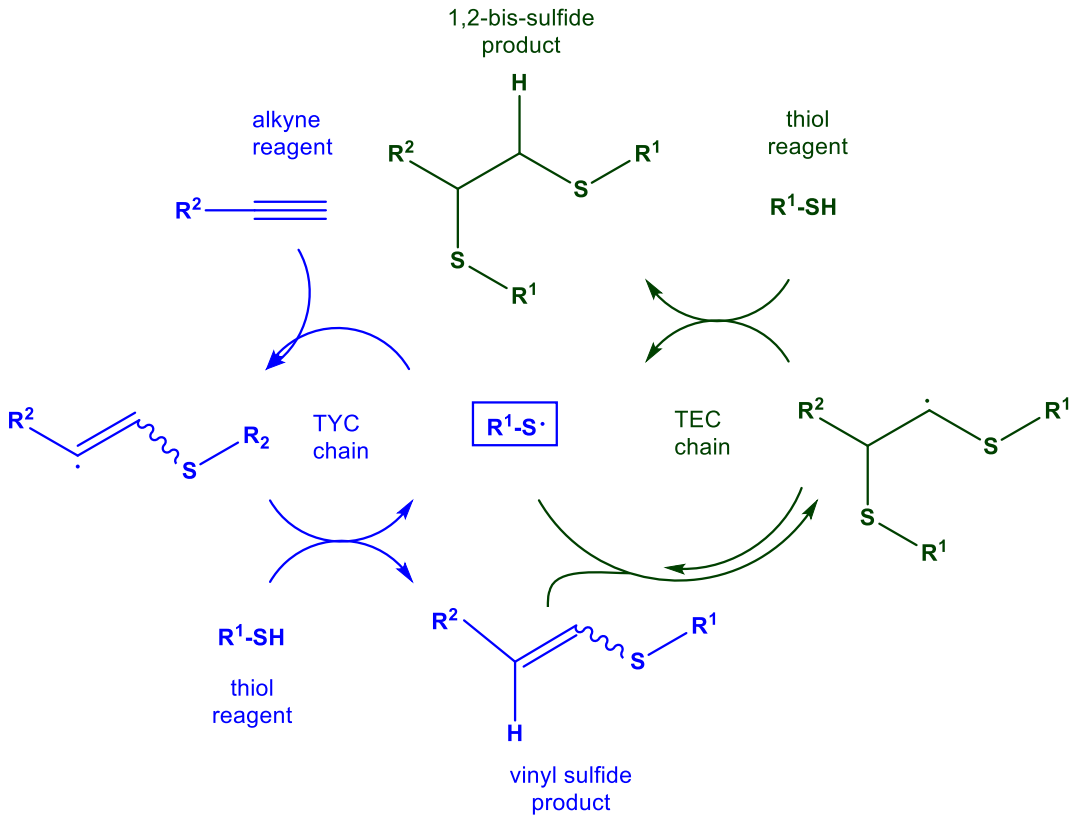

Figure 1.5 Schematic representation of thiol-yne polymerization reaction mechanism.

1.4.2. Thiol-epoxide ring opening polymerization

Thiol-epoxide ring opening polymerization involves a reaction between a thiol and an epoxide group. The highly strained epoxide rings can be opened in presence of a catalyst under suitable conditions. The syntheses of β-hydroxy sulphides are usually carried out using the thiol-epoxide ring opening reactions.[150, 151] β-hydroxy sulphides are important

intermediates which can be used for the synthesis of biologically interesting molecules and natural products.[152-154]

The base catalyzed thiol–epoxide polymerization mechanism involves a nucleophilic ring-opening reaction.[155] Thiolate anions are generated from the reaction between the base catalyst and the thiol, Figure 1.6.B. The ring opening of the epoxide by thiolate anions is then initiated, followed by the protonation of the alcolate anion takes place via the quaternary ammonium, which was originally formed via reaction of the base catalyst and thiol to generate the initial thiolate, as shown in Figure 1.6.B.

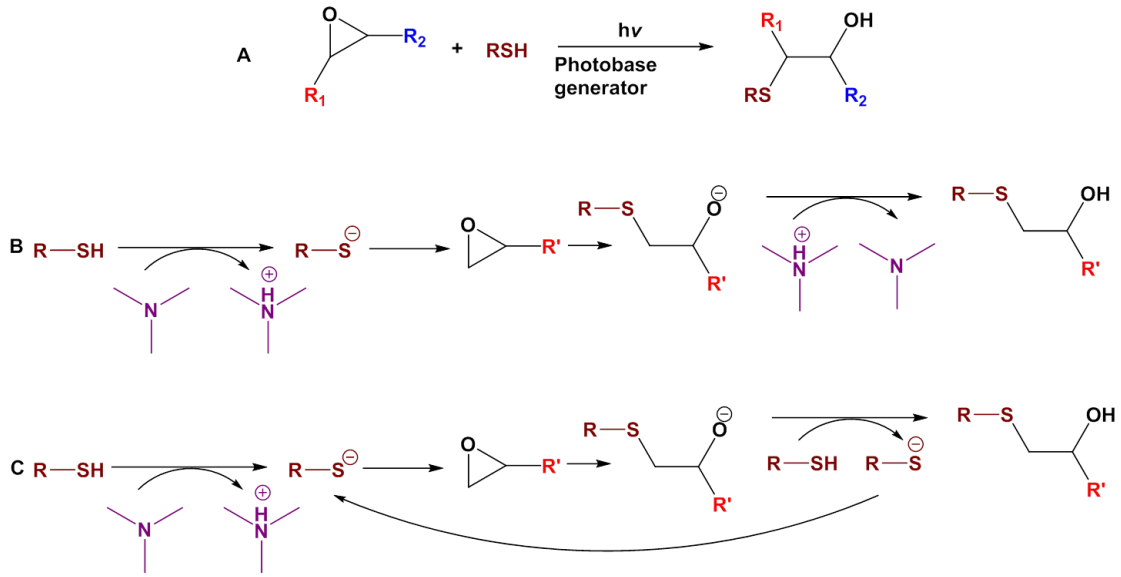

Figure 1.6 Schematic representation of reaction mechanism for the thiol-epoxide polymerization.

Strong bases are used as catalysts, through deprotonation of the thiol. Figure 1.6.C. shows, deprotonation of the thiol in the second step to regenerate the thiolate and complete a two-step anionic chain propagation process.

2. Scope of the thesis

Stimuli responsive and biodegradable polymers have fascinated researchers since long time. Polymeric nanoparticles prepared from these materials are promising for biomedical applications. A number of drugs, such as Adagen, Cimzia, Copaxone, Mircera, Oncaspar, Pegasys and Renagal, approved by FDA (Food and Drug Administration) are either based on polymer nanoparticles or contain polymer chains (e.g. PEGylation) as a part the formulation.[156] Stimulus such as temperature and pH have been thoroughly investigated. Oxidation responsive polymeric systems are relatively new and hence less explored. This work mainly focuses on the design and practical application of oxidation responsive polymers and their nanoparticles in the field of biomedicine.

Inflammatory response and related diseases are one of the major concerns of human morbidity and mortality around the world.[157] Inflammatory response in humans occurs due to many reasons including small cuts, inhalation of foreign bodies, mosquito bites, virus infections etc. Inflammation is a result of body's defense mechanism. Acute inflammation is shorter and less harmful comparing with chronic inflammation which lasts longer and can be even fatal.[158, 159]

Auto-immune diseases, infections, wound healing, or even carcinomas are general pathological reactions associated with inflammatory responses in humans. Anti-inflammatory drugs are often administrated to fight these conditions. Steroids based anti-inflammatory drugs are well known since 50 years and are used for the treatment of chronic inflammatory diseases such as rheumatoid arthritis.[160] Aspirin, ibuprofen, and naproxen etc. are famous non-steroidal anti-inflammatory drugs (NSAIDs).[161] Immune selective anti-inflammatory derivatives (ImSAIDs) are recently developed and are a new class of anti-inflammatory drugs.[162]

All kinds of anti-inflammatory drugs are still widely used even though they are known to cause a lot of unwanted side effects. Poor solubility and stability, reduced selectivity etc. are few problems to be addressed to enhance the drug efficiency. Responsive carriers which are site specific to inflammation could be an ideal choice for the site specific delivery of anti-inflammatory drugs. Suitable drug carriers developed from oxidation sensitive sulfur containing polymers are assessed in this work.

In this thesis we aim to develop three different libraries of biologically responsive polymers containing sulfur in the main chain, polysulfides, poly(β-hydroxy thioethers) and poly(β-

thioesters). These polymers were synthesized by thiol-yne, thiol-epoxide ring opening polymerization and thiol-ene reactions. Preparation of nanoparticles by nanoprecipitation, single emulsion and double emulsion methods using the above mentioned polymers were established.

Therefore the aims of this thesis can be summarized as follows:

1. Synthesis of two different sets of oxidation sensitive and one set of biodegradable polymer libraries, using thiol-yne, thiol-epoxide and thiol-ene reactions.

2. Preparation of nanoparticles from these polymers using three different techniques, nanoprecipitation, single emulsion and double emulsion techniques.

3. To study the nanoparticles size and zeta potential variations with different preparation techniques employed.

4. Estimation of degradation and oxidation responsive properties of these polymers under the influence of various concentration of hydrogen peroxide or various pH.

5. Nile red was used as a model dye to study the release kinetics and encapsulation efficiency.

6. Cellular experiments on Hela and HUVEC cells such as cell viability and cellular uptake were also monitored to determine the toxicity of nanoparticles.

3. Materials and Methods

3.1.Materials

Chemicals: 1,2-ethanedithiol (98 %), 1,5-pentanedithiol (96%), 1,6-hexanedithiol (96%), 1,8-octanedithiol (97%), 2-mercaptoethyl ether (95%), 2,2-(ethylenedioxy)diethanethiol (95%), 4-pentynoic acid (95 %), 1-pentyne (99 %), neopentyl glycol diglycidyl ether, di(ethylene glycol) diacrylate (75%), 2,2-dimethoxy-2-phenylacetophenone (99 %) (DMPA), 1,8-diazabicycloundec-7-ene (98%), trimethylphosphine solution (1.0 M in THF) DMSO-d_6 (99.9 %), $CDCl_3$ (99.8%), poly(vinyl alcohol), Rhodamine B and Nile Red (technical grade) 3-(4,5-dimethylthiazol-2-yl)-2,5-diphenyltetrazolium bromide (MTT) were purchased form Sigma-Aldrich (Steinheim, Germany) and used without purification unless otherwise noted. 4',6-diamidino-2-phenylindole (DAPI), hydrogen peroxide (30%) (H_2O_2), dichloromethane (DCM) and tetrahydrofuran (THF) was obtained from Merck (Darmstadt, Germany). Dimethyl sulfoxide (DMSO) was purchased from Roth chemicals (Karlsruhe, Germany).

Biological reagents: Dulbecco's modified Eagle's medium (DMEM), fetal bovine serum (FBS) donor bovine serum (DBS), phosphate buffered saline (PBS), penicillin/streptomycin mixture and trypsin were purchased from Invitrogen (Karlsruhe, Germany). Endothelial Cell Growth Medium (EGM-2) was purchased from Lonza Colonge AG(Colonge, Germany).

Cells: Hela cells were cultivated in 175 cm^2 tissue culture flasks at 37°C, in a humidified (90 %) and CO_2 (5 %) containing atmosphere. Cells were then trypsinized and passaged every second or third day. For passaging the cell culture medium is removed, about 13 mL of PBS are used to wash the cells. PBS is removed as well and about 3 mL trypsin solution (37°C) are pipetted into the flask and spread evenly all over the bottom. Excess of trypsin is removed and the flask is placed in the incubator for around 3 minutes. Trypsinized cells are gently resuspended by several times up/down pipetting in DMEM, and transferred into a new tissue culture flask or well plates.

HUVEC cells were also cultivated in 175 cm^2 tissue culture flasks at 37°C, in a humidified (90 %) and CO_2 (5 %) containing atmosphere. Cells were then trypsinized and passaged every second or third day. For passaging the cell culture medium is removed, about 13 mL of PBS are used to wash the cells. PBS is removed as well and about 3 mL trypsin solution (37°C) are pipetted into the flask and spread evenly all over the bottom. Excess of trypsin is removed and the flask is placed in the incubator for around 3 minutes. Trypsinized cells are gently resuspended by several times up/down pipetting in EGM-2, and transferred into a new tissue culture flask or well plates.

3.2.Methods

3.2.1. Instruments used and theoretical background

3.2.1.1.Nuclear magnetic resonance (NMR) Spectroscopy

Nuclear magnetic resonance (NMR) Spectroscopy is one of the most important and prominent analytical techniques often used by chemists to determine the structure of an organic compound. NMR spectroscopy is a non-destructive analytical method, using a very small amount of a sample (milligrams).[163] In the field of polymer science NMR spectroscopy is used for the determination of polymer structure, microstructure and also polymer dynamics.

The atomic nuclei posses spin or angular momentum, and the spinning of charges generate a magnetic moment associated with the angular momentum. The maximum experimentally observable component of the angular momentum of a nucleus possessing a spin is either a half-integral or integral multiple of $h/2\pi$, where h is the Planck's constant, according to the principles of quantum mechanics. If 'I' is the maximum component and known as the spin quantum number. There are $2I + 1$ possible orientations or states of the nucleus. The two most important nuclei in the polymer field are protons (^{1}H) and carbons (^{13}C) and they both have $I = 1/2$, so the possible magnetic quantum numbers are $+1/2$ and $-1/2$.

In the presence of a strong external magnetic field (B_0) they behave like small magnets and orient themselves with respect to the magnetic field, whereas in the absence of an external magnetic field the nuclei would randomly spin in their atomic or molecular environment. There are two possible alignments, either with the field, or against it, which differ very slightly in their energies, and it is this energy difference that can be supplied by the radio frequency radiation allowing the nuclear spins to change their state. The energy difference (ΔE) between spin states is directly proportional to the magnetic field strength, and because $\Delta E = h\nu$, the frequency of resonance ν, is also directly proportional to the strength of the external magnetic field. The proportionality constant can be shown to be $\gamma/2\pi$ where γ is the magnetogyroscopic ratio of the nucleus. The magnetogyroscopic ratio γ and the magnetic field strength B_0 determine the observation frequency for NMR signals. The sensitivity depends on the magnetogyroscopic ratio and the natural abundance. Protons have the highest sensitivity because they have the highest magnetogyroscopic ratio and natural abundance.

All polymers were first re-precipitated in n-hexane and then thoroughly dried overnight under reduced pressure (~10-15 mmHg) to remove all the solvent impurities. 10-15 mg of polymer

was weighed and dissolved in 0.5 ml NMR of solvents. All ^{1}H NMR spectra were acquired in DMSO-d_6 or $CDCl_3$ using a Bruker AVANCE DPX spectrometers operating at 500 MHz. Chemical shifts (δ) are given in ppm relative to the internal standard tetramethylsilane (TMS, δ = 0.00 ppm).

3.2.1.2.Raman spectroscopy

Raman spectroscopy is a well known vibrational spectroscopic technique used to study vibrational, rotational, and other low-frequency modes in a system.[164] Raman scattering is an inelastic scattering phenomena were the incident photons either gain or loose energy and causes a change in frequency. Wavenumbers in inverse length are generally used to report the Raman shifts. Spectral wavelength is converted to wavenumbers, using the following equation 1.

$$\Delta\omega = \left(\frac{1}{\lambda 0} - \frac{1}{\lambda 1}\right) \quad (1)$$

Where, Δω Raman shifts in wavenumbers, λ0 is the excitation wavelength and λ1 is the Raman spectra wavelength. To express the wavenumbers in inverse centimeters (cm^{-1}), the equation can be modified to equation 2.

$$\Delta\omega\ (cm^{-1}) = \left(\frac{1}{\lambda 0(nm)} - \frac{1}{\lambda 1(nm)}\right) \times (10^{7} nm)/(cm) \quad (2)$$

Raman spectroscopy was initially used to determine the molecular fingerprints of organic compounds. Recent advances in instrumentation like the introduction of diode-array detector, tunable lasers and Fourier transform (FT) made Raman spectroscopy a suitable analytical technique for the characterization of polymers and polymerization process. Raman spectroscopy is not only used to monitor the kinetics of polymerization, but also to retrieve information on the extent of polymerization and structural information on the end-product. The intensity of the v(C=C) stretching vibration is relatively strong in Raman spectrums, polymerization of unsaturated diene monomers shows a decrease in the intensity of the v(C=C) stretching vibration, as the reaction proceeds.[165] A comparison between the magnitude of initial and final peak intensities are done to calculate the conversion of monomer as a function of time at any given temperature.

In this work all Raman Spectra were acquired using a multiRAM, stand alone, Bruker RFS 27 Instrument. The spectral range is 4000 – 50 cm^{-1}. The laser source is Nd: YAG 1064 nm.

Samples were placed on the sample holder and directly measured, whereas nanoparticle suspension in water were filled in a 2 ml glass vial and measured.

3.2.1.3.Gel permeation chromatography (GPC)

Gel permeation chromatography (GPC) is also referred to as size exclusion chromatography (SEC), and is a commonly used analysis technique to determine the molecular weight and polydispersity index of a macromolecule. GPC/SEC is also a kind of chromatographic technique involving stationary and a mobile phase. The principle of separation is based on the size of polymer molecule in the solution. The stationary phase is comprised of stagnant liquid present in pores or beads and the flowing liquid act as the mobile phase. A GPC/SEC instrument consists of a pump that push the solvent through the instrument, an injection unit to introduce the sample to be tested onto the column, a column that holds the stationary phase, one or more detectors to detect the components as they leave the column, and software to control the different parts of the instrument and calculate and display the results.

All the polymers characterized were dissolved in THF, GPC grade (Merck, Darmstadt Germany) 2-4 mg/ml. The samples solutions were filtered using a 0.2 µm membrane filter prior to injection. Molecular weight (M_w) and polydispersity index PDI (M_w/M_n) values of the polymers were obtained by GPC using a Tosoh EcoSEC, TOSOH BIOSCIENCE GmbH (Stuttgart, Germany) equipped with an auto sampler and Tosoh EcoSEC RI refractive index detector. THF was used as eluent (flow rate 1 mL/min) at 30°C. All determinations were performed relative to linear polystyrene standards (Polymer Standard Service, MP 474− 2520000 Da).

3.2.1.4.Ultraviolet-visible spectroscopy (UV-Vis)

The response of a sample towards ultraviolet and visible region of an electromagnetic spectrum is measured using ultraviolet-visible spectroscopy. The sample is subjected to a light source with wavelength in the UV-Vis region, which leads to electronic transitions from the ground state to the higher excited state in molecular levels. Electronic transitions involving n, σ and π electrons are classified as; (a) σ to σ* transition that is present in compounds containing single bonds. (b) π to π* transition that takes place in compounds that contain double bonds. (c) n to σ* and n to π* transitions which are present in compounds containing lone-pair of electrons. The wavelength and amount of light that a compound absorbs depends on its molecular structure and the concentration of the compound used. The amount of light absorbed is usually expressed as either transmittance or absorbance, which is the difference between the incident radiation (*Io*) and the transmitted radiation (*I*).

Transmittance is given in terms of a fraction of 1 or as a percentage and is defined as follows, equation 1:

$$\mathrm{T}= \frac{I}{Io} \text{ or } \% \ \mathrm{T}= \left(\frac{I}{Io}\right) \times 100 \quad (1)$$

Absorbance and transmittance are related by the equation 2:

$$\mathrm{A} = -log\ \mathrm{T} \quad (2)$$

The Beer-Bouguer-Lambert law is shown in equation 3.

$$\mathrm{T} = \frac{I}{Io} = \ e^{-kbc} \quad (3)$$

Where the incident intensity is *Io*, the transmitted intensity is *I*, *e* is the base of natural logarithms, *k* is a constant, *b* is the path length (in centimeters) and *c* denotes the concentration of the absorbing species usually expressed in grams/liter or milligrams/liter. A linear expression can be derived using logarithmic values and commonly known as the Beer's law, equation 4

$$\mathrm{A} = -log\mathrm{T} = -\log\left(\frac{I}{Io}\right) = \log\left(\frac{Io}{I}\right) = \varepsilon bc \quad (4)$$

Here ε is known as the molar excitation coefficient, which is also dependent on wavelength, solvent and temperature. It is the characteristics of a substance under precisely defined set of conditions.[166]

UV-VIS spectra of nanoparticles dispersions were recorded at specified time intervals using a Varian Cary Eclipse spectrometer in a 1 cm quartz cuvette.

3.2.1.5.Dynamic light scattering (DLS)

Dynamic light scattering (DLS) referred also as a photon correlation spectroscopy, is a commonly used analytical technique to determine the hydrodynamic radius or particle size of a sample. Particles suspended in a liquid are constantly exhibiting Brownian motion (Reference). So as a result in a scattering experiment the phase relations of the light scattered by different particles change randomly. The number of particles in the scattering volume also fluctuates. The combined effects lead to a fluctuation of the scattering intensity, Figure 3.2 (a) which contains information about the time scale of the movement of the Brownian particles, or more physically, their diffusion process in terms of a time correlation function **(**Pecora, 1985**).** The correlation function is given by a digital correlator which is a signal comparer. The intensity of a signal is compared with itself at a particular point in time '*t*' and

a small time later $t+\tau$., if the intensity of signal at time = t is compared to the intensity a very small time later ($t+\delta t$), there will be a correlation between the intensities of two signals. Thus the autocorrelation function is given by equation 1

$$G_2(\tau) = \frac{< I(t).I(t+\tau) >}{< I(t) >^2} \quad (1)$$

However, for a fluctuating signal the correlation reduces with time. In the conventional DLS experiment the auto correlation function is given by equation 2. The Figure b shows the correlogram, i.e. correlation function, which decays with time. The auto correlation function is related to the diffusion coefficient by equation 2

$$G_1(\tau) = \exp(-q^2 D_t(\tau)) \quad (2)$$

This is obtained from the measured intensity auto correlation function using the Siegert relation (Berne & Pecora 1976b).

The size of a particle is calculated from the translational diffusion coefficient by using the Stokes- Einstein equation 3;

$$d_h = \frac{KT}{3\pi\eta D_t} \quad (3)$$

Where, d_h = hydrodynamic diameter, D_t = translational diffusion coefficient, K = Boltzmann's constant, T = absolute temperature, η = viscosity.

In the case of polymeric nanoparticle suspension, it is assumed that the light is scattered by a single scattering event i.e. multiple scattering is negligible. However, in real situations this assumption is valid only if the sample is very dilute (typically 10^{-5} to 10^{-2} weight %). However, study of concentrated (turbid) suspensions is significant from the industrial as well as fundamental research point of view. Additional averaging due to multiple scattering occurs in dynamic light scattering. The dynamic experiment shows additional spectral components at higher frequencies with a decreased resolution.[167] Thus investigation or characterization of turbid systems cannot be achieved by conventional dynamic light scattering.

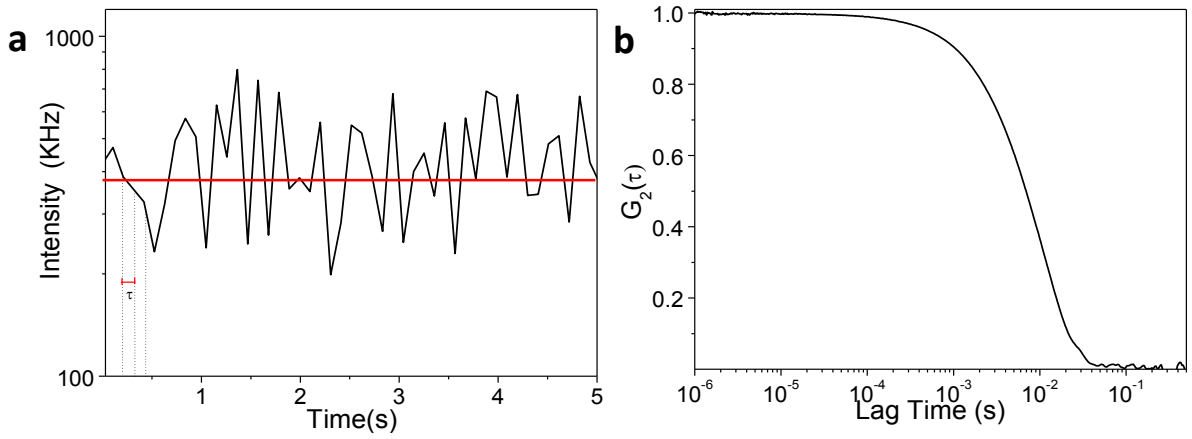

Figure 3.1 (a) Scattered intensity vs time in a dynamic light scattering experiment for polymeric nanoparticle suspension. (b) Auto Correlation function of a polymeric nanoparticle suspension.

Polymeric nanoparticles suspension were diluted to a concentration ranging between 0.1 mg/ml to 1 mg/ ml in water or buffer, and an optimized concentration of 0.5 mg/ml was finally used throughout the experiments. The hydrodynamic diameter and zeta potential of the nanoparticles were measured using a Malvern Zetasizer (Nano-ZS). All DLS measurements were done with a laser emitting at 632.8 nm at 25±1ºC and a fixed scattering angle of 175º. The intensity distribution was used to measure the particle size.

3.2.1.6.Scanning electron microscopy (SEM)

Scanning electron microscope (SEM) is a microscopic technique used to visualize the surface morphology of a sample; focused beam of high-energy electrons are used to generate a variety of signals at the surface of a solid sample. Vital information about the sample morphology, orientation of materials making up the sample, chemical composition or crystalline nature are gathered from the signals derived from electron –sample interactions. An electron gun generates the necessary amount of electron beam, which follows a vertical path through electromagnetic fields and lenses which focus the beam toward the sample placed in a vacuum chamber. The beam is focused to a fine point and raster scanned line by line over the sample.

Kinetic energy of accelerated electrons upon interaction with sample is dissipated in the form of secondary electrons, primary backscattered electrons, auger electrons and X-rays. These phenomena are dependent on the topography, the atomic number and the chemical state of the specimen. The signals from secondary electrons and backscattered electrons are commonly used for imaging purposes. Elemental microanalysis is done using the X-rays.

Images were obtained using the LEO 1530 Gemini scanning electron microscope (Zeiss, Germany). The samples were sputtered with a 10 nm gold layer using a Cressington 108 auto sputter coater before SEM measurement.

3.2.1.7.Transmission electron microscopy (TEM)

Transmission electron microscope (TEM) is one of the widely used electron microscopic techniques; images having higher spatial resolution than light microscopy are generated using a beam of electrons. Internal structural details, sample morphology, particle size etc. can be determined using this technique. The electrons are accelerated at high voltage (100-1000 kV) to a velocity approaching the speed of light (0.6-0.9 c) in a typical TEM. The associated wavelength is five orders of magnitude smaller than the light wavelength (0.04-0.008 Å). Nevertheless, the magnetic lens aberrations limit the convergence angle of the electron beam to 0.5° (instead of 70° for the glass lens used in optics), and reduce the TEM.. Atomic level material imaging and structure determination are possible at this resolution.

A PHILIPS CM 120 BioTwin TEM instrument was used to monitor the morphology of the resultant nanoparticles. The nanoparticles solution was placed onto carbon-coated copper grid followed by drying at room temperature for at least 72 h. The images were acquired at 200 kV.

3.2.1.8.Fluorescence spectroscopy

Fluorescence spectroscopy is a type of spectroscopy which is used to analyze fluorescence from a sample, it's also known as fluorometry or spectrofluorometry. The samples are irradiated using a definite wavelength of light (usually ultraviolet), which causes the excitation of molecules from the sample and hence emission at higher wavelengths. Qualitative and quantitative information's can be obtained using the emission spectrum.

Fluorescence is the relaxation of molecule from the singlet excited state to the singlet ground state with emission of light. The energy gap between the ground state and the excited state determines the energy and the wavelength of the light emitted. Figure 3.2 shows the electronic transition during fluorescence, by means of a simplified Jablonski diagram. The ratio of number photons emitted to the number of photons absorbed is known as the fluorescence quantum yield (Φ_F), or simply the efficiency of the fluorescence process.

In this research work fluorescent dye Nile red was used as the drug analog. The release of these dye from the polymeric nanoparticles was determined using the fluorescence spectroscopy. Fluorescence spectroscopy is recognized as one of the most sensitive technique, and it is possible to measure the concentration of the fluorescent substance at nano

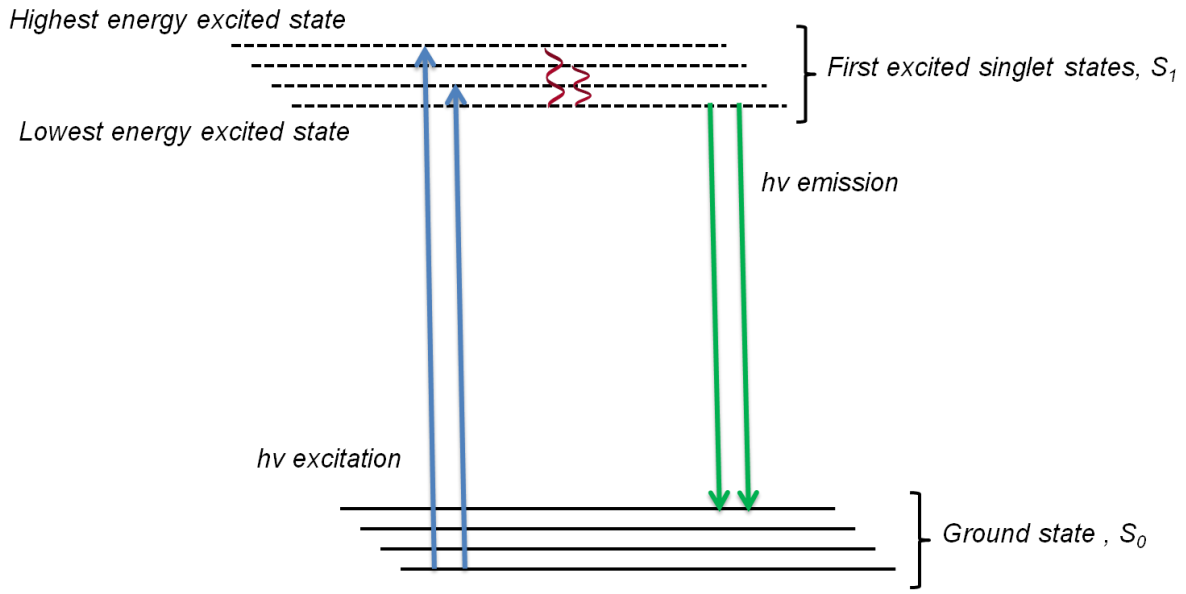

Figure 3.2 Electronic transition during fluorescence, a simplified Jablonski scheme.

gram levels. Fluorescence spectra were recorded at excitation wavelengths of 590 and 630 nm to monitor the release profile. Fluorescence spectra were obtained using a Varian Cary Eclipse fluorescence spectrophotometer.

3.2.1.9.Confocal laser scanning microscopy (CLSM)

Confocal laser scanning microscopy (CLSM) is a sophisticated microscopic technique used to obtain high resolution optical images with depth selectivity.[168] Optical sectioning is a process used in confocal microscopy to obtain in-focus images from selected depths, which is one of the advantages when compared with conventional microscopes.

Confocal images were obtained using a Leica TCS SP5 X confocal laser-scanning microscope (Wetzlar, Germany). Images were further processed using Leica LAS-AF Lite software.

3.3.Synthesis of polymers

3.3.1. Synthesis of oxidation responsive polysulfides via thiol-yne polymerization (General procedure)

Equimolar ratios of a alkyne and a dithiol were dissolved in 1 ml of THF. 2,2-dimethoxy-2-phenylacetophenone (2 wt % with respect to the monomers) was added to the solution and the whole reaction system was sealed with septum, and purged with argon for 10 min. The solution was then irradiated for 2 h under UV cabinet equipped with 5 X 8 W UV tubes (365

nm, 80 mW/cm^2) upon stirring. After the completion of the reaction, the polymer solution was precipitated using *n*-hexane. Precipitation was done three times, each time the sample was dissolved in THF. The final product was dried under vacuum to yield pale yellowish viscous substance.

3.3.1.1.Synthesis of polymer AU

4-Pentynoic acid (10 mmol, 0.98 g, 1 eq.) was added to a solution of 2,2-(ethylenedioxy)diethanethiol (10 mmol 1.82 g, 1 eq.) and dissolved in 1 ml of THF. 2,2-dimethoxy-2-phenylacetophenone (0.056 g, 2 wt % with respect to the monomers) was added to the solution and the whole reaction system was sealed with septum, and purged with argon for 10 min. The solution was then irradiated for 2 h under UV cabinet upon stirring. After the completion of the reaction, the polymer solution was precipitated using *n*-hexane. Precipitation was done three times, each time the sample was dissolved in THF. The final product was dried under vacuum to yield pale yellowish viscous substance.

^{1}H-NMR (500 MHz, $(CD_3)_2SO$, δ): 1.48-1.63 (m, 1H, -CH_2), 1.96-2.14 (m, 1H, -CH_2), 2.29-2.45 (m, 2H, CH_2), 2.60-2.75 (m, 5H, -CH_2-S-), 2.80-2.95 (m, 1H, -CH-S,), 3.24-3.77 (m, 8H, -CH_2-O).

3.3.1.2.Synthesis of polymer AV

4-Pentynoic acid (10 mmol, 0.98 g, 1 eq.) was added to a solution of 2-mercaptoethyl ether (10 mmol 1.38 g, 1 eq.) and dissolved in 1 ml of THF. 2,2-dimethoxy-2-phenylacetophenone (0.056 g, 2 wt % with respect to the monomers) was added to the solution and the whole reaction system was sealed with septum, and purged with argon for 10 min. The solution was then irradiated for 2 h under UV cabinet upon stirring. After the completion of the reaction, the polymer solution was precipitated using *n*-hexane. Precipitation was done three times, each time the sample was dissolved in THF. The final product was dried under vacuum to yield pale yellowish viscous substance.

^{1}H-NMR (500 MHz, $(CD_3)_2SO$, δ): 1.52-1.64 (m, 1H, CH_2), 1.96-2.12 (m, 1H, CH_2), 2.23 - 2.47 (m, 2H, CH_2), 2.55-2.78 (m, 5H, -CH_2-S), 2.81-2.99 (m, 1H, -CH-S), 3.48-3.68 (m, 4H -CH_2-O).

3.3.1.3.Synthesis of polymer AY

4-Pentynoic acid (10 mmol, 0.98 g, 1 eq.) was added to a solution of 1,8-octanedithiol (10 mmol 1.78 g, 1 eq.) and dissolved in 1 ml of THF. 2,2-dimethoxy-2-phenylacetophenone (0.056 g, 2 wt % with respect to the monomers) was added to the solution and the whole

reaction system was sealed with septum, and purged with argon for 10 min. The solution was then irradiated for 2 h under UV cabinet upon stirring. After the completion of the reaction, the polymer solution was precipitated using *n*-hexane. Precipitation was done three times, each time the sample was dissolved in THF. The final product was dried under vacuum to yield a pale yellowish viscous substance.

^{1}H-NMR (500 MHz, $(CD_3)_2SO$, δ): 1.22-1.40 (m, 8H, -CH_2), 1.45-1.63 (m, 5H, -CH_2), 2.00-2.09 (m, 1H, -CH_2), 2.30-2.45(m, 2H, -CH_2), 2.57-2.64(m, 5H, -CH_2,-S), 2.72-2.84 (m, 2H, -CH-S).

3.3.1.4.Synthesis of polymer ET

1-pentyne (10 mmol, 0.68 g, 1 eq.) was added to a solution of 1,2-ethanedithiol (10 mmol 0.94 g, 1 eq.) and dissolved in 1 ml of THF. 2,2-dimethoxy-2-phenylacetophenone (0.056 g, 2 wt % with respect to the monomers) was added to the solution and the whole reaction system was sealed with septum, and purged with argon for 10 min. The solution was then irradiated for 2 h under UV cabinet upon stirring. After the completion of the reaction, the polymer solution was precipitated using *n*-hexane. Precipitation was done three times, each time the sample was dissolved in THF. The final product was dried under vacuum to yield a pale yellowish viscous substance.

^{1}H-NMR (500 MHz, ($CDCl_3$, δ): 0.92-1.03 (t, 3H, -CH_3), 1.38-1.62 (m, 3H, -CH_2), 1.73-1.84 (m, 1H, CH_2), 2.72-2.86 (m, 5H, -CH_2-S), 2.86-2.95 (m, 1H, CH-S,).

3.3.1.5.Synthesis of polymer EU

1-pentyne (10 mmol, 0.68 g, 1 eq.) was added to a solution of 2,2-(ethylenedioxy)diethanethiol (10 mmol 1.82 g, 1 eq.) and dissolved in 1 ml of THF. 2,2-dimethoxy-2-phenylacetophenone (0.056 g, 2 wt % with respect to the monomers) was added to the solution and the whole reaction system was sealed with septum, and purged with argon for 10 min. The solution was then irradiated for 2 h under UV cabinet upon stirring. After the completion of the reaction, the polymer solution was precipitated using *n*-hexane. Precipitation was done three times, each time the sample was dissolved in THF. The final product was dried under vacuum to yield a pale yellowish viscous substance.

^{1}H-NMR (500 MHz, ($CDCl_3$, δ): 0.90-0.98 (t, 3H,-CH_3), 1.38-1.58 (m, 2H, -CH_2), 1.74-1.83 (m, 2H, -CH_2), 2.70-2.77(m, 5H, -CH_2-S), 2.87-2.95 (m, 2H, -CH-S), 3.61-3.70 (m, 8H, -CH_2-O).

3.3.1.6.Synthesis of polymer EV

1-pentyne (10 mmol, 0.68 g, 1 eq.) was added to a solution of 2-mercaptoethyl ether (10 mmol 1.38 g, 1 eq.) and dissolved in 1 ml of THF. 2,2-dimethoxy-2-phenylacetophenone (0.056 g, 2 wt % with respect to the monomers) was added to the solution and the whole reaction system was sealed with septum, and purged with argon for 10 min. The solution was then irradiated for 2 h under UV cabinet upon stirring. After the completion of the reaction, the polymer solution was precipitated using *n*-hexane. Precipitation was done three times, each time the sample was dissolved in THF. The final product was dried under vacuum to yield pale yellowish viscous substance.

^{1}H-NMR (500 MHz, ($CDCl_3$, δ): 0.89-0.99 (t, 3H, -CH_3), 1.38-1.61 (m, 3H, -CH_2), 1.74-1.91 (m, 1H, -CH_2), 2.69-2.79(m, 5H, -CH_2-S), 2.79-2.96 (m, 2H, -CH-S,), 3.55-3.78 (m, 4H, -CH_2-S).

3.3.2. Synthesis of poly (β-hydroxy thioethers) by thiol-epoxide ring opening polymerization (General procedure)

Equimolar ratios of a diepoxide and a dithiol were dissolved in 1 ml of THF. 1,8-Diazabicycloundec-7-ene (0.5 wt % with respect to the monomers used) was then added to the above solution. The solution was then irradiated for 2 h under UV light (365 nm) upon stirring. After the completion of the reaction the polymer solution was precipitated using *n*-hexane. Precipitation was done thrice, each time redissolving the sample in THF. The final product was dried under vacuum to yield viscous substance.

3.3.2.1.Synthesis of polymer EP1

Neopentyl glycol diglycidyl ether (10 mmol, 2.16 g, 1 eq.) was added to a solution of 1,2-ethanedithiol (10 mmol 0.94 g, 1 eq.) in 1 ml of THF. 1,8-Diazabicycloundec-7-ene (0.019 g, 0.5 wt % with respect to the monomers used) was then added to the above solution. The solution was then irradiated for 2 h under UV light (365 nm) upon stirring. After the completion of the reaction the polymer solution was precipitated using *n*-hexane. Precipitation was done thrice, each time redissolving the sample in THF. The final product was dried under vacuum to yield viscous substance.

^{1}H-NMR (500 MHz, ($CDCl_3$, δ): 0.85-0.95 (m, 6H, -CH_3), 2.54-2.79 (m, 4H, -CH_2-S), 2.80-2.84 (m, 4H, -CH_2), 3.12-3.35(m, 4H, -CH_2-O), 3.38-3.68 (m, 4H, -CH_2,), 3.93 (br, s, 2H, -CH-OH).

3.3.2.2.Synthesis of polymer EP2

Neopentyl glycol diglycidyl ether (10 mmol, 2.16 g, 1 eq.) was added to a solution of 1,5-pentanedithiol (10 mmol 1.36 g, 1 eq.) in 1 ml of THF. 1,8-Diazabicycloundec-7-ene (0.019 g, 0.5 wt % with respect to the monomers used) was then added to the above solution. The solution was then irradiated for 2 h under UV light (365 nm) upon stirring. After the completion of the reaction the polymer solution was precipitated using *n*-hexane. Precipitation was done thrice, each time redissolving the sample in THF. The final product was dried under vacuum to yield viscous substance.

^{1}H-NMR (500 MHz, ($CDCl_3$, δ): 0.88-0.96 (m, 6H, -CH_3), 1.58-1.80 (m, 6H, -CH_2), 2.53-2.70 (m, 8H, -CH_2-S), 3.21-3.41(m, 4H, -CH_2-O), 3.44-3.66 (m, 4H, -CH_2,-CH), 3.93 (br, s, 2H, -CH-OH).

3.3.2.3.Synthesis of polymer EP4

Neopentyl glycol diglycidyl ether (10 mmol, 2.16 g, 1 eq.) was added to a solution of 1,8-octanedithiol (10 mmol 1.78 g, 1 eq.) in 1 ml of THF. 1,8-Diazabicycloundec-7-ene (0.019 g, 0.5 wt % with respect to the monomers used) was then added to the above solution. The solution was then irradiated for 2 h under UV light (365 nm) upon stirring. After the completion of the reaction the polymer solution was precipitated using *n*-hexane. Precipitation was done thrice, each time redissolving the sample in THF. The final product was dried under vacuum to yield viscous substance.

^{1}H-NMR (500 MHz, ($CDCl_3$, δ): 0.85-0.95 (m, 6H, -CH_3), 2.54-2.79 (m, 4H, -CH_2), 2.80-2.84 (m, 4H, -CH_2), 3.12-3.35(m, 4H, -CH_2-O), 3.38-3.68 (m, 4H, -CH_2,), 3.93 (br, s, 2H, -CH-OH).

3.3.2.4.Synthesis of polymer EP5

Neopentyl glycol diglycidyl ether (10 mmol, 2.16 g, 1 eq.) was added to a solution of 2-mercaptoethyl ether (10 mmol 1.38 g, 1 eq.) in 1 ml of THF. 1,8-Diazabicycloundec-7-ene (0.019 g, 0.5 wt % with respect to the monomers used) was then added to the above solution. The solution was then irradiated for 2 h under UV light (365 nm) upon stirring. After the completion of the reaction the polymer solution was precipitated using *n*-hexane. Precipitation was done thrice, each time redissolving the sample in THF. The final product was dried under vacuum to yield a viscous substance.

^{1}H-NMR (500 MHz, ($CDCl_3$, δ): 0.88-0.94 (m, 6H, -CH_3), 2.64-2.84 (m, 8H, -CH_2-S), 3.18-3.41 (m, 4H, -CH_2-O), 3.12-3.35(m, 4H, -CH_2-O), 3.41-3.58 (m, 4H, -CH_2-CH), 3.58-3.70 (m, 4H, -CH_2-O), 3.93 (br, s, 2H, -CH-OH).

3.3.2.5.Synthesis of polymer EP6

Neopentyl glycol diglycidyl ether (10 mmol, 2.16 g, 1 eq.) was added to a solution of 2,2-(ethylenedioxy)diethanethiol (10 mmol 1.82 g, 1 eq.) in 1 ml of THF. 1,8-Diazabicycloundec-7-ene (0.019 g, 0.5 wt % with respect to the monomers used) was then added to the above solution. The solution was then irradiated for 2 h under UV light (365 nm) upon stirring. After the completion of the reaction the polymer solution was precipitated using *n*-hexane. Precipitation was done thrice, each time redissolving the sample in THF. The final product was dried under vacuum to yield a viscous substance.

^{1}H-NMR (500 MHz, ($CDCl_3$, δ): 0.85-0.94 (m, 6H, -CH_3), 2.64-2.93 (m, 8H, -CH_2-S), 3.20-3.36 (m, 4H, -CH_2-O), 3.38-3.54(m, 4H, -CH_2), 3.58-3.74(m, 8H, -CH_2), 3.93 (br, s, 2H, -CH-OH).

3.3.3. Synthesis of poly-β-thioesters using base catalyzed thiol-ene Michael addition (General procedure)

Equimolar rations of a diacryate and dithiol were dissolved in 1 ml of THF. 20 µl of trimethylphosphine (PMe_3) solution (1.0 M in THF) was then added to the above solution followed by stirring for 60 minutes at room temperature. After the completion of the reaction the polymer solution was precipitated using *n*-hexane. Precipitation was done thrice each time redissolving the sample in THF. The final product was dried under vacuum to yield the polymer.

3.3.3.1.Synthesis of polymer P7

1,2-ethanedithiol (98 %), (10 mmol, 0.98 g, 1 eq.) was added to a solution of di(ethylene glycol) diacrylate (10 mmol 2.14 g, 1 eq.) in 1 ml of THF. 20 µl of trimethylphosphine (PMe_3) solution (1.0 M in THF) was then added to the above solution followed by stirring for 60 minutes at room temperature. After the completion of the reaction the polymer solution was precipitated using *n*-hexane. Precipitation was done thrice each time redissolving the sample in THF. The final product was dried under vacuum to yield the polymer.

^{1}H-NMR (500 MHz, ($CDCl_3$, δ)): 2.65-2.67 (t, 4H, -CH_2-CO), 2.74-2.76 (t, 4H, -CH_2-S), 2.82-2.84 (t, 4H, -CH_2-S), 3.69-3.72 (t, 4H, -CH_2-O), 4.26-4.28 (t, 4H, -CH_2-O).

3.3.3.2.Synthesis of polymer P8

1,5-pentanedithiol (10 mmol 1.36 g, 1 eq.) was added to a solution of di(ethylene glycol) diacrylate (10 mmol 2.14 g, 1 eq.) in 1 ml of THF. 20 µl of trimethylphosphine (PMe_3) solution (1.0 M in THF) was then added to the above solution followed by stirring for 60 minutes at room temperature. After the completion of the reaction the polymer solution was precipitated using *n*-hexane. Precipitation was done thrice each time redissolving the sample in THF. The final product was dried under vacuum to yield the polymer.

^{1}H-NMR (500 MHz, ($CDCl_3$, δ)): 1.47-1.51 (m, 2H, -CH_2), 1.59-1.61 (m, 4H, -CH_2), 2.52-2.56 (t, 4H, -CH_2-S), 2.64-2.66 (t, 4H, -CH_2-CO), 2.78-2.80 (t, 4H, -CH_2-S), 3.69-3.72 (t, 4H, -CH_2-O), 4.27-4.29 (t, 4H, -CH_2-O).

3.3.3.3.Synthesis of polymer P9

1,6-hexanedithiol (98 %), (10 mmol, 1.50 g, 1 eq.) was added to a solution of di(ethylene glycol) diacrylate (10 mmol 2.14 g, 1 eq.) in 1 ml of THF. 20 µl of trimethylphosphine (PMe_3) solution (1.0 M in THF) was then added to the above solution followed by stirring for 60 minutes at room temperature. After the completion of the reaction the polymer solution was precipitated using *n*-hexane. Precipitation was done thrice each time redissolving the sample in THF. The final product was dried under vacuum to yield the polymer.

^{1}H-NMR (500 MHz, ($CDCl_3$, δ)): 1.39-1.41 (t, 4H, -CH_2), 1.58-1.60 (t, 4H, -CH_2), 2.51-2.54 (t, 4H, -CH_2-S), 2.64-2.66 (t, 4H, -CH_2-CO), 2.78-2.80 (t, 4H, -CH_2-S), 3.69-3.72 (t, 4H, -CH_2-O), 4.26-4.27 (t, 4H, -CH_2-O).

3.3.3.4.Synthesis of polymer P10

1,8-octanedithiol (10 mmol 1.78 g, 1 eq.) was added to a solution of di(ethylene glycol) diacrylate (10 mmol 2.14 g, 1 eq.) in 1 ml of THF. 20 µl of trimethylphosphine (PMe_3) solution (1.0 M in THF) was then added to the above solution followed by stirring for 60 minutes at room temperature. After the completion of the reaction the polymer solution was precipitated using *n*-hexane. Precipitation was done thrice each time redissolving the sample in THF. The final product was dried under vacuum to yield the polymer.

^{1}H-NMR (500 MHz, ($CDCl_3$, δ)): 1.30-1.34 (t, 4H, -CH_2), 1.34-1.37 (t, 4H, -CH_2), 1.58-1.61 (m, 4H, -CH_2), 2.51-2.54 (t, 4H, -CH_2-S), 2.65-2.67 (t, 4H, -CH_2-CO), 2.79-2.81 (t, 4H, -CH_2-S),3.64-3.65(m, 4H, -CH_2-O), 3.66-3.68(t, 4H, -CH_2-O), 3.71-3.73 (t, 4H, -CH_2), 4.27-4.29 (t, 4H, -CH_2-O).

3.3.3.5.Synthesis of polymer P11

2-mercaptoethyl ether (10 mmol 1.38 g, 1 eq.) was added to a solution of di(ethylene glycol) diacrylate (10 mmol 2.14 g, 1 eq.) in 1 ml of THF. 20 µl of trimethylphosphine (PMe_3) solution (1.0 M in THF) was then added to the above solution followed by stirring for 60 minutes at room temperature. After the completion of the reaction the polymer solution was precipitated using *n*-hexane. Precipitation was done thrice each time redissolving the sample in THF. The final product was dried under vacuum to yield the polymer.

^{1}H-NMR (500 MHz, ($CDCl_3$, δ)): 2.66-2.69 (t, 4H, -CH_2-S), 2.73-2.77 (t, 4H, -CH_2-CO), 2.85-2.87 (t, 4H, -CH_2-S), 3.64-3.67(m, 4H, -CH_2-O), 3.71-3.73(t, 4H, -CH_2-O), 4.27-4.29 (t, 4H, -CH_2-O).

3.3.3.6.Synthesis of polymer P12

2,2-(ethylenedioxy)diethanethiol (10 mmol 1.82 g, 1 eq.) was added to a solution of di(ethylene glycol) diacrylate (10 mmol 2.14 g, 1 eq.) in 1 ml of THF. 20 µl of trimethylphosphine (PMe_3) solution (1.0 M in THF) was then added to the above solution followed by stirring for 60 minutes at room temperature. After the completion of the reaction the polymer solution was precipitated using *n*-hexane. Precipitation was done thrice each time redissolving the sample in THF. The final product was dried under vacuum to yield the polymer.

^{1}H-NMR (500 MHz, ($CDCl_3$, δ)): 2.66-2.69 (t, 4H, -CH_2-S), 2.73-2.77 (t, 4H, -CH_2-CO), 2.84-2.86 (t, 4H, -CH_2-S), 3.64-3.65(m, 4H, -CH_2-O), 3.66-3.68(t, 4H, -CH_2-O), 3.71-3.73 (t, 4H, -CH_2), 4.26-4.28 (t, 4H, -CH_2-O).

3.4.Preparation of polymeric nanoparticles

Nanoparticles were prepared using three different methods, nanoprecipitation, single emulsion and double emulsion. The methods used determine the final structural and physical properties of the nanoparticles. Optimization of particle size, zeta potential and surface morphologies are one of the most important criteria to be achieved before final applications.

3.4.1. Nanoprecipitation

Nanoprecipitation is also referred to as a solvent displacement method.[169] A schematic representation of nanoprecipitation method is shown in Figure 3.3. It involves the precipitation of a polymer from an organic solution and the diffusion of the organic solvent in the aqueous medium in the presence or absence of a surfactant.[169-172] Particle formation

is due to the spontaneous precipitation and subsequent solidification of the polymer upon rapid solvent diffusion. The method was first introduced and patented by Fessi and co-workers.[169] The polymer is first dissolved in a water-miscible solvent (tetrahydrofuran, dimethyl sulfoxide, acetone etc.) of intermediate polarity, leading to the precipitation of nanospheres. This phase is then added into a stirred aqueous solution sometimes containing a stabilizer as a surfactant. Colloidal suspension is formed instantaneously as a result of polymer deposition on the interface between the water and the organic solvent, caused by fast diffusion of the solvent.[173] Nanoprecipitation is also considered as one of the easiest and mild technique for the preparation of polymeric nanoparticles due the fact that no external energy such as sonication or milling is required for the particle formation.[174] One of the limitations of this technique is its only limited to water-miscible solvents, in which the diffusion rate is enough to produce spontaneous emulsification.[173] Nanoprecipitation is extensively used technique for biodegradable polymers like PLGA, PLA and PCL, but can also be applied to various other polymers too.[175, 176]

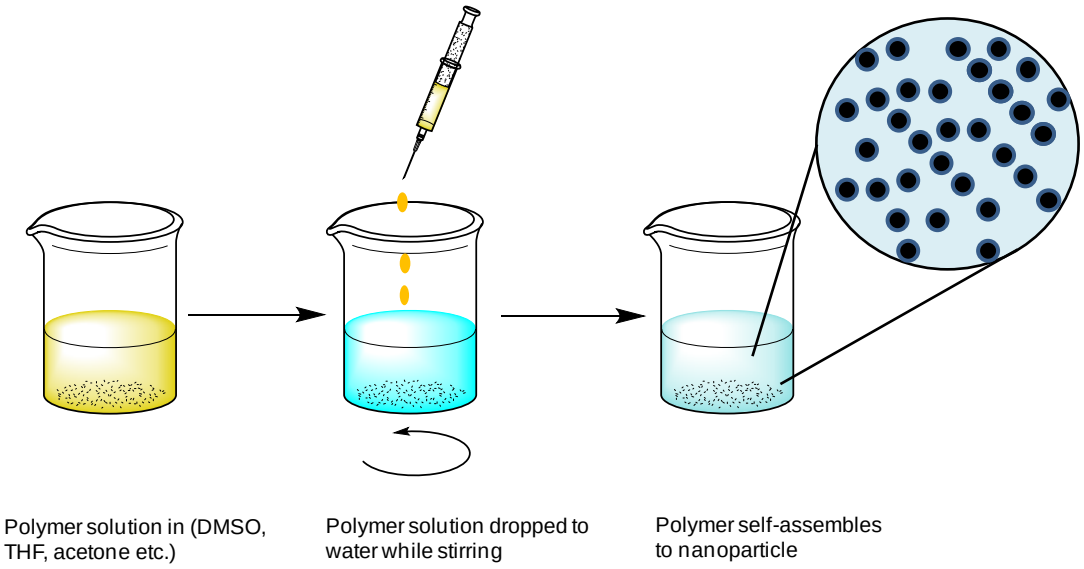

Figure 3.3 Schematic representation of steps involved in nanoprecipitation.

Nanoparticles were prepared using a previously described nanoprecipitation method [177]. 0.5 ml of polymer solution in DMSO (10 mg/mL, filtered with 0.45 µm polytetrafluoroethylene (PTFE) membrane) was added instantaneously (1 s) into a glass vial containing 4.5 mL of MilliQ water under stirring (700 rpm). After 30 minutes of stirring, the particles were separated using a cellulose membrane dialysis tube (MWCO 14,000 Da) from

Sigma-Aldrich (Steinheim, Germany) and further pre concentrated by centrifugation for 15 minutes at 10,000 rpm.

3.4.2. Single emulsion (O/W) technique

In this method, the polymer is first dissolved in an organic solvent like dichloromethane, chloroform or ethyl acetate. The drug or dye is then dissolved or dispersed into the above polymer solution, and this mixture is then emulsified into an aqueous solution to make an oil (O) in water (W) i.e., O/W emulsion by using a surfactant/emulsifying agent like poly(vinyl alcohol), gelatin, polysorbate-80, poloxamer-188, etc. This result in the formation of a stable emulsion, further the organic solvent is evaporated either by increasing the temperature, under reduced pressure or by continuous stirring.[178, 179] Figure 3.4. shows a schematic representation of single emulsion (O/W) technique.

The o/w single emulsion solvent evaporation method is one of the widely used microencapsulation techniques for the encapsulation of water insoluble cargos. Hydrophobic drugs are successfully retained within the microparticles prepared by this method. However, this method is not suitable for the entrapment of hydrophilic drugs because of rapid dissolution of the compounds into the aqueous continuous phase.

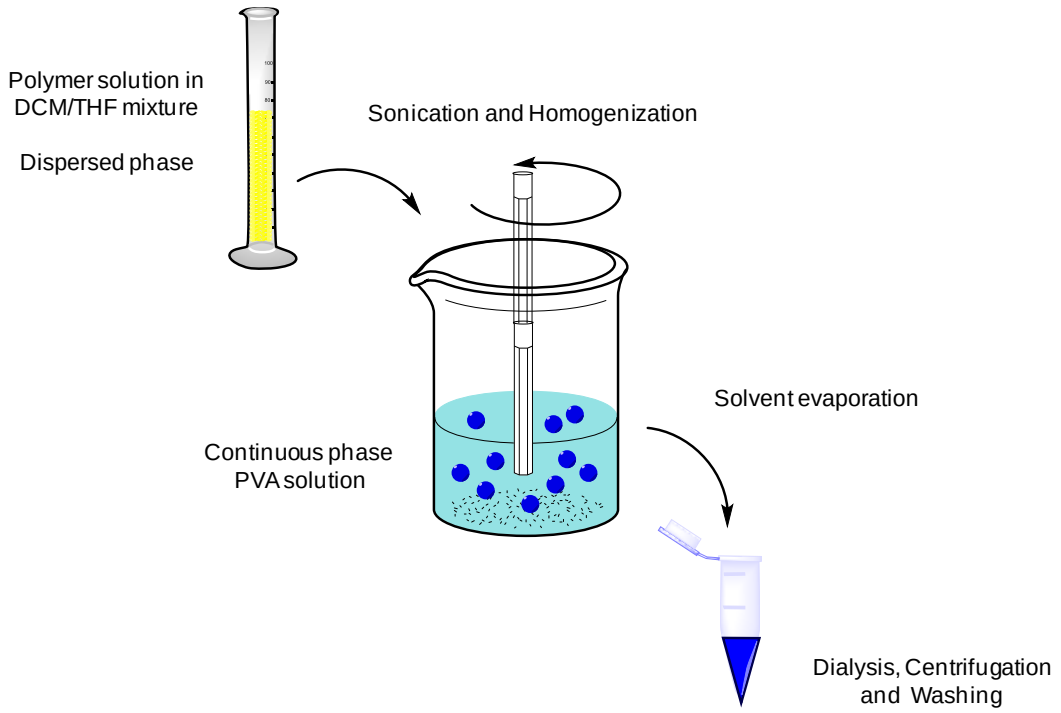

Figure 3.41 Schematic representation of steps involved in single emulsion (O/W) technique.

Nanoparticles were prepared by modification of the method reported by Mahmoud et al.[180] 17 mg of the synthesized polymer was dissolved in 2.5 ml of DCM/THF (10:1 v:v) mixture. The dissolved polymer was added to 20 ml of MilliQ water containing (0.05-1% w/v; 0.5-10 g/l) PVA. The mixture was then sonicated to prepare an emulsion, using a probe sonicator (Bandelin sonopuls hd 3200 (Berlin, Germany)) for 2 min (amplitude 50 %). The nanoparticle suspension was stirred overnight at 1000 rpm using a magnetic stirrer to evaporate the DCM/THF solvents. Dialysis of the nanoparticle suspension was performed to remove PVA excess (cellulose membrane dialysis tube (MWCO 14,000 Da), Sigma-Aldrich (Steinheim, Germany)). The nanoparticle suspension was further concentrated by centrifugation for 15 min at 10,000 rpm and used for further analysis.

3.4.3. Double emulsion technique (W/O/W) technique

An emulsion in an emulsion is known as double emulsion. A two step emulsification process is usually required for double emulsion.[181] W/O/W double emulsion technique is one of the popular methods, and was developed by Ogawa et al.[182] There are two different types of double emulsion, a water-in–oil-in-water (W/O/W) emulsion and an oil-in-water-in-oil (O/W/O), the former is more common in use than the latter. Herein we emphasis on (W/O/W) emulsion technique. Figure 3.5 shows a schematic representation of W/O/W double emulsion technique.

A W/O/W double emulsion technique mainly consists of four steps.[182, 183] In the first step, known also as primary emulsification, an aqueous solution of the active agent (internal water phase, W_1) is emulsified into an organic solution containing the biodegradable polymer (oil phase, O). In the second step re-emulsification process is carried out onto the primary emulsion. Primary emulsion (W_1/O) is further emulsified into a second aqueous phase containing a stabilizer (external water phase, W_2) to form a W_1/O/W_2 double emulsion. Solidification step involves the removal of organic solvent by evaporation or extraction which leads to the formation of solid particles. Finally the separation and purification of the particles are done by dialysis, centrifugation or filtration. Double emulsion techniques are popular and commonly used for the preparation of biodegradable hydrophobic microsphere containing hydrophilic pharmaceuticals, dyes, proteins and polypeptides for sustained release applications.

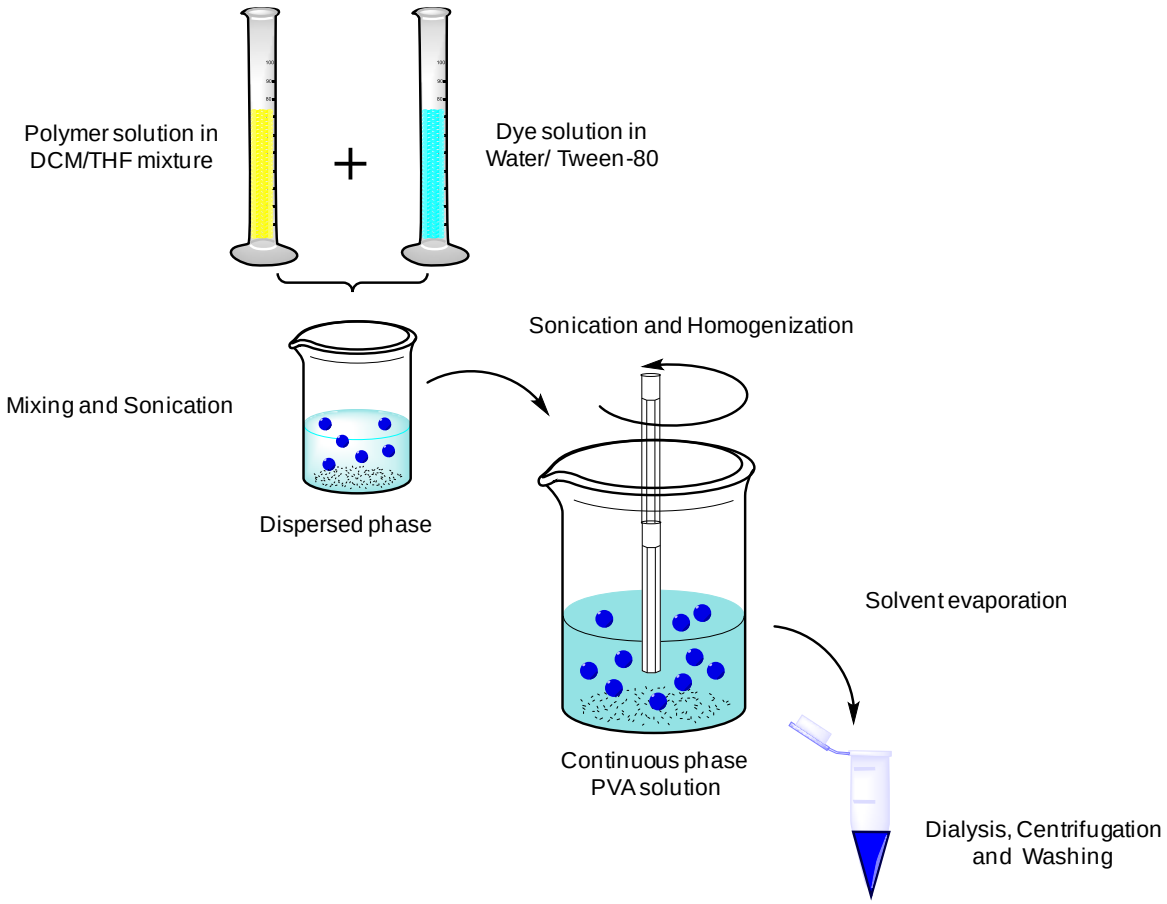

Figure 3.5 Schematic representation of steps involved in double emulsion technique (W/O/W) technique.

Nanoparticles were prepared by modification of the method reported by Liu et al. [184]. 17 mg of the synthesized polymer was dissolved in 2.5 ml of DCM/THF (10:1 v:v) mixture. 50 µl of Tween 80 was then dissolved in 500 µl of MilliQ water. Both solutions were combined and sonicated for 2 minutes (amplitude 50 %) using a probe sonicator to prepare the first emulsion. Finally, the first emulsion was added drop wise to 20 ml of MilliQ water containing (0.05-1% w/v; 0.5-10 g/l) PVA. The mixture was then sonicated using a probe sonicator for 2 minutes (amplitude 50 %) to prepare the final emulsion. The nanoparticle suspension was stirred overnight at 1000 rpm using a magnetic stirrer to evaporate the DCM/THF solvents. Dialysis of the nanoparticle suspension was performed to remove PVA excess using a dialysis membrane (cellulose membrane dialysis tube (MWCO 14,000 Da), Sigma-Aldrich (Steinheim, Germany)). The nanoparticle suspension was further concentrated by centrifugation for 15 min at 10,000 rpm.

3.5.Encapsulation efficiency

Encapsulation efficiency (% EE) is one of the most important criteria to be considered after the preparation of dye/drug encapsulated polymeric nanoparticles. It is an estimate of total encapsulation in percentage and given by the equation below.[185, 186]

$$\text{Encapsulation efficiency (\% EE)} = \frac{\text{Amount of drug/dye entrapped in NPs}}{\text{Initial amount of drug/dye added}} \times 100$$

UV or fluorescence spectroscopy can be used to estimate encapsulation efficiency. Because of the small size of nanoparticles, determinations of drug encapsulation or drug loading are not always an easy task. Separation of free drug from bound or entrapped drug is firstly done by ultracentrifugation or ultra filtration.

3.6.Cellular studies

3.6.1. Cellular uptake

The HeLa or HUVEC cells were utilized for the cell uptake experiments. Cells were plated in 6 well plate at a density of 2 X 10^4 cells per well, in DMEM medium or EGM -2 medium, 10 % Donor bovine serum (DBS) or FBS and 1% Penicillin-Streptomycin one day before the experiment. Nile Red encapsulated polymeric nanoparticles were reconstituted in DMEM or PBS. The final concentration was determined to be 50-100 μg/ml, treated with cells and allowed to react for 4 h at 37°C. After incubation the cells were washed with PBS three times. 4',6-diamidino-2-phenylindole (DAPI), blue was then used to counter-stain the cells. Cells were fixed using 3.7 % formaldehyde solution for further experiments.

3.6.2. Cellular viability- MTT assay

Biocompatibility of polymeric nanoparticles was investigated using an established procedure using the colorimetric MTT assay for quantitative assessment. The principle of this assay is the conversion of water-soluble MTT into an insoluble formazan dye by mitochondrial dehydrogenase only present in living cells.[187-190] Subsequently, the formazan concentration was determined by measuring the optical density [OD] using an automatic microplate reader at 570 nm with a background correction at 690 nm. Cytotoxicity was expressed as cell viability [%] of the treated cells relative to the untreated (negative control) calculated based on the following equation, and all data were expressed as mean (N=4) and relative standard deviation.

$$Cell\ viability\ [\%] = \frac{OD\ test\ cells}{OD\ negetive\ control} \times 100\ \%$$

HeLa or HUVEC cells were utilized for cell toxicity experiments. Cells were routinely maintained at 37ºC in 5% CO_2 in Dulbecco's Modified Eagle Medium (DMEM) supplemented with 10 % Donor bovine serum (DBS) and 1% penicillin-streptomycin for Hela cells. DMEM was replaced with EGM-2 for HUVEC cells. In preparation for the MTT test, the cells were placed in a 96-well plate. Various concentrations of nanoparticle dispersions were introduced to each well with 100 µl of media. To perform the MTT test, the media was removed after a 24 h incubation period and the wells were rinsed with 100 µl of PBS three times. 100 µl of 3-(4,5-dimethylthiazol-2-yl)-2,5-diphenyltetrazolium bromide (MTT) solution (0.5 mg/ml) was added to each well and allowed to react for 4 h at 37 °C. MTT-formazan crystals were then dissolved in the MTT solvent. Values were determined by subtracting the absorbance value measured at 690 nm from the value measured at 570 nm using a PerkinElmer (USA) plate reader.

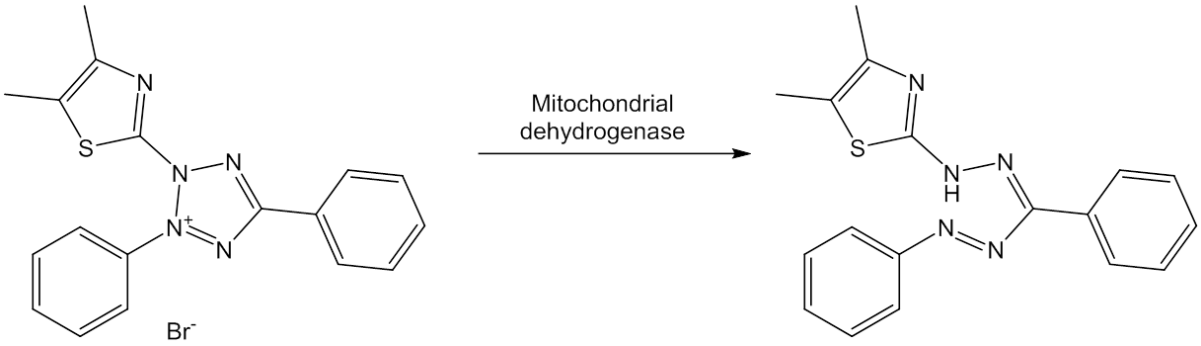

Figure 3.6 Conversion of MTT to insoluble formazan.

4. Results and Discussions

4.1. Oxidation-responsive polymer nanoparticles via thiol-yne click reaction

4.1.1. Synthesis of oxidation responsive polysulifides via thiol-yne click polymerization

Six linear polymers were synthesized via the thiol-yne reaction, employing two different alkynes (4-pentynoic acid with hydrophilic carboxyl group and hydrophobic 1–pentyne) and four different dithiols (Figure 4.1). An equimolar mixture of an alkyne with one of the dithiols in THF was irradiated with UV light (365 nm, 80mW/cm^2) for 2 hours followed by purification and characterization of the solid residue by NMR and Raman Spectroscopy.

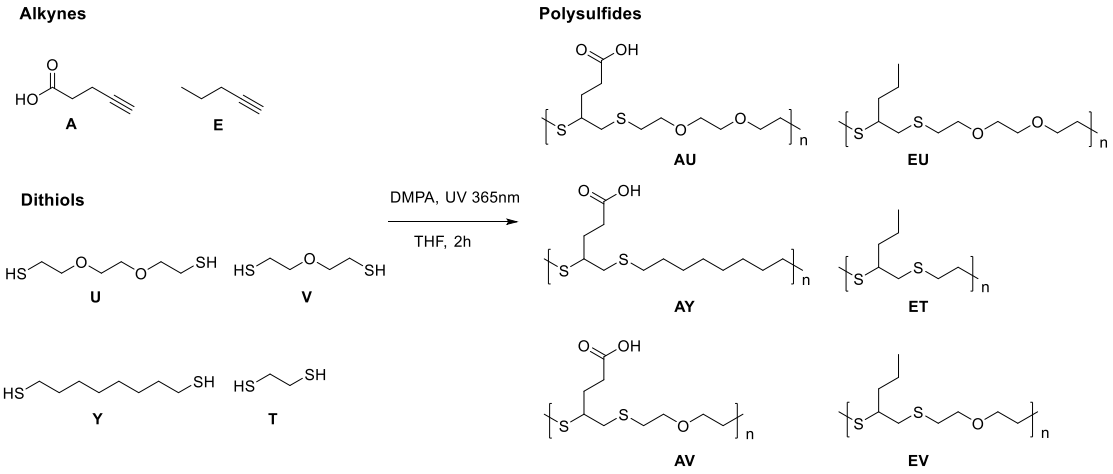

Figure 4.1 Thiol-yne click polymerization, reagents used and polymers formed.

4.1.2. NMR and Raman characterization of oxidation responsive polysulifides

^{1}HNMR spectra of all six polymers are shown in (Appendix A (a-f)). All measurements were performed in DMSO-d_6 or $CDCl_3$. Chemical shifts (δ) are given in ppm relative to the internal standard tetramethylsilane (TMS, δ = 0.00 ppm). In all cases -HC-S bond formation at 2.8 ppm and disappearance of (≡C-H) alkyne peak at 2.7 ppm were observed.

Monomer conversion was monitored using ^{1}H-NMR spectroscopy. 87 % conversion was obtained after 4 hours for the polymer type AU. During polymerization, the alkyne signal from the 4-pentynoic acid decreased while the peak from S-CH bond increased. Figure 4.2 a shows a first order kinetic plot for the polymerization of polymer AU. Figure 4.2 b shows the change in alkyne (≡C-H) and -HC-S peaks with time. Table 4.1 shows the monomer conversion after 2 hours for all the polymers synthesized.

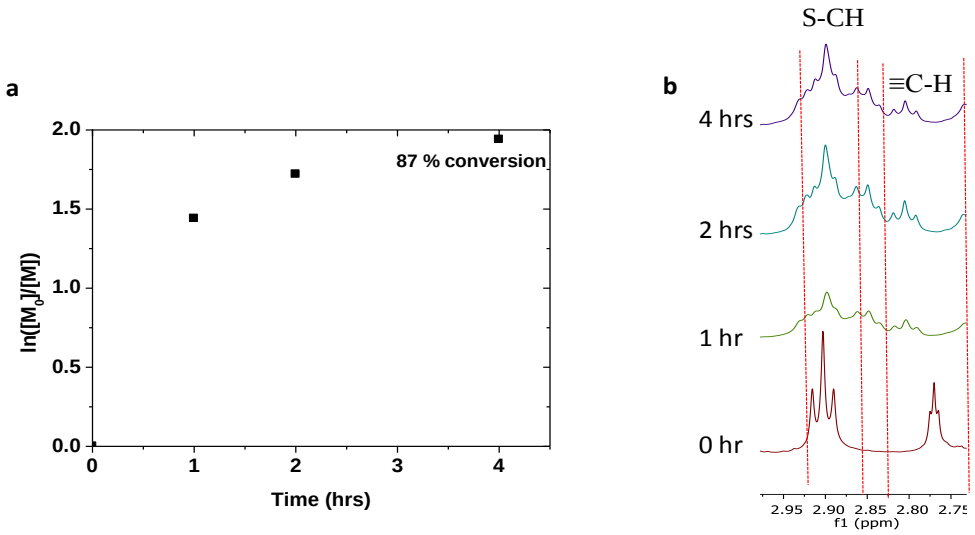

Figure 4.2 a) First order kinetic plot for the polymerization of AU, b) formation and disapperences of polymer and monomer peaks from ^{1}HNMR.

The plot is ln ([M_0]/[M]) (Monomer concentration at 0 time to total monomer concentration) vs time The reaction is observed to be first order [191], after the maximum conversion the ln ([M_0]/[M]) value stabilizes.

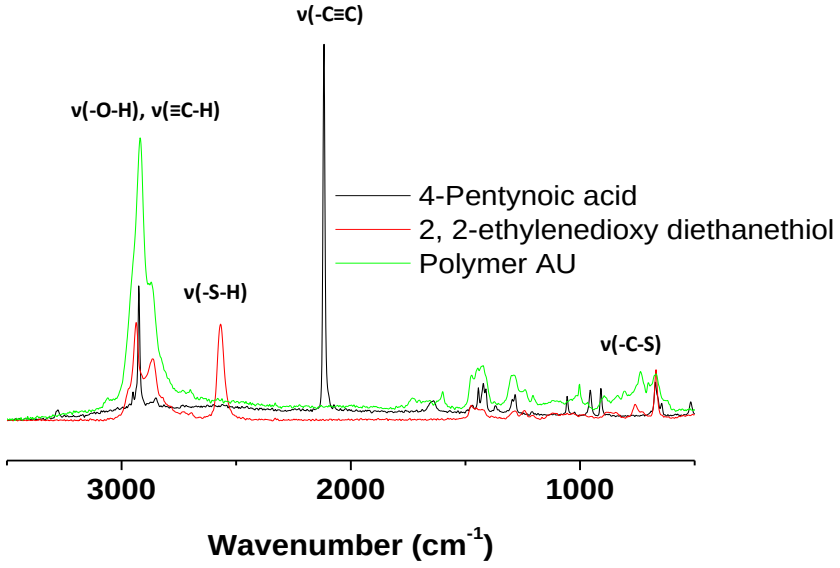

Figure 4.3 Solid state Raman spectroscopy of AU polymer and its monomers.

To further confirm the thiol-yne polymerization, a selected polymer AU was also characterized using Raman spectroscopy. Figure 4.3 shows the disappearance of the terminal alkyne group from 4-pentyonic acid (2117 cm^{-1}) and –S-H groups from dithiol (2568 cm^{-1}), as well as the formation of the C-S aliphatic bond (736 cm^{-1}).

4.1.3. Molecular weight characterization (GPC) of oxidation responsive polysulifides

Out of the eight possible combinations between the utilized alkynes and dithiols, six successfully resulted in polymers with molecular weight ranging between 1400 g/mol and 42700 g/mol according to GPC. Yield of the remaining two polymers (AT and EY) was very low and these compounds were not used in further experiments.

Table 4.1 GPC traces of polysulfide synthesized.

Polymers	M_w[a]	PDI[a]	Conversion[b]	Solubility				
	(g/mol)		(%)	THF	DMSO	H_2O	Ethanol	Acetone
AU	2600	1.2	85	+	+	-	-	-
AV	1400	1.1	88	+	+	-	-	-
AY	8700	1.4	58	+	+	-	-	-
ET	9600	1.8	91	+	+	-	-	-
EU	16200	2.1	80	+	+	-	-	-
EV	42700	3.9	73	+	-	-	-	-

[a] Measured by GPC against polystyrene standards in THF, [b] Measured by ^{1}HNMR, + Soluble – Not soluble

The GPC results show that the reaction of 4-pentynoic acid (A) with the more hydrophilic dithiols (2,2′-(ethylenedioxy)diethanethiol (U) and 2-mercaptoethyl ether (V)) yielded polymers with the lowest molecular weight (AU: M_w=2600 g/mol and AV: M_w=1400 g/mol). However, when a more hydrophobic dithiol was used (1,8-octanedithiol Y), the M_w of the produced polysulfide AY increased to 8700 g/mol. Similar results were reported by Turunc et al.[192] Polymers with higher molecular weights were obtained when 1-pentyne (E) was used as the monomer (Table 4.1). GPC traces of polymers are shown in Figure. 4.4.

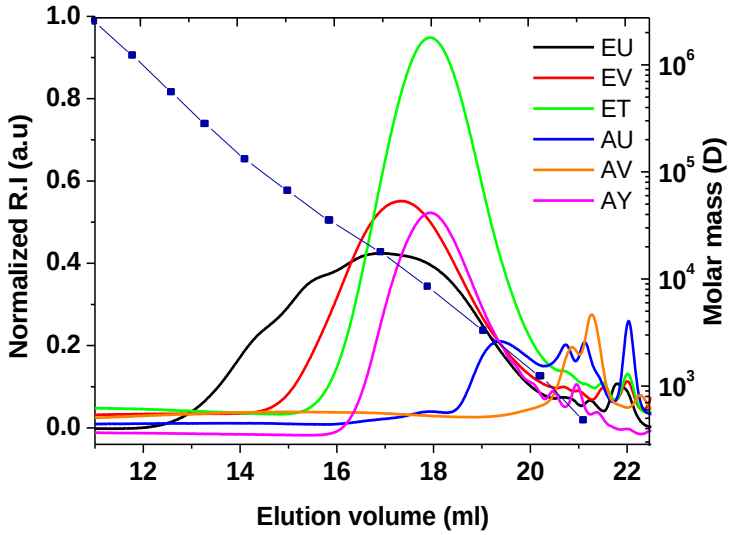

Figure 4.4 GPC trace of the polymers synthesized using thiol-yne click polymerization. Calibration curve polystyrene standards (Polymer Standard Service, MP 474− 2520000 Da).

4.1.4. Preparation of oxidation responsive polysulfide polymeric nanoparticles

A schematic representation of the preparation of oxidation responsive polymeric nanoparticles, drug loading and the process of controlled nanoparticle dissolution leading to the drug release in the presence of H_2O_2, is shown in Figure 4.5. The nanoprecipitation technique described by Schubert et al.[171] was implemented in order to investigate the ability of polysulfides to create nanoparticles in aqueous solution. A first assessment of the particle size of created nanocarriers was performed by DLS measurement (Table 4.2 and Figure 4.6).

The hydrodynamic diameter values revealed that the chemical structure of polymers strongly affects the size of the nanoparticles. Depending on the used polymer, the average particle size ranged from 61.9 to 210 nm.

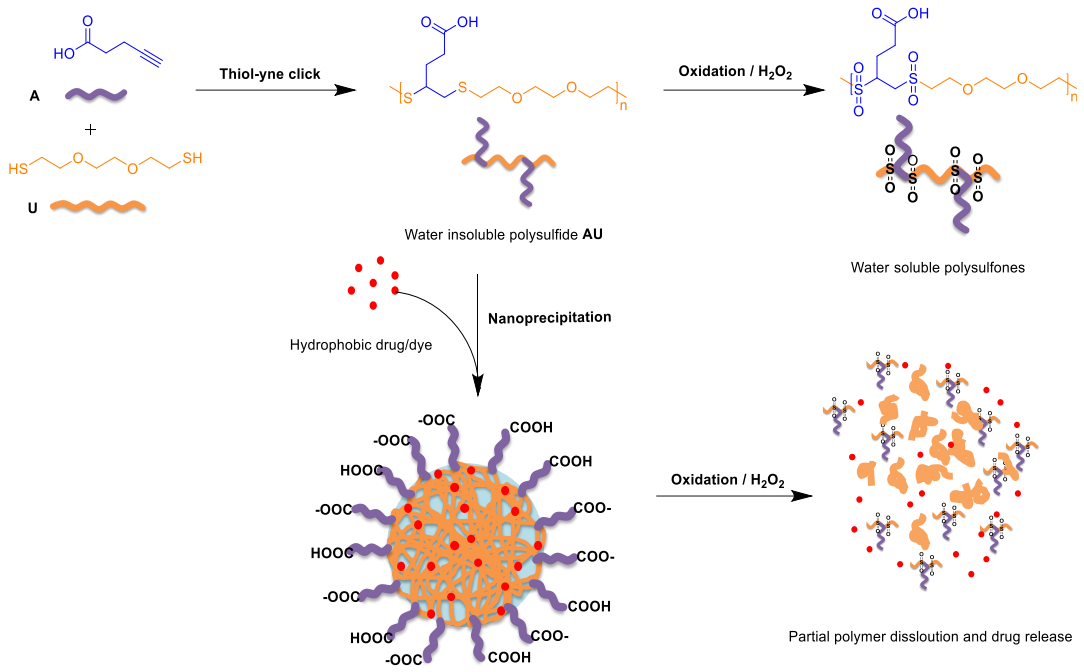

Figure 4.5 Schematic representation of the preparation of oxidation-responsive polymeric nanoparticles, drug loading and the process of controlled nanoparticle dissolution leading to the drug release in the presence of H_2O_2.

Zeta potential value was negative for all polymers and varied from -22 mV for AY to -66.5 mV for EU. The dispersion of nanoparticles obtained from ET was not stable, whereas the dispersion from EV could not be obtained due to its insolubility in DMSO. Scanning electron microscopy (SEM) images of representative AU polymer confirmed the size of created nanoparticles (Figure 4.7).

Table 4.2 DLS measurements of polymeric nanoparticles prepared by nanoprecipitation.

Polymers	Average Particle size, (nm)[a]	Zeta potential (mV)[a]	Notes[a]
AU	122.5 ± 30.5	-30.5 ± 3.6	Stable
AV	210.4 ± 25.8	-27.5 ± 4.1	Stable
AY	61.9 ± 10.1	-22.3 ± 2.7	Stable
ET	-	-	Not stable
EU	94.7 ± 15.1	-66.5 ± 3.4	Stable
EV	-	-	Not soluble in DMSO

[a] Measured by DLS

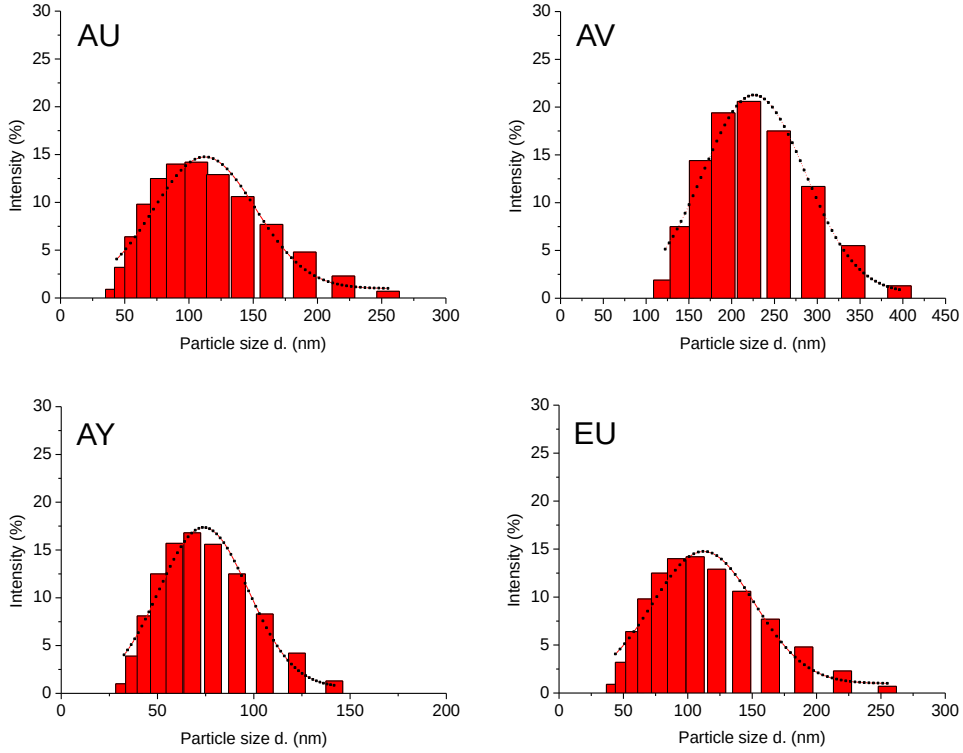

Figure 4.6 Particle size distribution of nanoparticles prepared by nanoprecipitation, measured by DLS.

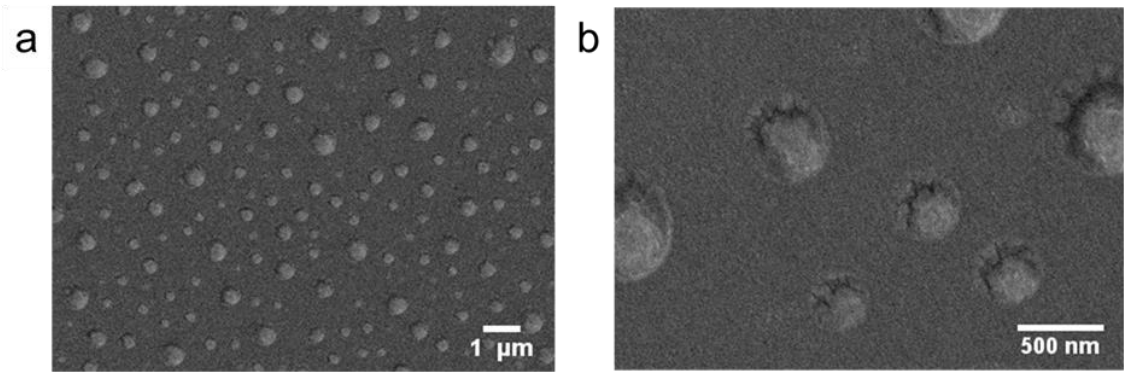

Figure 4.7 SEM images of nanoparticles prepared by the nanoprecipitation method.

In order to compare and find the best method to produce nanoparticles, single emulsion and double emulsion techniques were also used for polymer AU (Table 4.3 and 4.4). The change in particle size as a result of different concentration of PVA was investigated. When the concentration of PVA was raised from 0.05% w/v to 1 % w/v, the particle size showed an increase from 151 nm to 222 nm for single emulsion method and from 158 to 175 nm for double emulsion method.

Table 4.3 DLS measurements of AU polymeric nanoparticles prepared by single emulsion technique.

PVA (%)	Average Particle size, (nm)[a]	Zeta potential (mV)[a]	Notes[c]
0.05	151.5 ± 1.7	-44.5 ± 0.9	Stable
0.1	154.5 ± 0.9	-40.2 ± 0.2	Stable
0.5	205.9 ± 2.4	-26.8 ± 0.9	Stable
1	222.9 ± 2.8	-24.9 ± 0.7	Stable

[a] Measured by DLS

These results indicate that the particle size for nanoparticles obtained by the single and double emulsion techniques is significantly bigger than obtained by the nanoprecipitation method (122 nm). Taking this into account and considering that the degradation kinetics of nanoparticles is faster when using smaller particles, for further investigations the nanoparticles obtained by the nanoprecipitation method were preferred.

Table 4.4 DLS measurements of AU polymeric nanoparticles prepared by double emulsion technique.

PVA (%)	Average Particle size, (nm)[a]	Zeta potential (mV)[a]	Notes[c]
0.05	158.9 ± 2.3	-48.9 ± 3.6	Stable
0.1	153.4 ± 2.9	-37.0 ± 2.9	Stable
0.5	156.9 ± 1.9	-26.9 ± 1.2	Stable
1	175.9 ± 1.9	-20.0 ± 0.6	Stable

[a] Measured by DLS

4.1.5. Nanoparticle degradation induced by oxidation response of polysulfide nanoparticles in aqueous media

After establishing the best method to prepare nanoparticle dispersion, the oxidation responsiveness towards hydrogen peroxide (65 mM) in aqueous media was examined. The

degradation kinetics of the stable nanoparticle dispersion obtained from polymers AU, AV, AY and EU was investigated using DLS (Figure 4.8 a and b).

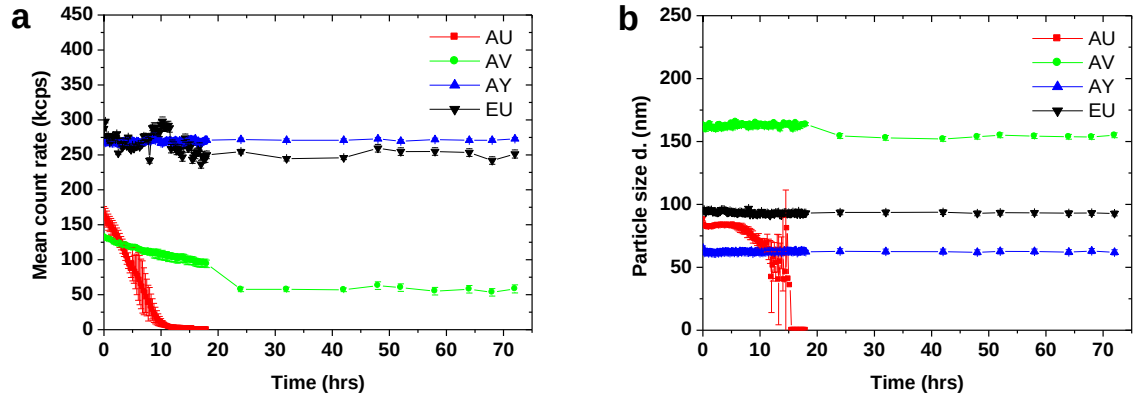

Figure 4.8 DLS data showing the degradation kinetics of various polymeric nanoparticles upon treatment with 65 mM H_2O_2. (a) Change in mean count rate with time. (b) Change of the average particle size d (nm) with time.

Nanoparticles from polymer AU showed the fastest oxidation response and were selected for further experiments. No significant change in particle size or mean count rate was observed for nanoparticles obtained from the other polymers. These results suggest that the hydrophilicity of the monomer repeating units and the molecular weight of the polymer, influence the oxidation response and therefore the degradation kinetics of the nanoparticles.

Subsequently, the degradation of AU polysulfide in the presence of hydrogen peroxide was investigated using ^{1}H-NMR, UV-Vis, DLS and TEM. Figure 4.9 depicts the changes in the ^{1}H-NMR spectra of the AU polymer before and after the treatment with hydrogen peroxide. These results clearly confirmed the oxidation of the polysulfide to the corresponding polysulfoxides, evidenced by the shift downfield (from 2.7 ppm (S-CH_2) to 3.8 ppm (SO_2-CH_2)) of the methylene signal directly bond to the sulfur. The oxidative response of nanoparticle dispersion was also examined using UV-Vis measurements (Figure 4.10). During the process of oxidation, the polymer chain become more hydrophilic and started to dissolve in aqueous solution, causing nanoparticle degradation and hence a reduction in scattered light intensity from the particle suspension.

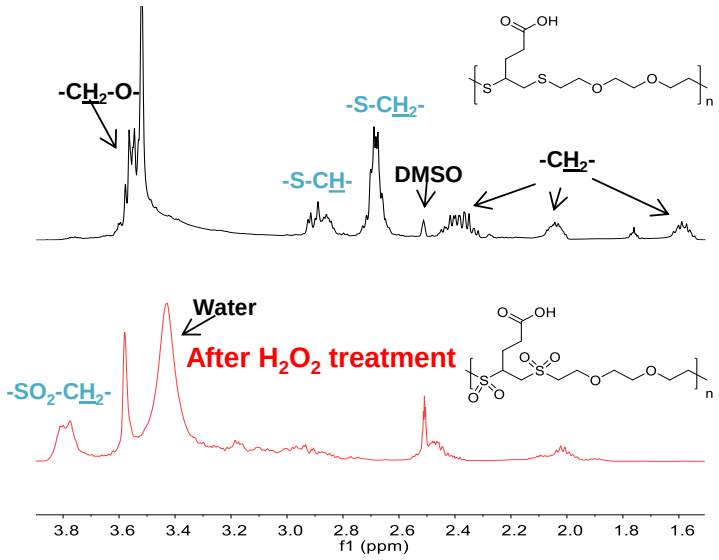

Figure 4.9 Oxidation of native polymer AU in the presence of 1 M hydrogen peroxide.

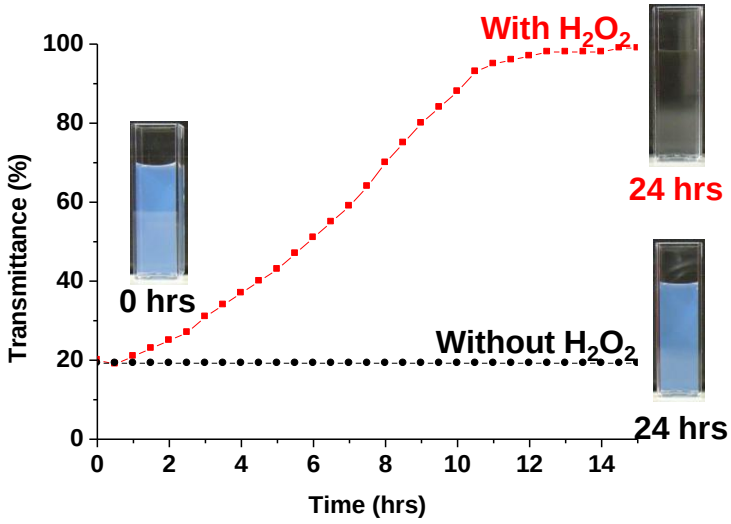

Figure 4.10 Change in % transmittance with respect to time in the presence and absence of hydrogen peroxide.

Nanoparticle suspension in the absence of H_2O_2 showed no change in turbidity even after 24 hours (Figure 4.10). A gradual increase in percentage transmittance, with approximately 99 % transmittance achieved in 12 hours, was noticed for the nanoparticle suspension with 65 mM addition of H_2O_2. Initial transmittance at 0 hour for both, treated and untreated suspensions was identical (20 %). Further experiments with variation in the concentration of H_2O_2 were also conducted. Higher concentration of H_2O_2 (10 %) resulted in a completely

transparent solution within five minutes. When lower concentrations of hydrogen peroxide were used (3 %) the complete transition took less than six hours. The changes in mean count rate of nanoparticle dispersion was monitored using DLS, which displays a sudden decrease in mean count rate with increase in the concentration of hydrogen peroxide. (Figure 4.11)

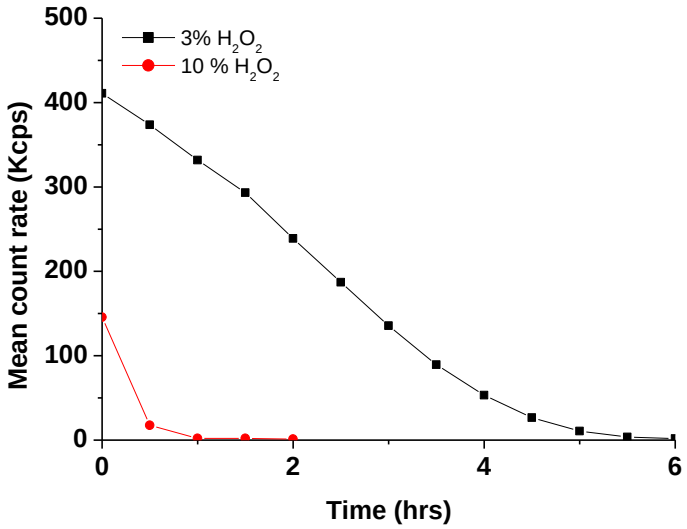

Figure 4.11 *Degradation kinetics and change in mean count rate (kcps) of AU polymeric nanoparticle suspension (0.5 mg/ml) in water: in the presence of 3 and 10 % H_2O_2.*

The initial particle size distribution of AU polymeric nanoparticles suspension (0.5 mg/ml) in water is shown in Figure 4.12a. In the absence of hydrogen peroxide, there was no significant change in the average diameter or mean count rate over a period of 15 hours measured by DLS. Figure 4.12b shows the change in particle size distribution and degradation kinetics over a period of 15 hours in the presence of 65 mM hydrogen peroxide, clearly confirming the degradation of nanoparticles. A large population of small particles with hydrodynamic values between 10 and 25 nm is evident in the DLS plot after 14 hours of treatment with H_2O_2. Initial mean count rate decreased from approximately 160 kilocounts per second (kcps) to less than 30 kcps within 8 hours. The decrease in mean count rate is caused by both, the sedimentation and the degradation of AU polymeric nanoparticles under oxidative environment.

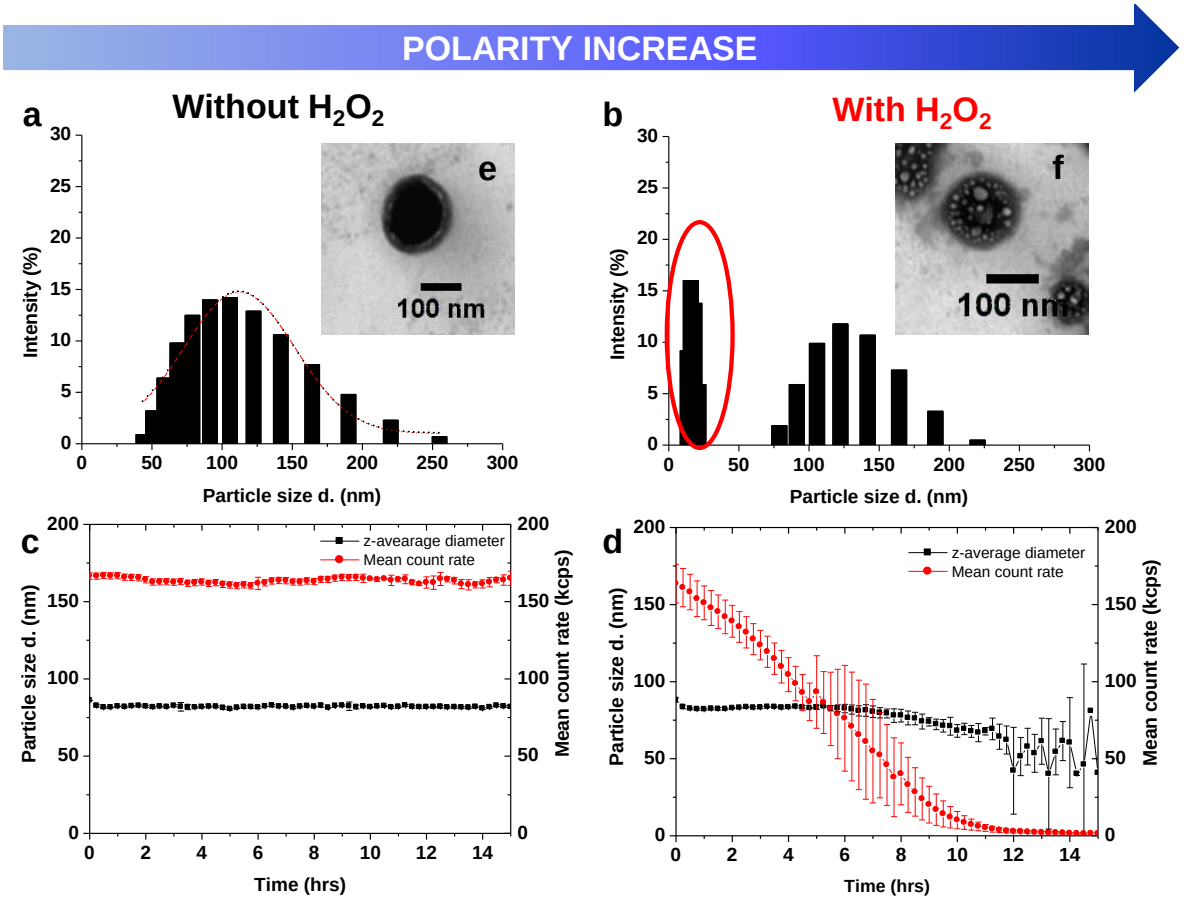

Figure 4.12 Particle size distribution (DLS) a) in the absence and b) in the presence of H_2O_2. Change in average diameter and mean count rate (DLS) c) in the absence d) in the presence of H_2O_2. TEM images e) before and f) after H_2O_2 treatment.

Transmission electron microscopy data was consistent with the results obtained by DLS analysis. Well-defined nanoparticles were observed for the AU polymer with an average diameter of 130 nm. Furthermore, TEM revealed that the particle morphology changed after H_2O_2 addition. Pore like structures with the diameter ranging from 10 to 30 nm could be observed on the surface of nanoparticles treated with H_2O_2 as a result of polymer oxidation (Figure 4.12 e and f).

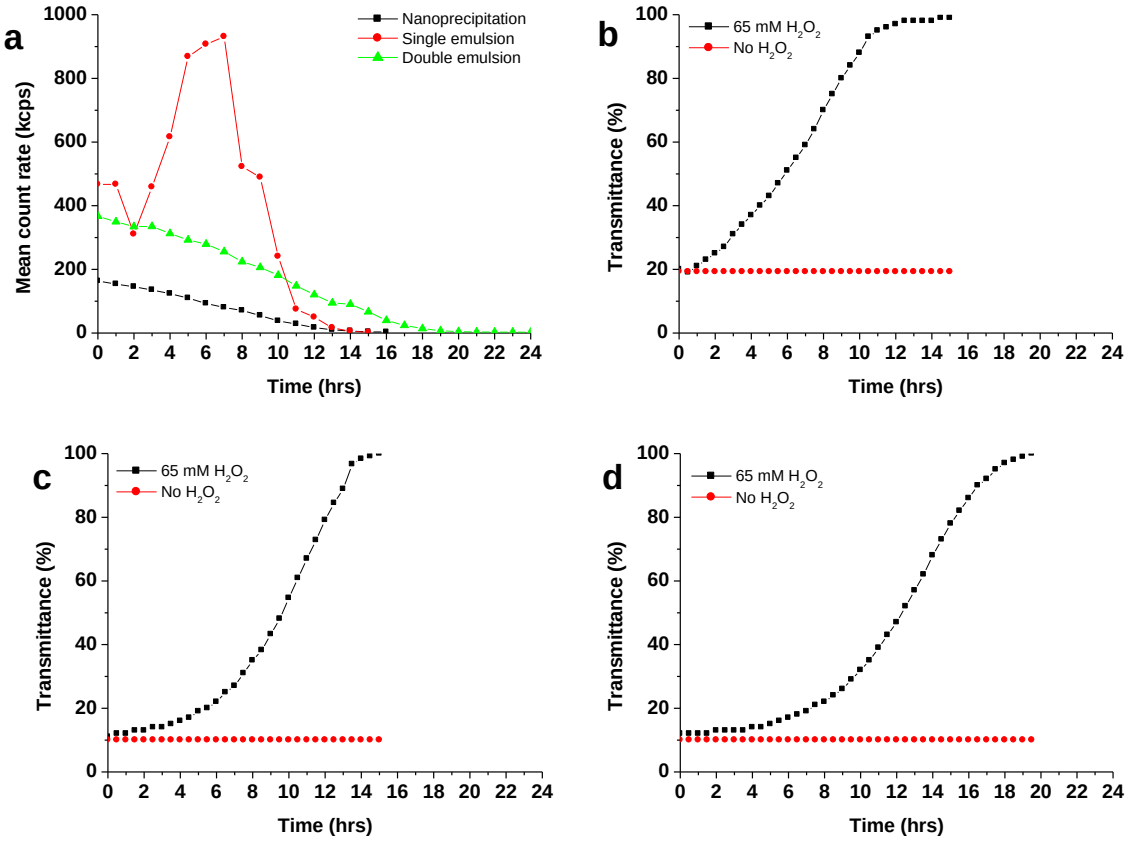

Figure 4.13 (a) Degradation kinetics and change in mean count rate (kcps) of AU nanoparticles prepared by various methods: nanoprecipitation (NP) single emulsion (SE) and double emulsion (DE) upon treatment with 65 mM H_2O_2 measured by DLS. Change in turbidity, in the presence and absence of H_2O_2 for nanoparticles prepared by (b) nanoprecipitation, (c) single emulsion and (d) double emulsion measured by UV-Vis spectrometry.

Degradation kinetics of AU polymeric nanoparticles prepared by single and double emulsion techniques in the presence of 65 mM hydrogen peroxide was also measured by DLS. The nanoparticles prepared by double emulsion showed a slower degradation compared to those prepared by single emulsion and nanoprecipitation techniques (Figure 4.13).

4.1.6. Encapsulation efficiency

Polymer AU showed the fastest oxidation response to hydrogen peroxide and therefore was chosen to investigate the creation of a stimuli-responsive drug delivery system. According to Blanco et al. and Hans et al., the encapsulation efficiency of nanoparticles depends on the molecular weight and concentration of the polymer used to create the nanoparticles dispersion [40, 41]. Nile Red is a hydrophobic dye used frequently as a model to investigate

the encapsulation efficiency and kinetics of dye release. Nile Red is known to be fluorescent in a hydrophobic environment; however a decrease in the fluorescence is observed when it is released into water.[193] In this case, the Nile Red encapsulation efficiency determined by fluorescence spectroscopy and was 32%. The calibration curve is shown in appendix Da. The low efficiency can be attributed to the low molecular weight of the polymer AU.

4.1.7. Release of encapsulated Nile Red.

Suspensions of polymer nanoparticles (0.5 mg/ml) with encapsulated Nile Red dye were prepared in PBS buffer (pH 7.4), and treated with 65 mM of H_2O_2. Fluorescence spectrometry was used to observe the release kinetics over a period of 15 hours. Figure 4.14. a and b show the gradual reduction in fluorescence intensity from 100 % to less than 20 % after 12 hours, in contrast to the almost invariable fluorescence intensity observed in control sample without H_2O_2 (Figure 4.14 a and c). These results indicate that the release of Nile Red due to the oxidative degradation of nanoparticles is indeed taking place, causing a change in its hydrophilicity and a reduction of the fluorescence intensity throughout time.

Physiological and pathological concentration of reactive oxygen species such as hydrogen peroxides in cellular levels are in the order of micromolar.[194] Therefore, in following experiments the concentration of hydrogen peroxide was reduced to biologically relevant levels. By this manner, 100 ug/ml of Nile red encapsulated inside AU nanoparticles (pH 7.4 PBS buffer) were treated with varied concentrations of H_2O_2 (0, 50, 200 and 500 μM). Figure 4.14 d shows a 50% decrease in the fluorescence intensity after ~ 100 hours of treatment when 50 μM of H_2O_2 was employed. This outcome clearly validates the effectiveness of controlled release from nanoparticles created from polysulfide AU in diluted concentrations of H_2O_2. To the best of our knowledge, this is the first time that the degradation of a polysulfide at a pathological concentration level of H_2O_2 has been demonstrated.

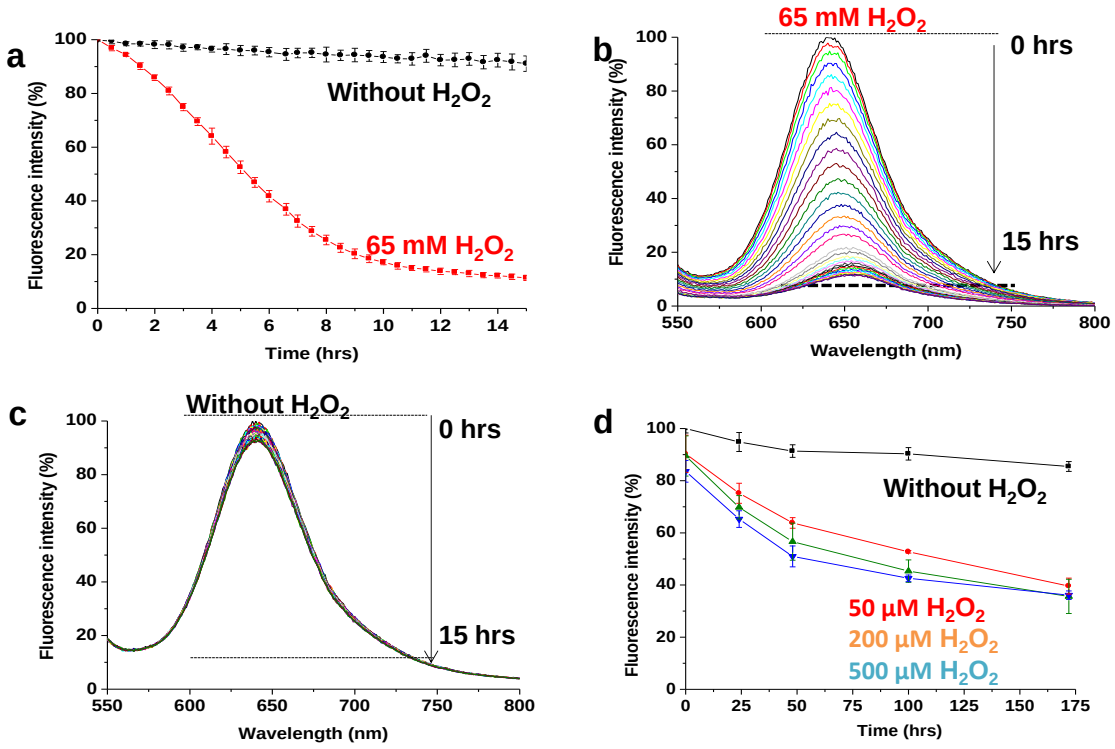

4.14 a) Change in fluorescence intensity (at 620 nm) of Nile Red encapsulated AU nanoparticles in the presence and in the absence of H_2O_2 (65 mM). The decrease of fluorescence corresponds to the release of the dye from the apolar particles to the polar aqueous solution. (b,c) Corresponding fluorescence spectra of solutions of Nile Red encapsulated AU nanoparticles with and without H_2O_2. (d) Release profiles of Nile red encapsulated AU nanoparticles (500 µg/ml) with various pathologically relevant concentrations of H_2O_2: 0 µM (black square), 50 µM (red circle), 200 µM (green up triangle), 500 µM (blue down triangle).

4.1.8. Cell viability-MTT assay

The cytotoxicity and cell viability of the created polymeric nanoparticles was evaluated using the MTT test. The assay was performed using AU polymeric nanoparticles in a range of 0.1 - 2.0 mg/ml. After 24h of contact with HeLa cells at 1.0 mg/ml nanoparticle concentration only a decrease of 20 % in cell viability was observed (Figure 4.15a). In the case of HUVEC there was a decrease of 18% cell viability. In both the cases the AU polymeric nanoparticle showed less toxicity. (Figure 4.15b).

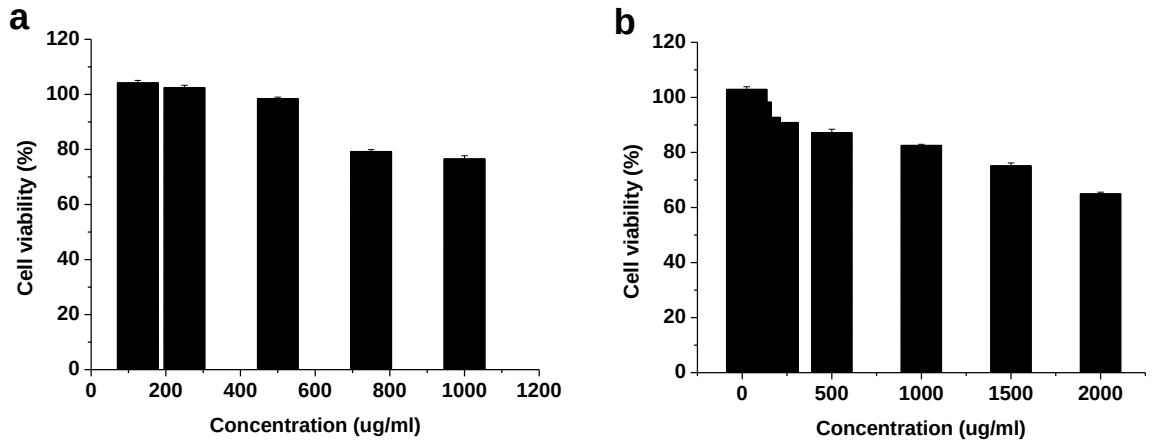

Figure 4.15 MTT assay-cell viability of free AU polymeric nanoparticles a) Hela cells b) HUVEC cells.

4.1.9. Cellular uptake

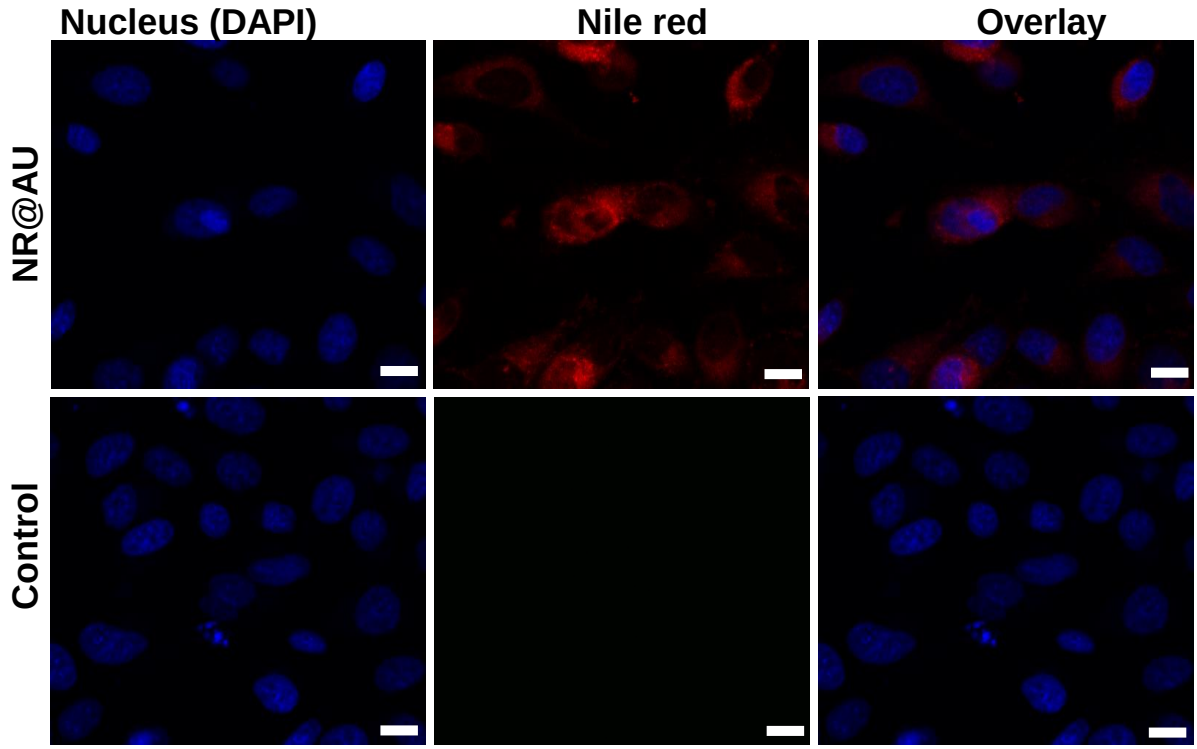

Figure 4.16 CSLM images of Hela cells treated with Nile Red encapsulated inside AU polymeric nanoparticles for 24 hrs at 37^0C. The images from left to right show: experiments with DAPI staining (blue), Nile Red staining (red) and the overlays of both images. The scale bars are 20 μm. The control experiment was performed without Nile Red addition.

In order to have a clear insight on how the polymeric nanoparticles interact with cells, cellular uptake studies were also performed on HeLa cell lines. The cellular uptake of polymeric nanoparticles with encapsulated Nile Red was monitored using confocal laser scanning microscopy (CLSM). Figure 4.16 shows the comparison of 50 μg/ml Nile Red@AU nanoparticle cellular uptake as well as the control experiments (without Nile Red). HeLa cell lines were stained with 4',6-diamidino-2-phenylindole (DAPI). In the control experiment the characteristic red fluorescence is not visible. In the samples with Nile Red, there is a clear evidence of particle internalisation due to endocytosis, and uniform distribution of Nile Red@AU nanoparticle can be observed in the cytoplasm.

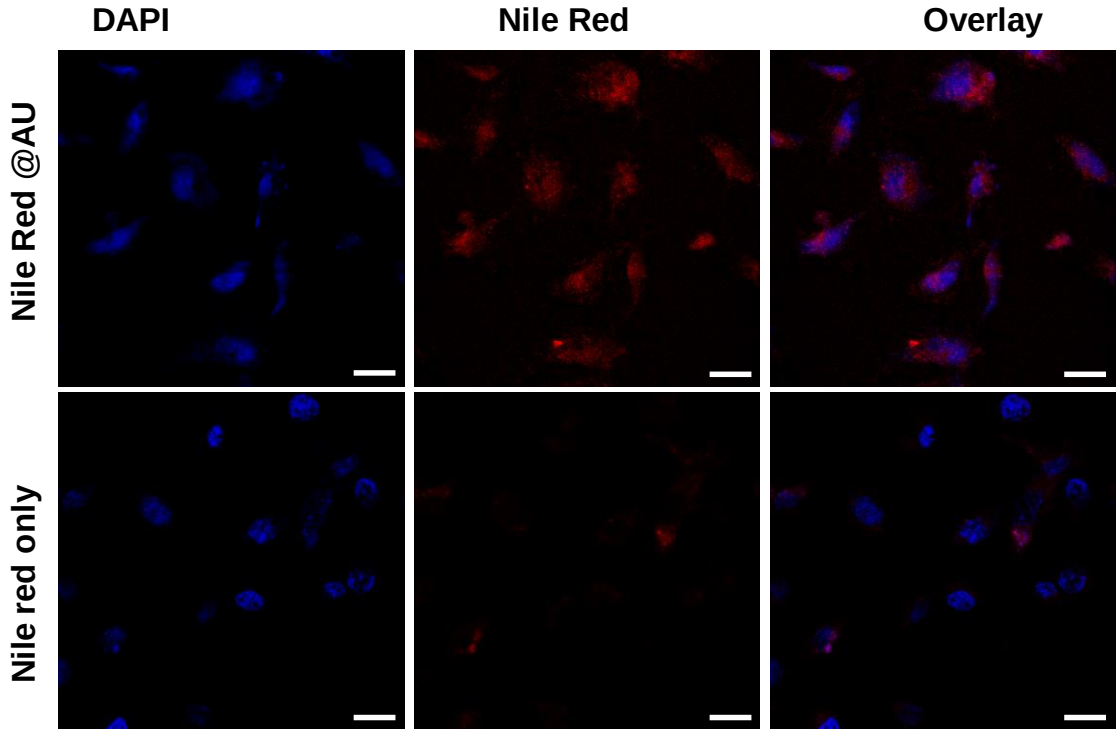

4.17 CSLM images of HUVECs treated with Nile Red encapsulated inside AU polymeric nanoparticles for 24 hrs at 37^0C. The images from left to right show: experiments with DAPI staining (blue), Nile Red staining (red) and the overlays of both images. The scale bars are 20 μm. The control experiment was performed with only Nile Red addition.

Similar experiments were also done using HUVECs. Figure 4.17 shows the comparison of 50 μg/ml Nile Red@AU nanoparticle cellular uptake as well as the control experiments (with Nile Red). HUVECs cell lines were stained with 4',6-diamidino-2-phenylindole (DAPI). In the control experiment the characteristic red fluorescence is not as prominent as that of the of Nile Red@AU nanoparticle. In the samples Nile Red@AU, there is a clear evidence of

particle internalisation due to endocytosis, and uniform distribution of Nile Red@AU nanoparticle can be observed in the cytoplasm.

4.1.10. General conclusion

The successful synthesis of novel hydrogen peroxide-responsive linear polysulfides by applying the thiol-yne click polymerization reaction was herein reported. Dispersions of stable polymeric nanoparticles were efficiently prepared by nanoprecipitation, and single and double emulsion techniques. These nanoparticles are sensitive towards biologically relevant low concentration of oxidising agents such as hydrogen peroxide, and have the potential to be applied in the control release of hydrophobic and hydrophilic drugs. It was demonstrated that, when polymers with a low molecular mass were used, the oxidation time and the required amount of hydrogen peroxide decrease, making them quickly soluble in aqueous solutions. Moreover, it was also showed that small size of nanoparticles (> 250 nm) improves efficient cellular uptake, turning these new structures into promising oxidation-responsive molecular cargos.

4.2.Synthesis of oxidation responsive poly(β-hydroxy thioether)s via thiol-epoxide ring opening polymerization

Thiol-epoxide ring opening polymerization is a relatively new method for the synthesis of functional materials. A new class of polymers, poly(β-hydroxy thioether) was synthesized using a base catalyzed ring opening of epoxides in presence of thiols.[195] This approach utilizes the nucleophilic characteristics of thiols and the ring strain of epoxides. This method also facilitates an easy and quick way to generate linear polymers with hydroxyl substitution. Post modification of these polymers can be carried out by using appropriate and reactive functional groups.

Here a modified synthetic approach for the synthesis of linear poly(β-hydroxy thioether) is reported. Five different linear poly(β-hydroxy thioether)s were synthesized using a combination of one diepoxide (neopentyl glycol diglycidyl ether) and five different dithiols. Figure 4.18, shows monomers, reagents and polymers synthesized by thiol-epoxide ring opening reaction. In all the cases the monomer ratio was fixed to be 1:1. The monomer conversion after 2 hours is reported in Table 4.5. Synthesized polymers were designated as EP1, EP2, EP4, EP5 and EP6. Obtained polymers are viscous in appearance and soluble in organic solvents such as THF, acetone ethanol and chloroform (Table 4.5).

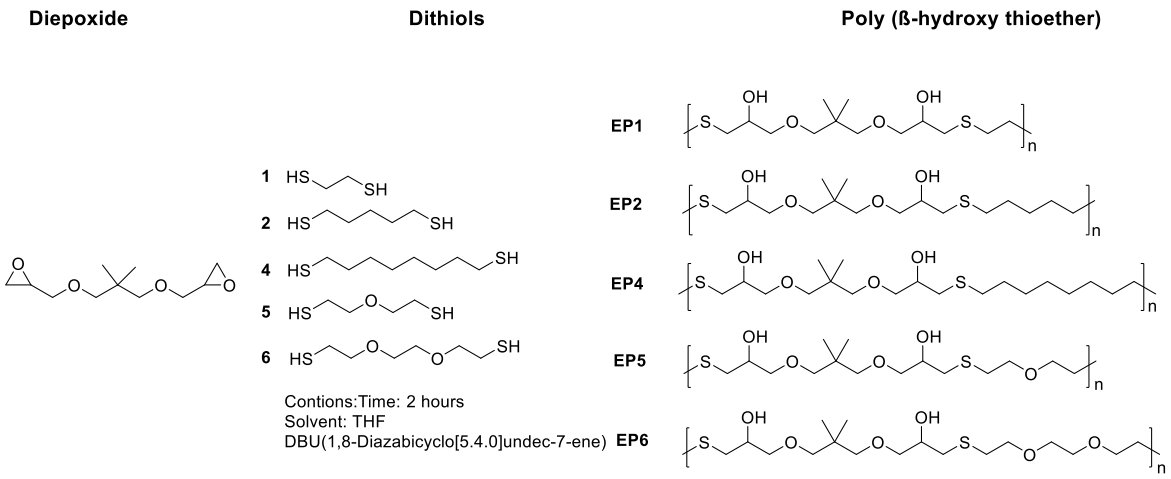

Figure 4.18 Structure of monomers used and different poly(β-hydroxy thioether) formed.

4.2.1. [1]HNMR and Raman characterization of oxidation responsive poly(β-hydroxy thioether)s

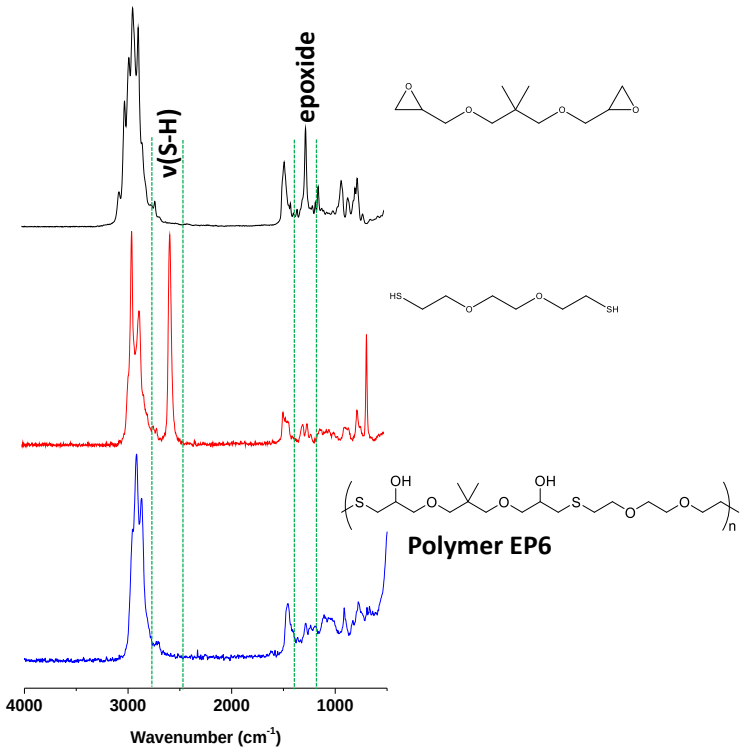

Figure 4.19 Solid state Raman spectroscopy of EP6 polymer and its monomers.

[1]H-NMR spectra of all five polymers are shown in (Appendix B (a-e)). All spectra were acquired in $CDCl_3$. Chemical shifts (δ) are given in ppm relative to the internal standard

tetramethylsilane (TMS, δ = 0.00 ppm). In all the cases the -HC-S bond formation at 3.93 ppm and disappearance of epoxide peaks (-CH_2) at 2.58 ppm were observed. The monomer conversion is also reported in the Table 4.5. To further confirm the thiol-epoxide polymerization, a selected polymer EP6 was also characterized using Raman spectroscopy. Figure 4.19 shows the disappearance of the epoxide peak (1250 cm^{-1}) and the terminal -SH group from dithiol (2568 cm^{-1}).

4.2.2. Molecular weight characterization (GPC) of oxidation responsive poly(β-hydroxy thioether)s

The GPC results show (Table 4.5, Figure 4.20) that synthesised polymers have average molecular weight M_w in the range between 4800 and 8900 g/ mol. The poly dispersity index (PDI) value was between 1.7 and 1.9.

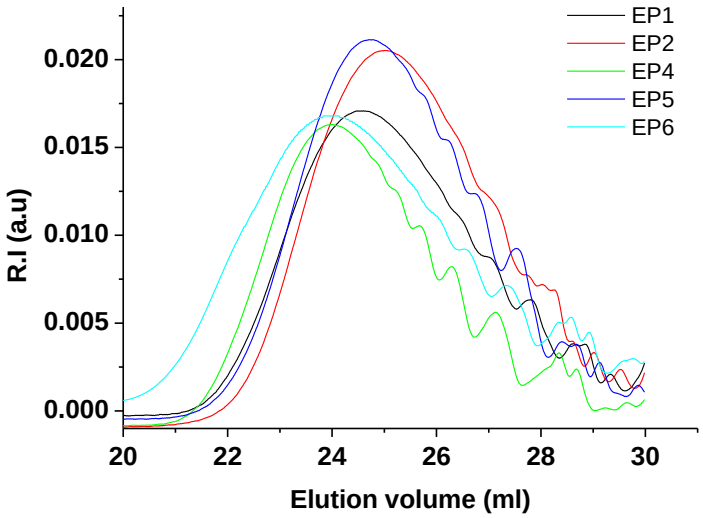

Figure 4.20 GPC of various poly(β-hydroxy thioether)s synthesized by thiol-epoxide ring opening polymerization. Calibration curve polystyrene standards (Polymer Standard Service, MP 474− 2520000 Da).

Table 4.5 GPC traces of various poly(β-hydroxy thioether)s.

Polymers	M_w[a] (g/mol)	PDI[a]	Conversion[b] (%)	Solubility				
				THF	DMSO	H_2O	Ethanol	Acetone
EP1	5.8	1.8	94	+	+	-	+	+
EP2	4.8	1.7	60	+	+	-	+	+
EP4	7.3	1.8	66	+	+	-	+	+
EP5	5.4	1.7	88	+	+	-	+	+
EP6	8.9	1.9	89	+	+	-	+	+

[a] Measured by GPC against polystyrene standards in THF, [b] Measured by ^{1}H-NMR, + Soluble – Not soluble

4.2.3. Preparation of oxidation responsive poly(β-hydroxy thioether)s nanoparticles

All five poly(β-hydroxy thioether)s were employed to prepare nanoparticles dispersion by nanoprecipitation.

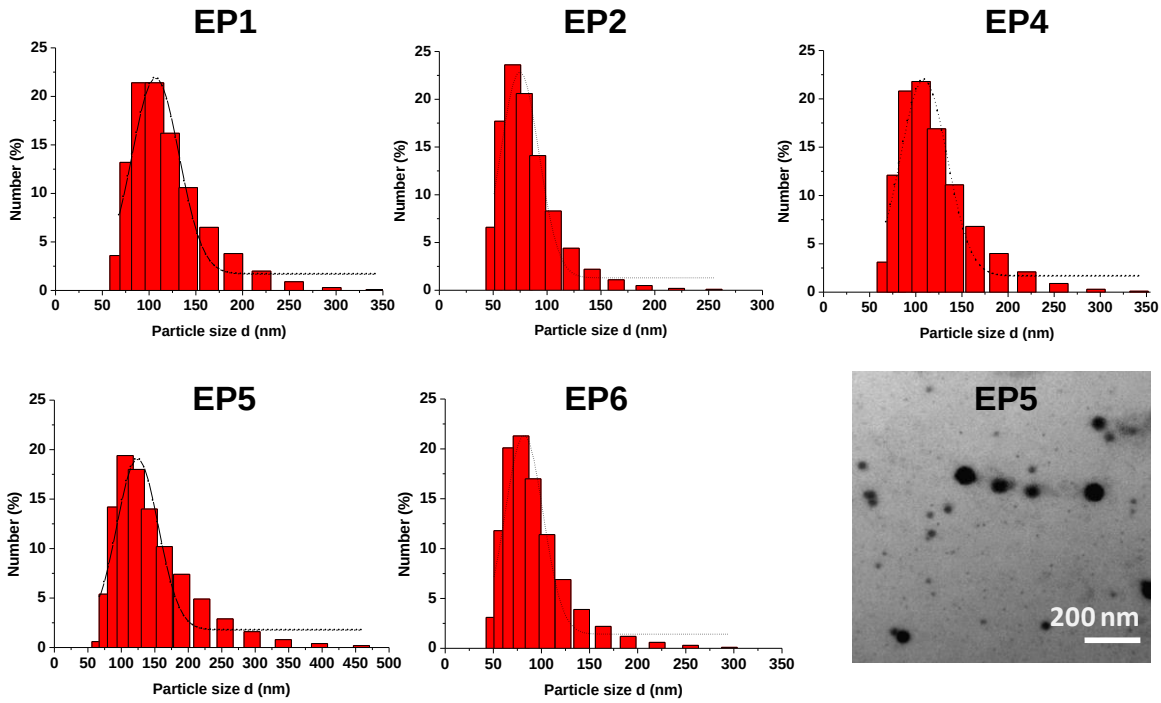

Figure 4.21 Particle size distribution of poly(β-hydroxy thioether) nanoparticles prepared by nanoprecipitation, measured by DLS.

The poly(β-hydroxy thioether)s were dissolved in acetone and added to MilliQ water. The stirring was kept at 1000 rpm and the particle formation at the interface was observed with a

change in solution turbidity. The obtained nanoparticles solution was allowed to stir for an additional six hours to evaporate acetone from the solution. The nanoparticles solution was further dialyzed against water using cellulose membrane dialysis tube to remove the impurities, further the particle solution was pre concentrated by centrifugation. The particle solutions showed good stability for 6-8 weeks without any significant change in particle size and zeta potential measured by DLS, over a period of time (Table 4.6). The number average particle size was between 110 and 195 nm with zeta potential values between -25 and -35 mV. The particle size distrubtion of various poly(β-hydroxy thioether) nanoparticles is shown in Figure 4.21. TEM image of EP5 nanoparticles are also shown in the Figure 4.21. which confirms the presence of spherical nanoparticles and in accordance with the DLS datas.

Table 4.6 DLS measurements of poly(β-hydroxy thioether) nanoparticles prepared by nanoprecipitation.

Polymers	Average particle size, DLS (nm)[a]	Zeta potential, DLS (mV)[a]	Nanoparticle stability[b]
EP 1	151.3± 6.5	-32.0 ± 4.8	Stable
EP 2	115.7 ± 4.0	-34.5 ± 2.6	Stable
EP 4	145.4 ± 5.4	-31.4 ± 3.7	Stable
EP 5	192.6± 2.5	-27.7± 2.0	Stable
EP 6	142.9 ±8.3	-26.5 ± 3.4	Stable

[a, b] Measured by DLS.

The EP5 polymer was selected and polymeric nanoparticles were also prepared using single emulsion and double emulsion techniques. (Table 4.7 and 4.8). The change in particle size as a result of different concentration of PVA was investigated. When the concentration of PVA was raised from 0.05% w/v to 1 % w/v, the particle size showed decrease from 251.5 ± 18.8 nm to 202.8 ± 6.5 nm for single emulsion method. The decrease in particle size is usually attributed to the presence of higher concentration of the surfactant which makes the nanoparticle stable; the zeta potential showed an increase in value and the highest zeta potential value -18.6 ± 7.4 was obtained for the smallest nanoparticle.

Table 4.7 DLS measurements of EP5 polymeric nanoparticles prepared by single emulsion technique.

PVA (%)	Average Particle size, (nm)[a]	Zeta potential (mV)[a]	Notes[a]
0.05	251.5 ± 18.8	-11.9 ± 2.8	Stable
0.1	225.5 ± 15.4	-15.3 ± 5.6	Stable
0.5	217.9 ± 10.5	-16.8 ± 5.0	Stable
1	202.8 ± 6.5	-18.6 ± 7.4	Stable

[a] Measured by DLS

Double emulsion nanoparticles were prepared as described earlier. The smallest value of average particle size 98.8 ± 3.5 was obtained for nanoparticles prepared with the highest concentration of PVA (1% w/v). An increasing trend in average particle size was seen when the concentration of PVA was reduced.

Table 4.8 DLS measurements of EP5 polymeric nanoparticles prepared by double emulsion technique.

PVA (%)	Average Particle size, (nm)[a]	Zeta potential (mV)[a]	Notes[a]
0.05	173.7 ± 14.3	-6.6 ± 2.8	Stable
0.1	107.9 ± 6.8	-10.4 ± 2.8	Stable
0.5	110.8 ± 4.0	-10.8 ± 2.5	Stable
1	98.8 ± 3.5	-12.5 ± 0.5	Stable

[a] Measured by DLS

These results also indicate that the zeta potential for nanoparticles obtained by single and double emulsion techniques was significantly lower than that obtained by the nanoprecipitation method. Taking this into account and considering that degradation kinetics and nanoparticle stability, for further investigations the nanoparticles obtained by the nanoprecipitation method were preferred.

4.2.4. Nanoparticle degradation oxidation response of poly(β-hydroxy thioether) nanoparticles in aqueous media

Further experiments with different concentrations of H_2O_2 were performed. 50, 100, 200 and 500 mM concentration of H_2O_2 was used to study the kinetics of nanoparticles degradation using DLS technique. When lower concentration (50 mM) of H_2O_2 was used, the complete transition took more than 36 hours. The change in the mean count rate and the average particle size of nanoparticles dispersion was monitored. The sudden decrease of the mean count rate and the particle size was observed for increasing H_2O_2 concentrations. (Figure 4.22 a and b).

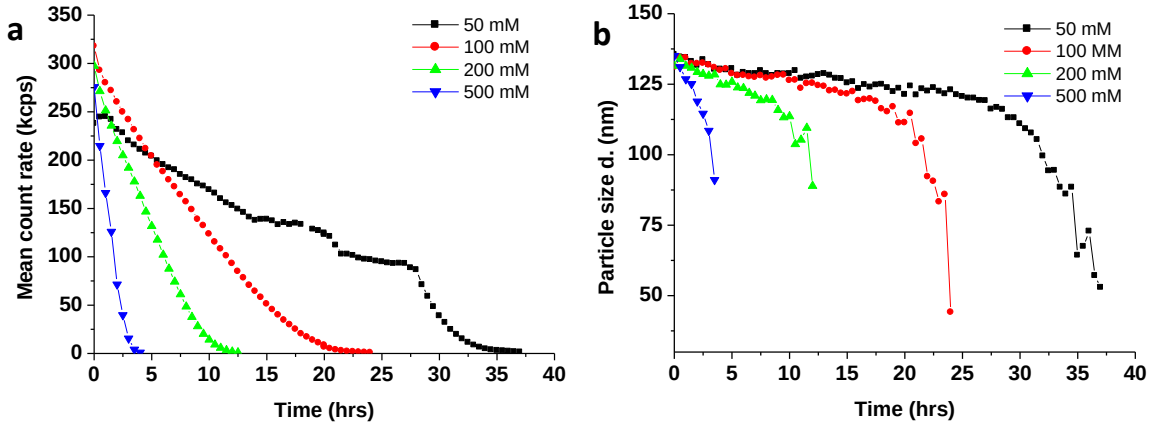

Figure 4.22 Degradation kinetics, change in a) mean count rate and b) average paticle size for EP5 nanoparticle suspension with various concentration of hydrogen peroxide.

When lower concentration of H_2O_2 was used, the degradation was much slower. The transition was more visible with an abrupt change in mean count rate after 20 hours due to prolonged exposure, as seen in figure 4.22 a.

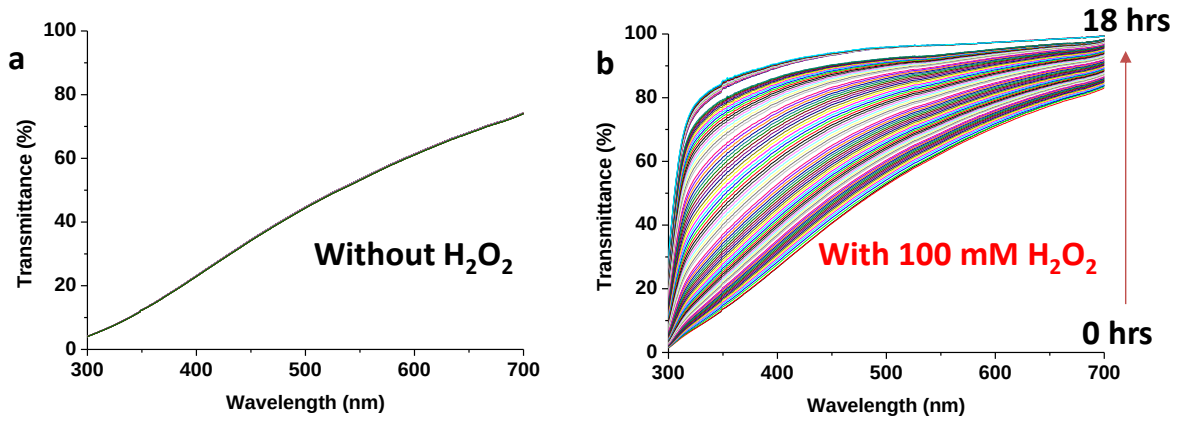

Figure 4.23 Change in % transmittance with respect to time in the a) absence and b) presence of 100 mM hydrogen peroxide.

The nanoparticles suspension in the absence of H_2O_2 showed no change in turbidity even after 24 hours (Figure 4.23 a). A gradual increase in percentage transmittance, with approximately 99% transmittance achieved in 18 hours, was noticed for the nanoparticle suspension with the 100 mM addition of H_2O_2 (Figure 4.24 b). Initial transmittance at 0 hour for both, treated and untreated suspensions was identical (20 %) at 400 nm.

4.2.5. Nile Red encapsulated in poly(β-hydroxy thioether) nanoparticles

Nanoparticles with Nile Red were prepared in a similar way as described earlier in chapter 4.1.4. 10 mg of synthesized polymers and 0.1 mg of Nile Red was dissolved in 1 ml of acetone. The solution was stirred for 3.5 hours, and finally added to 9 ml of MilliQ water under magnetic stirring (1000 rpm). Next, the solution was allowed to stir for six hours to evaporate the organic solvent. Nanoparticles were separated using cellulose membrane dialysis tube (MWCO 14,000 Da) and further pre concentrated by centrifugation for 15 minutes at 9500 g.

4.2.6. Encapsulation efficiency

Encapsulation efficiency is one of the most important parameters in drug delivery applications. The nanoparticle suspension with Nile Red was first centrifuged at 9500 g for 15 mins and than the supernatant was removed. Next, nanoparticles were further resuspended in Milli-Q water and again centrifuged at 9500 g for 15 mins. The final precipitate was dissolved in acetone and the fluroscence or absorbance measurement was used to determine the encapsulation efficiency. Standard calibration curve for Nile Red in acetone is shown in

appendix D. Encapsulation efficiency for the poly(β-hydroxy thioether) nanoparticles were found to be between 30- 50 %.

4.2.7. Nile Red release and degradation kinetics of poly(β-hydroxy thioether) nanoparticles

To investigate the oxidation sensitivity of all the five poly(β-hydroxy thioether) nanoparticle prepared. Nile red encapsulated nanoparticle suspension was treated with 100 mM of H_2O_2. The release kinetic was monitored over a period of 16 hours. From the Figure 4.24 it is obivious that the release was faster from EP 5 and EP 6 nanoparticles compared to other nanoparticles investigated. Nile red fluorescence was reduced to less than 5 % for both EP 5 and EP 6. EP 4 synthesised from 1,8-octanedithiol monomer, showed the slowest release kinetics compared with other polymers, only 54 % Nile red fluorescence was observed after 16 hours. EP 2 and EP 1 showed around 11 % Nile red fluorescence after 16 hours of H_2O_2 treatment.

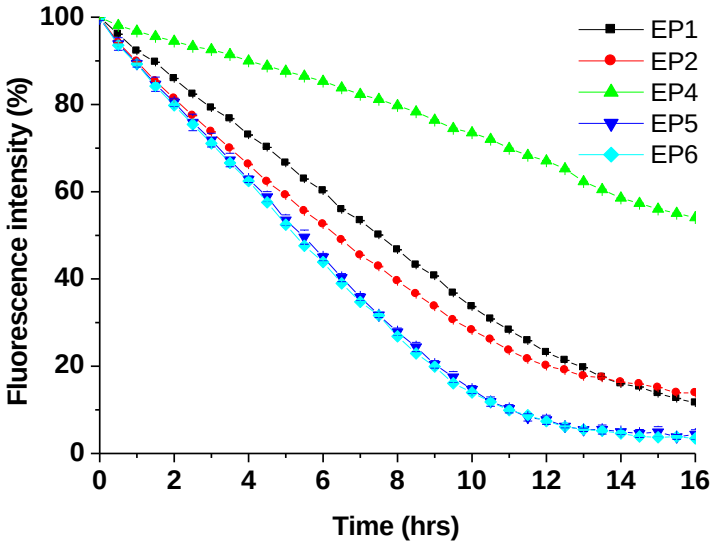

4.24 Change in fluorescence intensity (at 620 nm) of Nile Red encapsulated EP5 nanoparticles in the presence and in the absence of various concentrations of H_2O_2 (100mM).

The release of Nile Red from poly(β-hydroxy thioether) nanoparticles induced by H_2O_2 was monintored by fluorescence spectroscopy. Compared to polysulfide nanoparticles, poly(β-hydroxy thioether)s showed slower response to oxidating agent. Figure 4.25 a shows the release of Nile Red from EP5 nanoparticles with various concentration of H_2O_2. The 80 % drop in fluroscence intensity was observed after 2-3 hours for suspention with 1 M of H_2O_2.

With lower concentration of H_2O_2 (100 mM) the degradation time was longer and took 14 hours. Figure 4.25 b shows the change in fluorescence intensity in the absence and presence of hydrogen peroxide for the Nile red encapsulated EP5 nanoparticle solution. It is not clear what causes the slight increase in fluorescence at 4 hrs. The Influence of released Nile red could be one of the possible reasons.

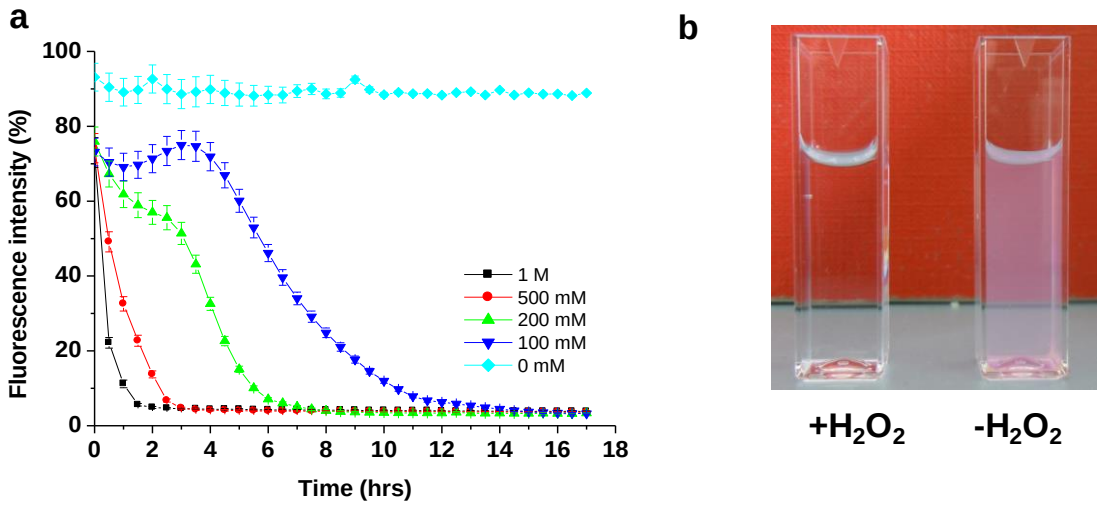

Figure 4.25 a) Change in fluorescence intensity (at 620 nm) of Nile Red encapsulated EP5 nanoparticles in the presence and in the absence of various concentrations of H_2O_2 (100mM, 200 mM, 500 mM and 1 M). b) Sample fluorescence in the presence and in the absence of H_2O_2 after 18 hours.

4.2.8. Cellular uptake

The cellular uptake of polymeric nanoparticles with encapsulated Nile Red was monitored by confocal laser scanning microscopy (CLSM). Figure 4.26 shows the cellular uptake of EP5 nanoparticles suspention with encapsulated Nile Red with HeLa cell lines were stained with 4',6-diamidino-2-phenylindole (DAPI). In the control experiment without Nile red the characteristic red fluorescence is not visible. In the samples with Nile Red, there is a clear evidence of particle internalisation due to endocytosis and uniform distribution of Nile Red @ EP5 nanoparticles can be observed in the cytoplasm.

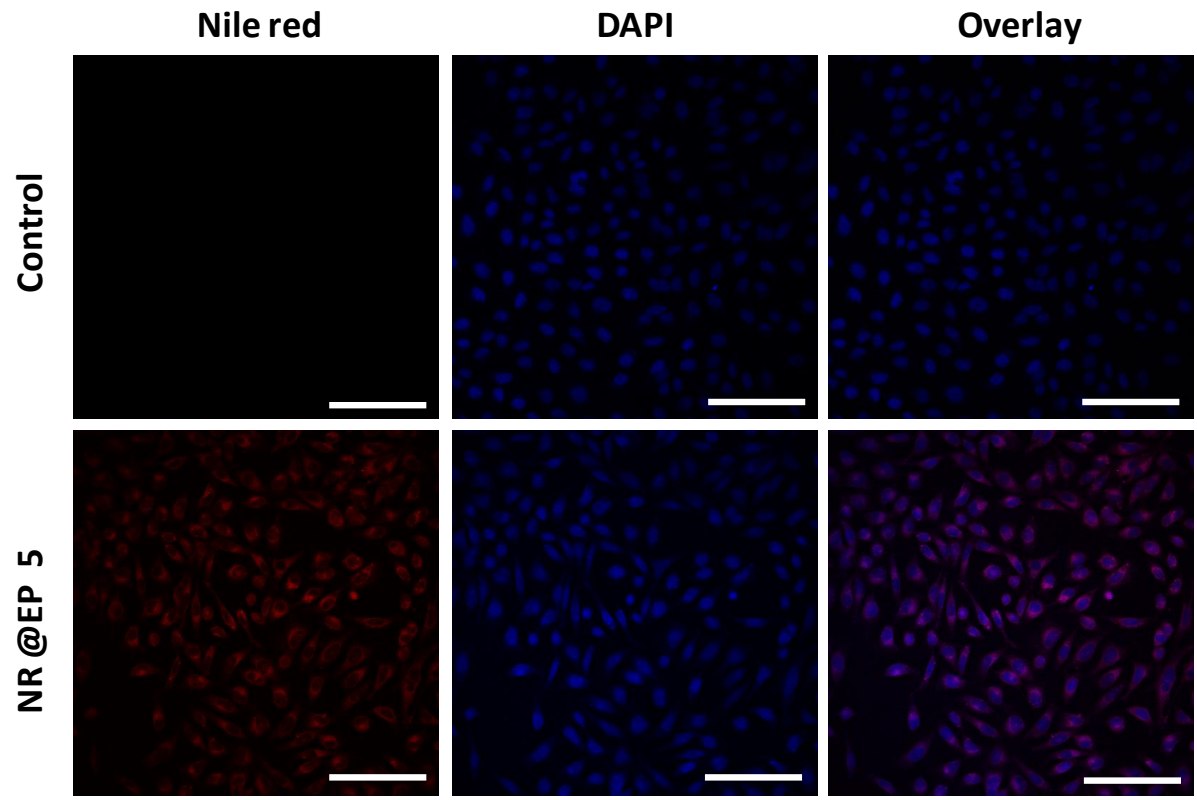

Figure 4.26 CSLM images of Hela cells treated with Nile red encapsulated EP5 polymeric nanoparticles for 24 hrs at 37^0C. The images from left to right show: experiments with Nile Red staining (red), DAPI staining (blue) and the overlays of both images. The scale bars are 100 µm. The control experiment was performed without Nile Red addition.

4.2.9. Cell viability-MTT assay

The cell viability of poly(β-hydroxy thioether)s polymeric nanoparticles was evaluated using the MTT assay. The assay was performed using nanoparticle concentration in the range of 0 - 2.0 mg/ml. HUVEC cells with a cell density of 5000 cells per well were used. After incubation for 4 hours with nanoparticle solution, only a decrease of 70-50 % in cell viability was observed even at a concentration of 2 mg/ml. Nanoparticle derived from EP1 polymer showed the highest level of toxicity among the rest of polymers measured. (Figure 4.27).

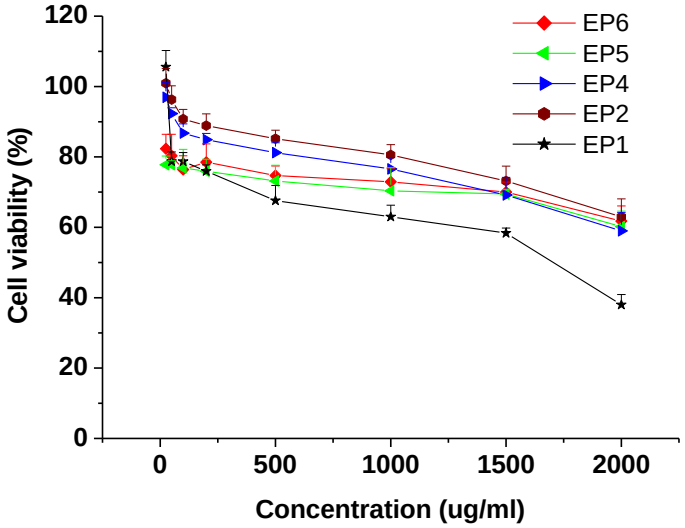

Figure 4.27 MTT assay-cell viability of poly (β-hydroxy thioethers) polymeric nanoparticles.

4.2.10. General conclusion

The synthesis of hydrogen peroxide-responsive linear poly(β-hydroxy thioether)s by thiol-epoxide polymerization reaction is herein reported. Stable dispersions of polymeric nanoparticles were efficiently prepared by nanoprecipitation, and single and double emulsion techniques. Synthesized poly(β-hydroxy thioether)s are less sensitive towards hydrogen peroxide, compared to the linear polysulfides prepared by thiol-yne reactions. However, it was demonstrated that, when 100 mM of H_2O_2 was used, the degradation of nanoparticles was achieved in 14 hours. The cell viability and the cellular uptake with Hela cells were efficient. Linear poly(β-hydroxy thioether)s can be utilized as a promising oxidation-responsive molecular cargos for the delivery of anti-inflammatory hydrophobic drugs for its controlled and delayed release at the site of a chronic infalammation.

4.3.Syntheses of poly(β-thioester)s via base-catalyzed Michael-type nucleophilic thiol-ene polyaddition

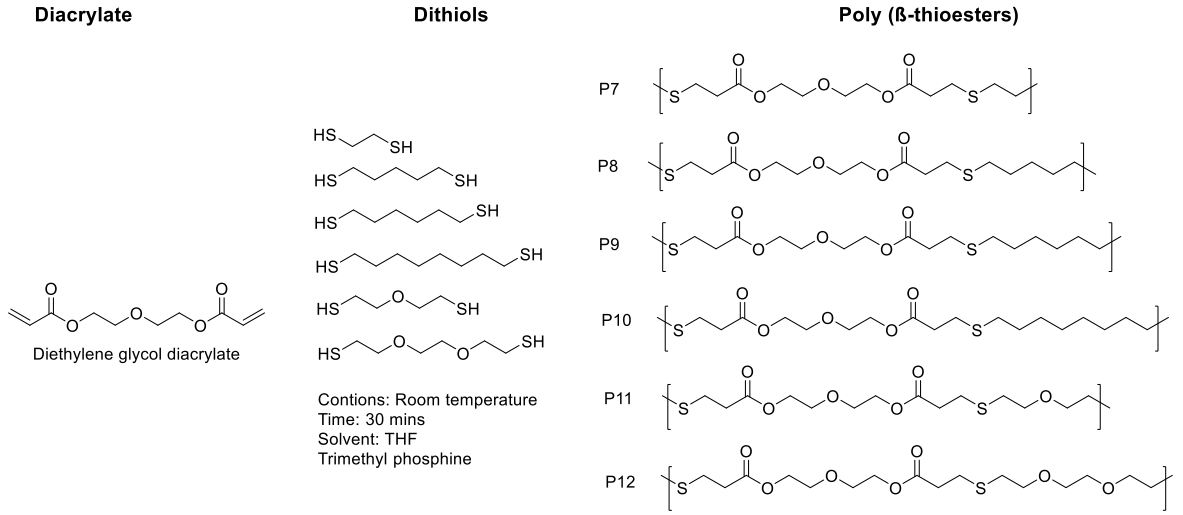

Figure 4.28 Structure of monomers used and different poly(β-thioester) formed.

Poly(β-thioester)s were synthesized via base-catalyzed Michael-type nucleophilic thiol-ene click polyaddition using a combination of six different dithiols and one diacrylate. During polymerization each diacrylate functional group was combined with one thiol to generate a thioester bond. Figure 4.28 shows the chemical structures of monomers and polymers formed. The reaction was carried out in the presence of trimethylphosphine (PMe_3) as catalyst. Structures of six linear polymers synthesized are also shown in appendix C (a-f). Synthesized poly(β-thioester)s were designated as P7, P8, P9, P10, P11 and P12. The monomers ratio was fixed to be 1:1. Polymerization time was optimized for a minimum reaction time of 60 minutes to achive the complete conversion of monomers. Obtained polymers were reprecipitated in n-hexane at least three times and dried under vacuum before further analysis. All polymers were viscous and gel-like , which is a characteristic property of polymers synthesized using polar monomers like di(ethylene glycol) diacrylate.[196] The monomer conversion after one hour and their respective solubility with some common solvents are reported in Table 4.7.

^{1}H-NMR and Raman characterization of biodegradable poly(β-thioester)s ^{1}HNMR spectra of all polymers were measured in $CDCl_3$ and are shown in (Appendix C (a-f)). The disappearance of characteristic C-H peak of alkene at 6.12 ppm, in addition to the formation of S-CH_2 peak at 2.85 ppm confirmed successful polymerization.

Kinetics of the thiol-ene polymerization and the percentage conversion of the monomer was monitored in detail by ^{1}H-NMR. Polymer P10 was synthesized using a 1:1 molar ratio 1,8-octanedithiol and di(ethylene glycol) diacrylate. Obtained polymers were reprecipitated in n-hexane at least three times and dried under vacuum before further analysis. ^{1}H-NMR spectra of polymers were obtained at different time points, which shows The gradual disappearance of characteristic alkene protons (δ 5.83, 6.17 and 6.40 ppm) present in diacrylate molecules together with gradual increase of S-CH_2 peak at 2.85 ppm were observed (Figure 4.29).

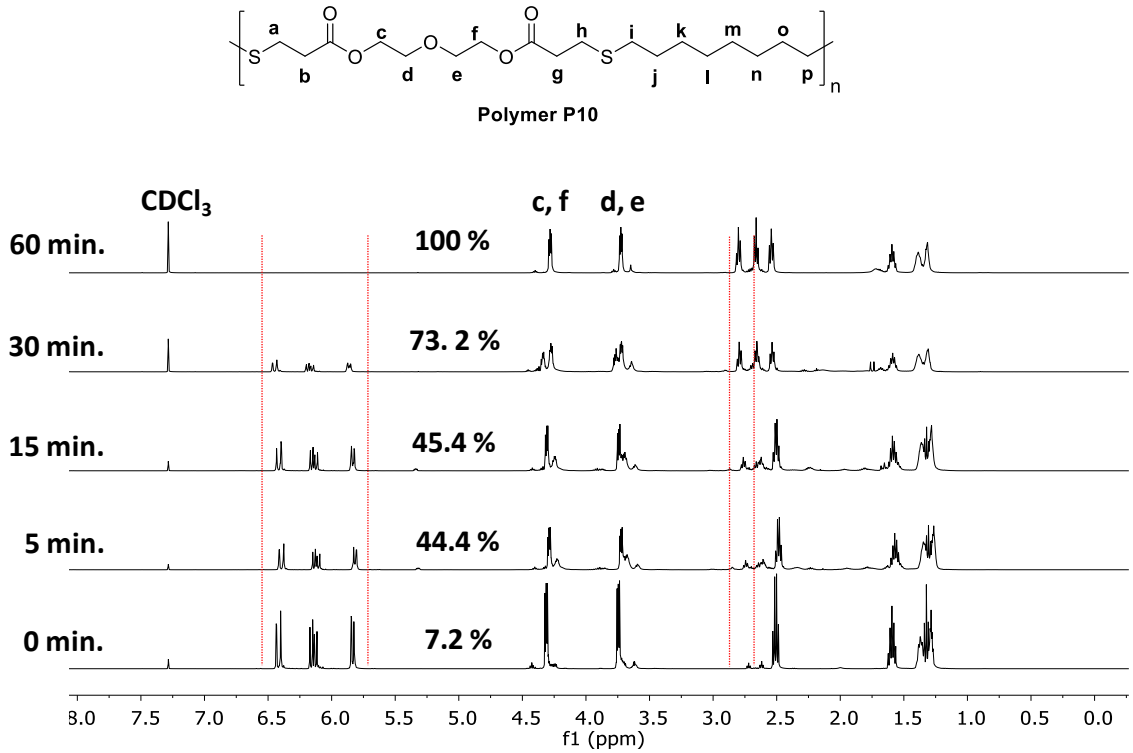

Figure 4.29 Time lapse ^{1}H NMR spectra's of polymer P10

4.3.1. Molecular weight characterization (GPC) of biodegradable poly(β-thioesters)

The GPC results show (Table 4.9, Figure 4.30), that obtained polymers have average molecular weight M_w in that range of 9800 to 53900 g/ mol. The poly dispersity index (PDI) was relatively high and varied depending upon the dithiol used. The polymer P7, prepared by using 1,2-ethane dithiol and di(ethylene glycol) diacrylate showed a higher PDI of 31.7. The lowest PDI (6.8) was obtained for the polymer P9.

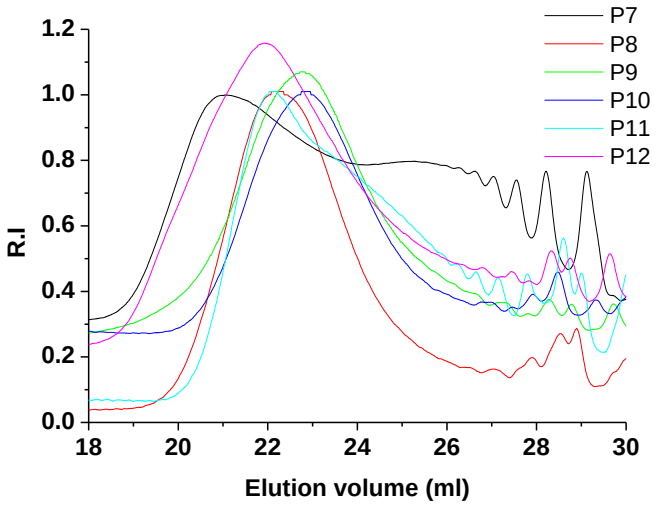

Figure 4.30 GPC of various poly(β-thioester)s synthesized using thiol-ene click polymerization. Calibration curve polystyrene standards (Polymer Standard Service, MP 474− 2520000 Da).

Table 4.9 GPC traces of various poly(β-thioester)s.

Polymers	M_w[a] (g/mol)	PDI[a]	Conversion[b] (%)	Solubility				
				THF	DMSO	H_2O	Ethanol	Acetone
P7	53.9	31.7	98	+	+	-	-	+
P8	16.7	8.7	95	+	+	-	-	+
P9	23.3	6.8	96	+	+	-	-	+
P10	13.2	10.5	98	+	+	-	-	+
P11	9.8	14.2	96	+	+	-	-	+
P12	29.5	9.8	98	+	+	-	-	+

[a] Measured by GPC against polystyrene standards in THF, [b] Measured by ^{1}HNMR, + Soluble – Not soluble

4.3.2. Preparation of biodegradable poly(β-thioester)s polymeric nanoparticles

All six poly(β-thioester)s nanoparticle dispersions were prepared by nanoprecipitation (Table 4.10). The poly (β-thioester) were dissolved in acetone and added to MilliQ water containing (0.05 % w/v) PVA as a surfactant. While stirring at 1000 rpm the particle formation at the interface was observed indicated by a change in solution turbidity. The obtained nanoparticles dispersion was allowed to stir for an additional six hours to evaporate acetone

from the solution. The nanoparticles dispersion was further dialyzed against water using cellulose membrane dialysis tube to remove the excess of PVA. Next, the nanoparticle dispersion was pre concentrated by centrifugation. Polymeric nanoparticles dispersion prepared from P7 was not stable, whereas P8, P9, P10 P11 and P12 formed stable suspension of nanoparticles. The nanoparticle dispersions showed considerable good stability for at least 4-5 weeks without any significant change in particle size and zeta potential controlled by DLS measurements, over a period of time. The number average particle size (d) was between 100 and 180 nm with zeta potential values between -8 and -52 mV.

Table 4.10 Particle size and zeta potential of poly(β-thioester)s nanoprecipitated particles measured by DLS.

Polymers	Average Particle size, DLS (nm)[a]	Zeta potential, DLS (mV)[a]	Remarks[b]
P7	163.5 ± 12.2	-19.3 ± 1.4	Not stable
P8	154.4 ± 2.8	-51.3 ± 2.6	Stable
P9	176.2 ± 29.4	-17.4 ± 1.6	Stable
P10	134.6 ± 17.0	-47.1 ± 4.0	Stable
P11	141.4 ± 3.7	-8.9 ± 1.3	Stable
P12	100.8 ± 6.8	-42.9 ± 3.3	Stable

[a]Measured by DLS, [b] Stability of nanoparticles after nanoprecipitation.

In order to have a clear insight of the particle morphology, SEM was used to visualize the nanoparticles. Representative SEM images of P8 polymeric nanoparticles are shown in Figure 4.31. Depicted nanoparticles are spherical with the size below 200 nm.

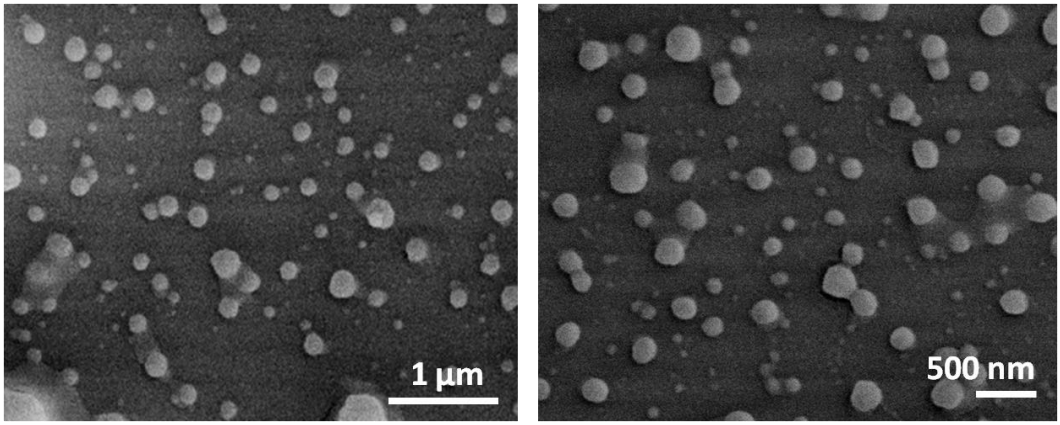

Figure 4.31 (a) Representative SEM images of poly (β-thioester) (polymer P8) nanoparticles.

4.3.3. Nile red encapsulated poly(β-thioesters) nanoparticles

A schematic representation for the preparation of polymer, encapsulation of dyes and hydrolysis of poly(β-thioesters) nanoparticle is shown in Figure 4.32.

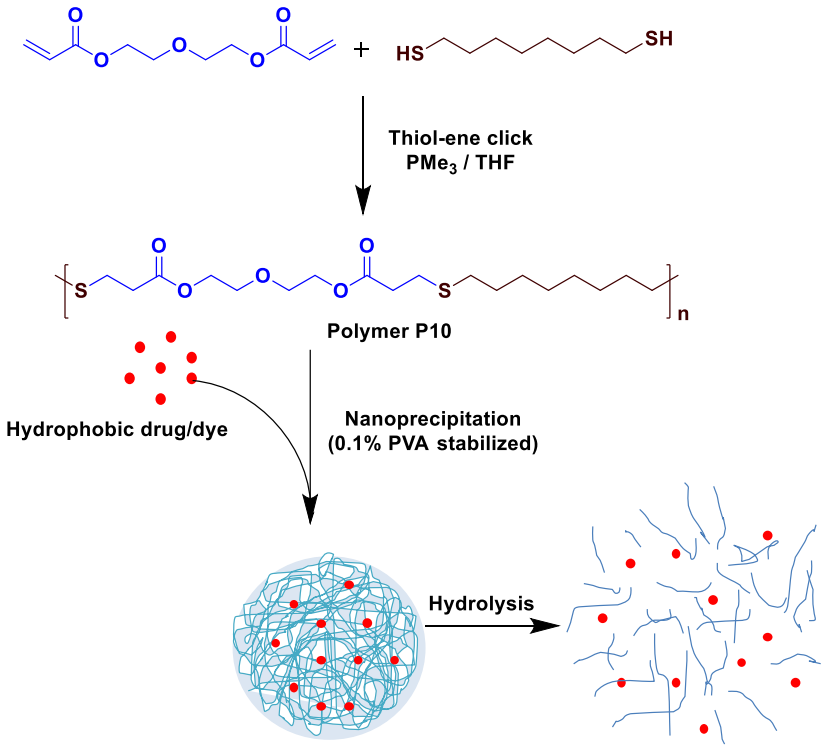

Figure 4.32 Schematic representation of preparation, hydrolysis and dye release from poly (β-thioester) polymer nanoparticles.

Nile red encapsulated nanoparticles were prepared in a similar way as described earlier. 10 mg of polymer and 0.1 mg of Nile Red was dissolved in 1 ml of acetone. This solution was stirred for 3.5 hours, and finally added to 9 ml of MilliQ water containing (0.05 % w/v or 0.5 g/l) PVA under magnetic stirring (1000 rpm), the solution was allowed to stir for at least six hours to evaporate the organic solvent. Particles were separated using cellulose membrane dialysis tube (MWCO 14,000 Da) and further pre concentrated by centrifugation for 15 minutes at 10,000 rpm.

4.3.4. Encapsulation efficiency

Encapsulation efficiency is one of the most important parameters in drug delivery applications. The nanoparticle suspension with Nile Red was first centrifuged at 9500 g for 15 mins and then the supernatant was removed. Next, nanoparticles were further resuspended in Milli-Q water and again centrifuged at 9500 g for 15 mins. The final precipitate was

dissolved in acetone and the fluroscence or absorbance measurement was used to determine the encapsulation efficiency. The encapsulation efficiency was determined to between 35-55 % Appendix D shows a calibration curve for Nile Red in acetone.

4.3.5. Nile red release and degradation kinetics of poly(β-thioesters) nanoparticles

The Nile red release form the nanoparticles were determined using fluorescence spectroscopy. 0.2-0.5 mg/ml Nile red encapsulated poly(β-thioester) nanoparticles were diluted with different buffer solutions. The release kinetics was monitored at 37^0C. The release profile of the dye from polymer P10 under different buffers are show below (Figure 4.33). The most hydrophobic poly(β-thioester) P10 showed the least amount of dye release when water was used. However, more than 50% of the release was observed in 16 hours under pH 5.01 when 200 mM of NaOAc buffer was used.

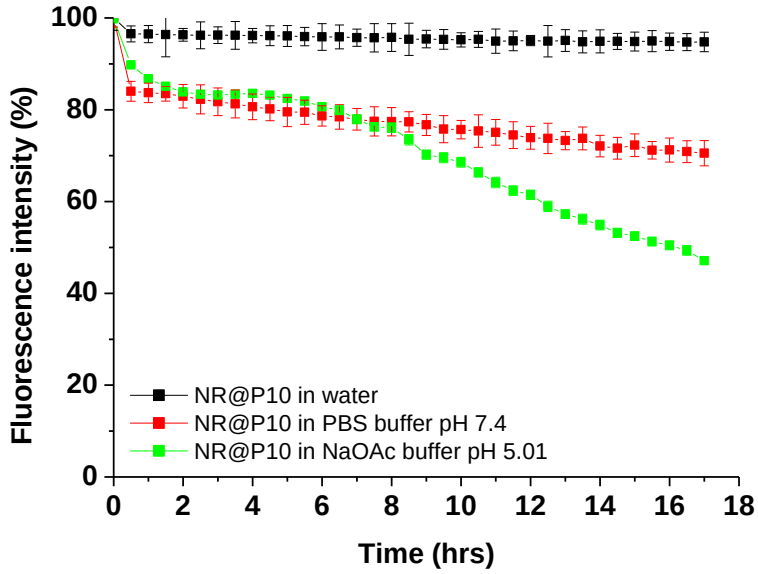

Figure 4.33 Release profle of nile red from poly(β-thioester) P10 polymer nanoparticles.

4.3.6. Cellular uptake

The cellular uptake of polymeric nanoparticles with encapsulated Nile Red was monitored using confocal laser scanning microscopy (CLSM). Figure 4.34, shows the comparison of Nile Red encapsulated P10 nanoparticle cellular uptake. HeLa cell lines were stained by 4',6-diamidino-2-phenylindole (DAPI). In the control experiment the characteristic red fluorescence is not visible. In the samples with Nile Red, there is a clear evidence of particle internalisation, and uniform distribution of Nile Red @ P10 nanoparticle can be observed in the cytoplasm.

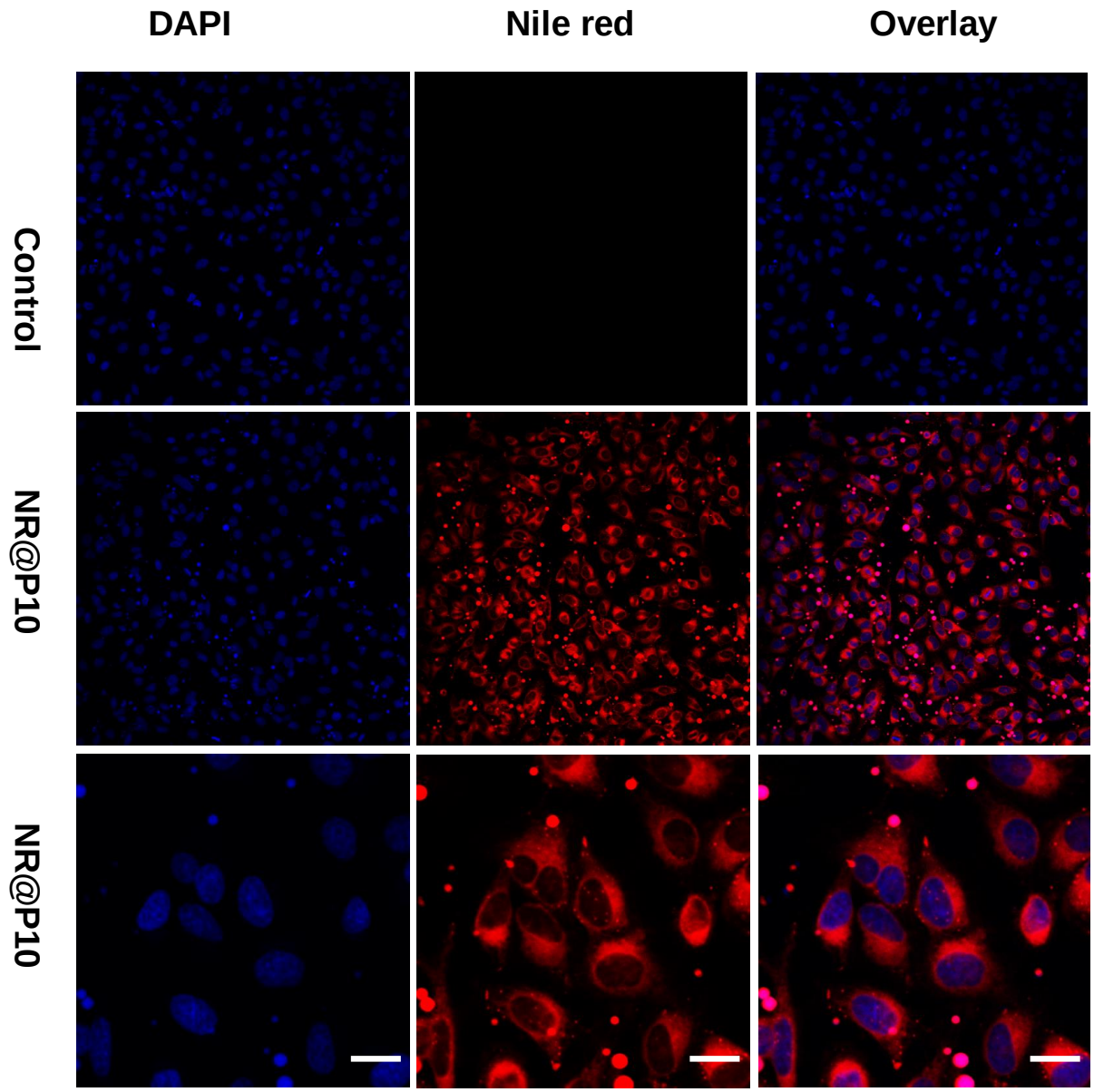

Figure 4.34 CSLM images of Hela cells treated with Nile red encapsulated inside P10 poly (β-thioester) polymeric nanoparticles for 24 hrs at 37^0C. The images from left to right show: experiments with DAPI staining (blue), Nile Red staining (red) and the overlays of both images. The scale bars are 20 µm. The control experiment was performed without Nile Red addition.

4.3.7. Cell viability-MTT assay

The cell viability of poly(β- thioester) polymeric nanoparticles was evaluated using MTT assay. The assay was performed using nanoparticle concentration in the range of 0 - 1.0 mg/ml. Hela cells with a cell density of 20000 cells per well were used. After incubation for 4

hours with nanoparticle solution, only a decrease of 20-10 % in cell viability was observed at a concentration of 1 mg/ml. Nanoparticle derived from P11 polymer showed the highest level of toxixcity among the rest of polymers measured. (Figure 4.35).

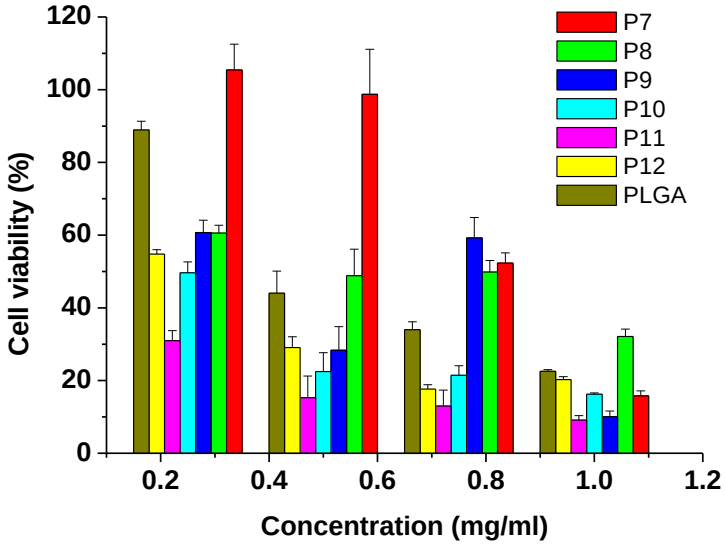

Figure 4.35 MTT assay-cell viability of poly(β-thioesters) polymeric nanoparticles.

4.3.8. General conclusion

The synthesis of linear poly(β-hydroxy thioesters) by thiol-ene nucleiophic addition polymerization reaction is herein reported. Dispersions of stable polymeric nanoparticles were efficiently prepared by nanoprecipitation stabilized by PVA as surfactant. The nanoparticles undergo hydrolysis when treated with NaOAc buffer at pH 5.01. The cell viability and the cellular uptake with Hela cells were efficient. So we anticipate that the linear poly(β-hydroxy thioesters) can be utilized as a promising biodegradable cargo for the delivery of hydrophobic drugs or dyes.

5. Summary and Outlook

The aim of this thesis was to synthesize sulfur contacting polymer libraries, which can be used as delivery matrices for triggered release of payloads. Herein three polymeric libraries were synthesized using three different synthetic approaches. The coupling of dithiols with alkynes, diepoxide and diacrylate was established to generate linear polysulfides, poly(β-hydroxy thioethers) and poly(β-thioester), respectively. The polymerization reactions carried out in these studies are facile, rapid and more convenient in comparison with other polymerization techniques. The reaction time was optimized and was mostly under 4 hours. These coupling reactions are efficient for the preparation of polymer libraries. However more studies are required to establish polymers with predefined molecular weight and better polydispersity index.

Stimuli responsive nanoparticles are prominent in the area of biomedicine, the preparation of nanosized particles not only depends on the technique used but also various other parameters involved during the preparation steps. Three commonly used techniques were used for the preparation of nanoparticles from the synthesized linear polymers.

Oxidation responsive polysulfides and poly(β-hydroxy thioethers)

It was possible to demonstrate that that the linear polysulfides and poly(β-hydroxy thioethers) prepared using the thiol-yne and thiol-epoxide reactions are sensitive to hydrogen peroxide. I have shown that different parameters, such as the preparation tecnique, size and chemical nature of the polymer, influence the degradation kinetics and, hence, the payload release kinetics. Linear polysulfides were more responsive to hydrogen peroxide when compared with poly(β-hydroxy thioethers). Polysulfide AU showed the highest sensitivity towards H_2O_2 when compared with the rest of the polymers studied in the thesis. The fact has to be admitted that the sensitivity towards hydrogen peroxide are of the order of millimolar range, which makes the nanoparticle degradation kinetics slower in the phathological and physiological conditions.

Outlook and perspective

In my study, the polysulfides and poly(β-hydroxy thioethers) have demonstrated substantial oxidation-responsive character to hydrogen peroxide. Other advantages of this polymers include the controllable synthesis of the polymer and their low cytotoxicity, facile process for the drug carrier preparation and further possibility to encapsulate hydrophobic cargos. Polysulfides and poly(β-hydroxy thioethers) are, therefore, expected to have promising applications in anti-inflammatory therapy.

Even though considerable progress has been made so far in the field of ROS responsive materials, there are several challenges to be addressed for future development. It is important to design materials that can distinguish between the low levels of ROS from normal cellular activities and the increased levels of ROS from pathological sites. Biocompatibility of ROS-sensitive materials is also an important factor to be considered when designing novel ROS-sensitive drug delivery systems. Inflammatory response can be triggered by activated macrophages and neutrophils resulting in the generation of large amount of ROS (respiratory burst) that can adversely act on ROS-responsive materials. For optimal outcomes, solubility change and degradation should be controlled at a rate suitable for pathologies. Interaction between polymer composition, material properties, and biological effects should be thoroughly understood in order to design the next-generation ROS-responsive biomaterials. In spite of its current challenges, ROS-responsive materials offer a novel treatment possibility and hold great potential in the field of biomedicine.

Biodegradable poly(β-thioesters)

The biodegradable poly(β-thioesters) are promising materials for biomedical applications. Polymer libraries were synthesised using co-polymerization of various dithiols and diacrylates. The reaction showed high efficieny and almost 98% conversion was achieved. However, the polydispersity index was relatively high. The molecular weight distrubition can be controlled by changing the monomer ratios and reaction time. Thiol-ene Michael addition is a non-radical fast reaction with high yields that proceeds at room temperature with minute amounts of a tertiary phosphine or amine used as catalyst. Poly(β-thioesters) synthesized using thiol-ene Michael addition is a relatively new area and more research will be essential for developing new polymers with enhanced properties. The synthesis of these polymers were easier when compared with other biodegradable polymers. However, the degradation kinetics is slow, there is a possibility of enhancing the degradation behaviour with the correct choice of monomers.

Biodegradable polymer materials may find application in limitless number of areas such as agriculture, automotives, medicine, and packaging which require environmentally friendly polymers. If the level of biodegradation can be tailored to specific needs, each industry is able to create its own ideal material. Controlling biodegradation is a challenge to be achieved especially in the area of biomedicines. Biodegradable polymeric nanoparticulate systems are being increasingly recognized as drug delivery systems which find a wide variety of

applications in the pharmaceutical industry, hence biodegradable polymer matrix with specific degradation kinetics is essential for efficient delivery systems.

References

[1] M. Mittal, M.R. Siddiqui, K. Tran, S.P. Reddy, A.B. Malik, Reactive Oxygen Species in Inflammation and Tissue Injury, Antioxid Redox Sign, 20 (2014) 1126-1167.
[2] A.R. Saltiel, C.R. Kahn, Insulin signalling and the regulation of glucose and lipid metabolism, Nature, 414 (2001) 799-806.
[3] B. Jeong, A. Gutowska, Lessons from nature: stimuli-responsive polymers and their biomedical applications, Trends in Biotechnology, 20 (2002) 305-311.
[4] D. Schmaljohann, Thermo- and pH-responsive polymers in drug delivery, Advanced Drug Delivery Reviews, 58 (2006) 1655-1670.
[5] A. Nelson, Stimuli-responsive polymers: Engineering interactions, Nat Mater, 7 (2008) 523-525.
[6] A.S. Hoffman, Stimuli-responsive polymers: Biomedical applications and challenges for clinical translation, Advanced Drug Delivery Reviews, 65 (2013) 10-16.
[7] A. Kumari, S.K. Yadav, S.C. Yadav, Biodegradable polymeric nanoparticles based drug delivery systems, Colloids and Surfaces B: Biointerfaces, 75 (2010) 1-18.
[8] E.S. Gil, S.M. Hudson, Stimuli-reponsive polymers and their bioconjugates, Progress in Polymer Science, 29 (2004) 1173-1222.
[9] E. Fleige, M.A. Quadir, R. Haag, Stimuli-responsive polymeric nanocarriers for the controlled transport of active compounds: Concepts and applications, Advanced Drug Delivery Reviews, 64 (2012) 866-884.
[10] H.-m. Ding, Y.-q. Ma, Controlling Cellular Uptake of Nanoparticles with pH-Sensitive Polymers, Sci. Rep., 3 (2013).
[11] L.Y.T. Chou, K. Ming, W.C.W. Chan, Strategies for the intracellular delivery of nanoparticles, Chemical Society Reviews, 40 (2011) 233-245.
[12] W.B. Liechty, D.R. Kryscio, B.V. Slaughter, N.A. Peppas, Polymers for Drug Delivery Systems, Annual review of chemical and biomolecular engineering, 1 (2010) 149-173.
[13] F. Puoci, F. Iemma, N. Picci, Stimuli-responsive molecularly imprinted polymers for drug delivery: a review, Current drug delivery, 5 (2008) 85-96.
[14] W. Fischer, A Second Note on the Term "Chalcogen", Journal of Chemical Education, 78 (2001) 1333.
[15] A. Kultys, S. Pikus, Polyurethanes containing sulfur. III. New thermoplastic HDI-based segmented polyurethanes with diphenylmethane unit in their structure, Journal of Polymer Science Part A: Polymer Chemistry, 39 (2001) 1733-1742.
[16] L.R.e.o.c. Rudnick, Synthetics, mineral oils, and bio-based lubricants : chemistry and technology, Second edition. ed.
[17] A. Napoli, M. Valentini, N. Tirelli, M. Muller, J.A. Hubbell, Oxidation-responsive polymeric vesicles, Nat Mater, 3 (2004) 183-189.
[18] O. Türünç, M.A.R. Meier, A novel polymerization approach via thiol-yne addition, Journal of Polymer Science Part A: Polymer Chemistry, 50 (2012) 1689-1695.
[19] H. Tian, Z. Tang, X. Zhuang, X. Chen, X. Jing, Biodegradable synthetic polymers: Preparation, functionalization and biomedical application, Progress in Polymer Science, 37 (2012) 237-280.

[20] B.D. Ulery, L.S. Nair, C.T. Laurencin, Biomedical applications of biodegradable polymers, Journal of Polymer Science Part B: Polymer Physics, 49 (2011) 832-864.
[21] J. Vandenbergh, K. Ranieri, T. Junkers, Synthesis of (Bio)-Degradable Poly(β-thioester)s via Amine Catalyzed Thiol−Ene Click Polymerization, Macromolecular Chemistry and Physics, 213 (2012) 2611-2617.
[22] S. Mitchell, Biological interactions of sulfur compounds, Taylor & Francis, London, 1996.
[23] S. Parcell, Sulfur in human nutrition and applications in medicine, Alternative medicine review : a journal of clinical therapeutic, 7 (2002) 22-44.
[24] J.T. Brosnan, M.E. Brosnan, The Sulfur-Containing Amino Acids: An Overview, The Journal of Nutrition, 136 (2006) 1636S-1640S.
[25] A.A. Brakhage, Molecular regulation of beta-lactam biosynthesis in filamentous fungi, Microbiol Mol Biol Rev, 62 (1998) 547-585.
[26] M.H. Brodnitz, J.V. Pascale, L. Van Derslice, Flavor components of garlic extract, Journal of Agricultural and Food Chemistry, 19 (1971) 273-275.
[27] P. Morales, E. Ferna´ndez-García, M. Nuñez, Production of Volatile Compounds in Cheese by Pseudomonas fragi Strains of Dairy Origin, Journal of Food Protection, 68 (2005) 1399-1407.
[28] V. Varlet, X. Fernandez, Review. Sulfur-containing Volatile Compounds in Seafood: Occurrence, Odorant Properties and Mechanisms of Formation, Food Science and Technology International, 16 (2010) 463-503.
[29] T.E. Siebert, M.R. Solomon, A.P. Pollnitz, D.W. Jeffery, Selective Determination of Volatile Sulfur Compounds in Wine by Gas Chromatography with Sulfur Chemiluminescence Detection, Journal of Agricultural and Food Chemistry, 58 (2010) 9454-9462.
[30] C. Qian Michael, X. Fan, K. Mahattanatawee, Volatile Sulfur Compounds in Food, in: ACS Symposium Series, American Chemical Society, 2011, pp. 0.
[31] L. Pripis-Nicolau, G. de Revel, A. Bertrand, A. Lonvaud-Funel, Methionine catabolism and production of volatile sulphur compounds by Œnococcus œni, Journal of Applied Microbiology, 96 (2004) 1176-1184.
[32] T.B. Aldrich, A Chemical Study of the Secretion of the Anal Glands of Mephitis Mephitiga (Common Skunk), with Remarks on the Physiological Properties of This Secretion, J Exp Med, 1 (1896) 323-340.
[33] O. Mozziconacci, T.D. Williams, C. Schöneich, Intramolecular Hydrogen Transfer Reactions of Thiyl Radicals from Glutathione: Formation of Carbon-Centered Radical at Glu, Cys, and Gly, Chemical Research in Toxicology, 25 (2012) 1842-1861.
[34] M.D. Sevilla, D. Becker, S. Swarts, J. Herrington, Sulfinyl radical formation from the reaction of cysteine and glutathione thiyl radicals with molecular oxygen, Biochemical and Biophysical Research Communications, 144 (1987) 1037-1042.
[35] W.T. Lowther, N. Brot, H. Weissbach, J.F. Honek, B.W. Matthews, Thiol–disulfide exchange is involved in the catalytic mechanism of peptide methionine sulfoxide reductase, P Natl Acad Sci USA, 97 (2000) 6463-6468.
[36] J. Luong, R. Gras, R.A. Shellie, H.J. Cortes, Direct measurement of part-per-billion levels of dimethyl sulfoxide in water by gas chromatography with stacked injection and chemiluminescence detection, Journal of Separation Science, 35 (2012) 1486-1493.
[37] L. Tong, Acetyl-coenzyme A carboxylase: crucial metabolic enzyme and attractive target for drug discovery, CMLS, Cell. Mol. Life Sci., 62 (2005) 1784-1803.
[38] J. Chen, M. Zhao, F. Feng, A. Sizovs, J. Wang, Tunable Thioesters as "Reduction" Responsive Functionality for Traceless Reversible Protein PEGylation, Journal of the American Chemical Society, 135 (2013) 10938-10941.

[39] R.J. Mancini, J. Lee, H.D. Maynard, Trehalose Glycopolymers for Stabilization of Protein Conjugates to Environmental Stressors, Journal of the American Chemical Society, 134 (2012) 8474-8479.
[40] M. Yan, J. Du, Z. Gu, M. Liang, Y. Hu, W. Zhang, S. Priceman, L. Wu, Z.H. Zhou, Z. Liu, T. Segura, Y. Tang, Y. Lu, A novel intracellular protein delivery platform based on single-protein nanocapsules, Nat Nano, 5 (2010) 48-53.
[41] D. Witt, Recent Developments in Disulfide Bond Formation, Synthesis, 2008 (2008) 2491-2509.
[42] T.C.P. Lee, Properties and applications of elastomeric polysulfides, Rapra Technology Ltd., Shawbury, Shrewsbury, 1999.
[43] T. Higashihara, K. Matsumoto, M. Ueda, Sulfonated aromatic hydrocarbon polymers as proton exchange membranes for fuel cells, Polymer, 50 (2009) 5341-5357.
[44] J.M. Bae, I. Honma, M. Murata, T. Yamamoto, M. Rikukawa, N. Ogata, Properties of selected sulfonated polymers as proton-conducting electrolytes for polymer electrolyte fuel cells, Solid State Ionics, 147 (2002) 189-194.
[45] P. Radziwon, B. Boczkowska-Radziwon, J. Giedrojc, J. Schenk, M.Z. Wojtukiewicz, J. Kloczko, H.K. Breddin, Effects of Polysulfonate Derivative (GL 522-Y-1) on Coagulation in vitro and Thrombosis in vivo, Pathophysiology of Haemostasis and Thrombosis, 28 (1998) 86-92.
[46] U.C. Chaturvedi, R. Shrivastava, Interaction of viral proteins with metal ions: role in maintaining the structure and functions of viruses, FEMS Immunology & Medical Microbiology, 43 (2005) 105-114.
[47] M. Hosoya, J. Balzarini, S. Shigeta, E. Declercq, Differential Inhibitory Effects of Sulfated Polysaccharides and Polymers on the Replication of Various Myxoviruses and Retroviruses, Depending on the Composition of the Target Amino-Acid-Sequences of the Viral Envelope Glycoproteins, Antimicrob Agents Ch, 35 (1991) 2515-2520.
[48] V.D. Prajapati, P.M. Maheriya, G.K. Jani, H.K. Solanki, Carrageenan: A natural seaweed polysaccharide and its applications, Carbohydrate Polymers, 105 (2014) 97-112.
[49] A. Kultys, A. Puszka, Transparent poly(thiourethane-urethane)s based on dithiol chain extender, J Therm Anal Calorim, 117 (2014) 1427-1439.
[50] G. Gubitz, M.G. Schmid, Chiral separation by chromatographic and electromigration techniques. A review, Biopharmaceutics & drug disposition, 22 (2001) 291-336.
[51] Biology and brimstone, Nat Chem Biol, 2 (2006) 169-169.
[52] J.e.o.c. Barber, C.e.o.c. Rostron, Pharmaceutical chemistry.
[53] K.S. Soppimath, T.M. Aminabhavi, A.R. Kulkarni, W.E. Rudzinski, Biodegradable polymeric nanoparticles as drug delivery devices, Journal of Controlled Release, 70 (2001) 1-20.
[54] M.L. Hans, A.M. Lowman, Biodegradable nanoparticles for drug delivery and targeting, Current Opinion in Solid State and Materials Science, 6 (2002) 319-327.
[55] R.C. Mundargi, V.R. Babu, V. Rangaswamy, P. Patel, T.M. Aminabhavi, Nano/micro technologies for delivering macromolecular therapeutics using poly(d,l-lactide-co-glycolide) and its derivatives, Journal of Controlled Release, 125 (2008) 193-209.
[56] E. Leo, B. Brina, F. Forni, M.A. Vandelli, In vitro evaluation of PLA nanoparticles containing a lipophilic drug in water-soluble or insoluble form, International Journal of Pharmaceutics, 278 (2004) 133-141.
[57] M.A. Woodruff, D.W. Hutmacher, The return of a forgotten polymer—Polycaprolactone in the 21st century, Progress in Polymer Science, 35 (2010) 1217-1256.
[58] J. Panyam, V. Labhasetwar, Biodegradable nanoparticles for drug and gene delivery to cells and tissue, Advanced Drug Delivery Reviews, 55 (2003) 329-347.

[59] L.A. Guzman, V. Labhasetwar, C. Song, Y. Jang, A.M. Lincoff, R. Levy, E.J. Topol, Local Intraluminal Infusion of Biodegradable Polymeric Nanoparticles: A Novel Approach for Prolonged Drug Delivery After Balloon Angioplasty, Circulation, 94 (1996) 1441-1448.
[60] K. Madhavan Nampoothiri, N.R. Nair, R.P. John, An overview of the recent developments in polylactide (PLA) research, Bioresource technology, 101 (2010) 8493-8501.
[61] Y. Zhao, Z. Wang, J. Wang, H. Mai, B. Yan, F. Yang, Direct synthesis of poly(D,L-lactic acid) by melt polycondensation and its application in drug delivery, Journal of Applied Polymer Science, 91 (2004) 2143-2150.
[62] L.L. Madison, G.W. Huisman, Metabolic engineering of poly(3-hydroxyalkanoates): from DNA to plastic, Microbiology and molecular biology reviews : MMBR, 63 (1999) 21-53.
[63] G.Q. Chen, Q. Wu, The application of polyhydroxyalkanoates as tissue engineering materials, Biomaterials, 26 (2005) 6565-6578.
[64] F.J.v. Natta, J.W. Hill, W.H. Carothers, Studies of Polymerization and Ring Formation. XXIII.1 ε-Caprolactone and its Polymers, Journal of the American Chemical Society, 56 (1934) 455-457.
[65] A. Alani, J.C. Knowles, W. Chrzanowski, Y.L. Ng, K. Gulabivala, Ion release characteristics, precipitate formation and sealing ability of a phosphate glass-polycaprolactone-based composite for use as a root canal obturation material, Dental Materials, 25 (2009) 400-410.
[66] K.W. Ng, H.N. Achuth, S. Moochhala, T.C. Lim, D.W. Hutmacher, In vivo evaluation of an ultra-thin polycaprolactone film as a wound dressing, J Biomat Sci-Polym E, 18 (2007) 925-938.
[67] E.J. Frazza, E.E. Schmitt, A new absorbable suture, J Biomed Mater Res, 5 (1971) 43-58.
[68] M.D. Dhanaraju, D. Gopinath, M.R. Ahmed, R. Jayakumar, C. Vamsadhara, Characterization of polymeric poly(epsilon-caprolactone) injectable implant delivery system for the controlled delivery of contraceptive steroids, J Biomed Mater Res A, 76 (2006) 63-72.
[69] K.J. Lowry, K.R. Hamson, L. Bear, Y.B. Peng, R. Calaluce, M.L. Evans, J.O. Anglen, W.C. Allen, Polycaprolactone/glass bioabsorbable implant in a rabbit humerus fracture model, J Biomed Mater Res, 36 (1997) 536-541.
[70] P.D. Dalton, T. Woodfield, D.W. Hutmacher, Snapshot: Polymer scaffolds for tissue engineering, Biomaterials, 30 (2009) 701-702.
[71] C.S. Marvel, A. Kotch, Polythiolesters, Journal of the American Chemical Society, 73 (1951) 1100-1102.
[72] T. Lütke-Eversloh, K. Bergander, H. Luftmann, A. Steinbüchel, Biosynthesis of Poly(3-hydroxybutyrate-co-3-mercaptobutyrate) as a Sulfur Analogue to Poly(3-hydroxybutyrate) (PHB), Biomacromolecules, 2 (2001) 1061-1065.
[73] M.A.C. Stuart, W.T.S. Huck, J. Genzer, M. Muller, C. Ober, M. Stamm, G.B. Sukhorukov, I. Szleifer, V.V. Tsukruk, M. Urban, F. Winnik, S. Zauscher, I. Luzinov, S. Minko, Emerging applications of stimuli-responsive polymer materials, Nat Mater, 9 (2010) 101-113.
[74] A.W. Jackson, D.A. Fulton, Making polymeric nanoparticles stimuli-responsive with dynamic covalent bonds, Polym Chem-Uk, 4 (2013) 31-45.
[75] B. Priya, P. Viness, E.C. Yahya, C.d.T. Lisa, Stimuli-responsive polymers and their applications in drug delivery, Biomedical Materials, 4 (2009) 022001.
[76] H. Priya James, R. John, A. Alex, K.R. Anoop, Smart polymers for the controlled delivery of drugs – a concise overview, Acta Pharmaceutica Sinica B, 4 (2014) 120-127.

[77] J.C. Garbern, E. Minami, P.S. Stayton, C.E. Murry, Delivery of basic fibroblast growth factor with a pH-responsive, injectable hydrogel to improve angiogenesis in infarcted myocardium, Biomaterials, 32 (2011) 2407-2416.
[78] R.V. Kulkarni, R. Boppana, G. Krishna Mohan, S. Mutalik, N.V. Kalyane, pH-responsive interpenetrating network hydrogel beads of poly(acrylamide)-g-carrageenan and sodium alginate for intestinal targeted drug delivery: Synthesis, in vitro and in vivo evaluation, Journal of Colloid and Interface Science, 367 (2012) 509-517.
[79] K. Wang, X. Xu, Y. Wang, X. Yan, G. Guo, M. Huang, F. Luo, X. Zhao, Y. Wei, Z. Qian, Synthesis and characterization of poly(methoxyl ethylene glycol-caprolactone-co-methacrylic acid-co-poly(ethylene glycol) methyl ether methacrylate) pH-sensitive hydrogel for delivery of dexamethasone, International Journal of Pharmaceutics, 389 (2010) 130-138.
[80] I.M. El-Sherbiny, Enhanced pH-responsive carrier system based on alginate and chemically modified carboxymethyl chitosan for oral delivery of protein drugs: Preparation and in-vitro assessment, Carbohydrate Polymers, 80 (2010) 1125-1136.
[81] W.K. Bae, M.S. Park, J.H. Lee, J.E. Hwang, H.J. Shim, S.H. Cho, D.-E. Kim, H.M. Ko, C.-S. Cho, I.-K. Park, I.-J. Chung, Docetaxel-loaded thermoresponsive conjugated linoleic acid-incorporated poloxamer hydrogel for the suppression of peritoneal metastasis of gastric cancer, Biomaterials, 34 (2013) 1433-1441.
[82] K. Li, L. Yu, X. Liu, C. Chen, Q. Chen, J. Ding, A long-acting formulation of a polypeptide drug exenatide in treatment of diabetes using an injectable block copolymer hydrogel, Biomaterials, 34 (2013) 2834-2842.
[83] M.-H. Hsiao, M. Larsson, A. Larsson, H. Evenbratt, Y.-Y. Chen, Y.-Y. Chen, D.-M. Liu, Design and characterization of a novel amphiphilic chitosan nanocapsule-based thermo-gelling biogel with sustained in vivo release of the hydrophilic anti-epilepsy drug ethosuximide, Journal of Controlled Release, 161 (2012) 942-948.
[84] C.L. Hastings, H.M. Kelly, M.J. Murphy, F.P. Barry, F.J. O'Brien, G.P. Duffy, Development of a thermoresponsive chitosan gel combined with human mesenchymal stem cells and desferrioxamine as a multimodal pro-angiogenic therapeutic for the treatment of critical limb ischaemia, Journal of Controlled Release, 161 (2012) 73-80.
[85] M. Licciardi, G. Amato, A. Cappelli, M. Paolino, G. Giuliani, B. Belmonte, C. Guarnotta, G. Pitarresi, G. Giammona, Evaluation of thermoresponsive properties and biocompatibility of polybenzofulvene aggregates for leuprolide delivery, International Journal of Pharmaceutics, 438 (2012) 279-286.
[86] F.M. Winnik, Phase transition of aqueous poly-(N-isopropylacrylamide) solutions: a study by non-radiative energy transfer, Polymer, 31 (1990) 2125-2134.
[87] F.M. Winnik, Fluorescence studies of aqueous solutions of poly(N-isopropylacrylamide) below and above their LCST, Macromolecules, 23 (1990) 233-242.
[88] H.G. Schild, Poly(N-isopropylacrylamide): experiment, theory and application, Progress in Polymer Science, 17 (1992) 163-249.
[89] J.S. Scarpa, D.D. Mueller, I.M. Klotz, Slow hydrogen-deuterium exchange in a non-.alpha.-helical polyamide, Journal of the American Chemical Society, 89 (1967) 6024-6030.
[90] S. Dai, P. Ravi, K.C. Tam, pH-Responsive polymers: synthesis, properties and applications, Soft Matter, 4 (2008) 435-449.
[91] B. Jaquet, D. Wei, B. Reck, F. Reinhold, X. Zhang, H. Wu, M. Morbidelli, Stabilization of polymer colloid dispersions with pH-sensitive poly-acrylic acid brushes, Colloid Polym Sci, 291 (2013) 1659-1667.
[92] C. Zhao, S. Nie, M. Tang, S. Sun, Polymeric pH-sensitive membranes—A review, Progress in Polymer Science, 36 (2011) 1499-1520.
[93] M.a.R.e. Aguilar, J.e. San Roma\n, Smart polymers and their applications.

[94] M. Zelzer, S.J. Todd, A.R. Hirst, T.O. McDonald, R.V. Ulijn, Enzyme responsive materials: design strategies and future developments, Biomaterials Science, 1 (2013) 11-39.
[95] R. Jin, L.S. Teixeira, P.J. Dijkstra, C.A. van Blitterswijk, M. Karperien, J. Feijen, Enzymatically-crosslinked injectable hydrogels based on biomimetic dextran-hyaluronic acid conjugates for cartilage tissue engineering, Biomaterials, 31 (2010) 3103-3113.
[96] A.A. Aimetti, M.W. Tibbitt, K.S. Anseth, Human neutrophil elastase responsive delivery from poly(ethylene glycol) hydrogels, Biomacromolecules, 10 (2009) 1484-1489.
[97] K.J. van Bommel, M.C. Stuart, B.L. Feringa, J. van Esch, Two-stage enzyme mediated drug release from LMWG hydrogels, Organic & biomolecular chemistry, 3 (2005) 2917-2920.
[98] V.K. Garripelli, J.K. Kim, S. Son, W.J. Kim, M.A. Repka, S. Jo, Matrix metalloproteinase-sensitive thermogelling polymer for bioresponsive local drug delivery, Acta Biomater, 7 (2011) 1984-1992.
[99] M. Huo, J. Yuan, L. Tao, Y. Wei, Redox-responsive polymers for drug delivery: from molecular design to applications, Polym Chem-Uk, 5 (2014) 1519-1528.
[100] S. Aleksanian, B. Khorsand, R. Schmidt, J.K. Oh, Rapidly thiol-responsive degradable block copolymer nanocarriers with facile bioconjugation, Polym Chem-Uk, 3 (2012) 2138-2147.
[101] Z.-Q. Yu, J.-T. Sun, C.-Y. Pan, C.-Y. Hong, Bioreducible nanogels/microgels easily prepared via temperature induced self-assembly and self-crosslinking, Chemical Communications, 48 (2012) 5623-5625.
[102] M.N. Levine, R.T. Raines, Trimethyl lock: a trigger for molecular release in chemistry, biology, and pharmacology, Chemical Science, 3 (2012) 2412-2420.
[103] H. Nishide, K. Oyaizu, Toward Flexible Batteries, Science, 319 (2008) 737-738.
[104] C.M. Quinzii, L.C. Lopez, R.W. Gilkerson, B. Dorado, J. Coku, A.B. Naini, C. Lagier-Tourenne, M. Schuelke, L. Salviati, R. Carrozzo, F. Santorelli, S. Rahman, M. Tazir, M. Koenig, S. DiMauro, M. Hirano, Reactive oxygen species, oxidative stress, and cell death correlate with level of CoQ10 deficiency, FASEB J, 24 (2010) 3733-3743.
[105] V.J. Thannickal, B.L. Fanburg, Reactive oxygen species in cell signaling, Am J Physiol Lung Cell Mol Physiol, 279 (2000) L1005-1028.
[106] M.A.C. Stuart, W.T.S. Huck, J. Genzer, M. Muller, C. Ober, M. Stamm, G.B. Sukhorukov, I. Szleifer, V.V. Tsukruk, M. Urban, F. Winnik, S. Zauscher, I. Luzinov, S. Minko, Emerging applications of stimuli-responsive polymer materials, Nat Mater, 9 (2010) 101-113.
[107] M.W. Lawless, K.J. O'Byrne, S.G. Gray, Targeting oxidative stress in cancer, Expert Opin Ther Tar, 14 (2010) 1225-1245.
[108] M.A. Smith, C.A. Rottkamp, A. Nunomura, A.K. Raina, G. Perry, Oxidative stress in Alzheimer's disease, Bba-Mol Basis Dis, 1502 (2000) 139-144.
[109] W.R. Markesbery, Oxidative stress hypothesis in Alzheimer's disease, Free Radical Bio Med, 23 (1997) 134-147.
[110] H. Tsutsui, S. Kinugawa, S. Matsushima, Oxidative stress and heart failure, Am J Physiol Heart Circ Physiol, 301 (2011) H2181-2190.
[111] D.J. Grieve, A.M. Shah, Oxidative stress in heart failure - More than just damage, Eur Heart J, 24 (2003) 2161-2163.
[112] S.H. Lee, M.K. Gupta, J.B. Bang, H. Bae, H.-J. Sung, Current Progress in Reactive Oxygen Species (ROS)-Responsive Materials for Biomedical Applications, Advanced Healthcare Materials, 2 (2013) 908–915.
[113] A. Napoli, M. Valentini, N. Tirelli, M. Muller, J.A. Hubbell, Oxidation-responsive polymeric vesicles, Nat Mater, 3 (2004) 183-189.

[114] V.V. Khutoryanskiy, N. Tirelli, Oxidation-responsiveness of nanomaterials for targeting inflammatory reactions, Pure Appl Chem, 80 (2008) 1703-1718.
[115] P. Han, N. Ma, H. Ren, H. Xu, Z. Li, Z. Wang, X. Zhang, Oxidation-responsive micelles based on a selenium-containing polymeric superamphiphile, Langmuir, 26 (2010) 14414-14418.
[116] N. Ma, Y. Li, H.F. Ren, H.P. Xu, Z.B. Li, X. Zhang, Selenium-containing block copolymers and their oxidation-responsive aggregates, Polym Chem-Uk, 1 (2010) 1609-1614.
[117] K.E. Broaders, S. Grandhe, J.M. Frechet, A biocompatible oxidation-triggered carrier polymer with potential in therapeutics, J Am Chem Soc, 133 (2011) 756-758.
[118] C. de Gracia Lux, S. Joshi-Barr, T. Nguyen, E. Mahmoud, E. Schopf, N. Fomina, A. Almutairi, Biocompatible polymeric nanoparticles degrade and release cargo in response to biologically relevant levels of hydrogen peroxide, J Am Chem Soc, 134 (2012) 15758-15764.
[119] M. Kuhlmann, S. Singh, J. Groll, Controlled ring-opening polymerization of substituted episulfides for side-chain functional polysulfide-based amphiphiles, Macromol Rapid Commun, 33 (2012) 1482-1486.
[120] C.E. Hoyle, A.B. Lowe, C.N. Bowman, Thiol-click chemistry: a multifaceted toolbox for small molecule and polymer synthesis, Chem Soc Rev, 39 (2010) 1355-1387.
[121] J. Han, Y. Zheng, B. Zhao, S. Li, Y. Zhang, C. Gao, Sequentially Hetero-functional, Topological Polymers by Step-growth Thiol-yne Approach, Sci. Rep., 4 (2014).
[122] C.D. Vo, G. Kilcher, N. Tirelli, Polymers and Sulfur: what are Organic Polysulfides Good For? Preparative Strategies and Biological Applications, Macromol Rapid Comm, 30 (2009) 299-315.
[123] M.K. Gupta, T.A. Meyer, C.E. Nelson, C.L. Duvall, Poly(PS-b-DMA) micelles for reactive oxygen species triggered drug release, J Control Release, 162 (2012) 591-598.
[124] D. Velluto, D. Demurtas, J.A. Hubbell, PEG-b-PPS Diblock Copolymer Aggregates for Hydrophobic Drug Solubilization and Release: Cyclosporin A as an Example, Molecular Pharmaceutics, 5 (2008) 632-642.
[125] P. Hu, N. Tirelli, Scavenging ROS: Superoxide Dismutase/Catalase Mimetics by the Use of an Oxidation-Sensitive Nanocarrier/Enzyme Conjugate, Bioconjugate Chem, 23 (2012) 438-449.
[126] E.A. Mahmoud, J. Sankaranarayanan, J.M. Morachis, G. Kim, A. Almutairi, Inflammation Responsive Logic Gate Nanoparticles for the Delivery of Proteins, Bioconjugate Chem, 22 (2011) 1416-1421.
[127] C.S. Marvel, R.R. Chambers, Polyalkylene Sulfides from Diolefins and Dimercaptans, Journal of the American Chemical Society, 70 (1948) 993-998.
[128] E. Takeshi, M. Kazuhide, Molecular Design and Polymerization Behavior of Monomers Polymerizable via Radical Ring-opening, in: Controlled/Living Radical Polymerization: Progress in ATRP, American Chemical Society, 2009, pp. 33-48.
[129] E. Ranucci, F. Bignotti, P. Ferruti, M. Casolaro, New polymeric acids containing potentially hydrolyzable bonds, Macromolecules, 24 (1991) 4554-4558.
[130] C.S. Marvel, E.H.H. Shen, R.R. Chambers, Polymercaptals and Polymercaptols1, Journal of the American Chemical Society, 72 (1950) 2106-2109.
[131] B. Tarasiuk, W. Podkoscielny, W. Majewski, Products of polycondensation of 4,4′-biphenyldithiol with some hydrocarbon dihalides, Die Angewandte Makromolekulare Chemie, 251 (1997) 13-21.
[132] O. Nuyken, F. Siebzehnrübl, Novel sulfur-containing telechelics with alternating aliphatic-aromatic structure units, Polymer Bulletin, 19 (1988) 371-375.

[133] T. Posner, Beiträge zur Kenntniss der ungesättigten Verbindungen. II. Ueber die Addition von Mercaptanen an ungesättigte Kohlenwasserstoffe, Berichte der deutschen chemischen Gesellschaft, 38 (1905) 646-657.
[134] Correspondence, Journal of the Society of Chemical Industry, 57 (1938) 752-754.
[135] C.E. Hoyle, T.Y. Lee, T. Roper, Thiol–enes: Chemistry of the past with promise for the future, Journal of Polymer Science Part A: Polymer Chemistry, 42 (2004) 5301-5338.
[136] T. Clark, L. Kwisnek, C.E. Hoyle, S. Nazarenko, Photopolymerization of Thiol-Ene Systems Based on Oligomeric Thiols, J Polym Sci Pol Chem, 47 (2009) 14-24.
[137] M. Heggli, N. Tirelli, A. Zisch, J.A. Hubbell, Michael-type addition as a tool for surface functionalization, Bioconjug Chem, 14 (2003) 967-973.
[138] N.A. LeBel, A. DeBoer, Stereochemistry of the free-radical addition of thiolacetic acid to 2-chloro-4-tert-butylcyclohexene, Journal of the American Chemical Society, 89 (1967) 2784-2785.
[139] J.F. Harris, F.W. Stacey, The Free Radical Addition of Trifluoromethanethiol to Fluoroölefins, Journal of the American Chemical Society, 83 (1961) 840-845.
[140] J.F. Harris, F.W. Stacey, The Free Radical Addition of Hydrogen Sulfide to Fluoroethylenes, Journal of the American Chemical Society, 85 (1963) 749-754.
[141] N.A. LeBel, R.F. Czaja, A. DeBoer, Stereochemistry of free-radical additions of thiols to substituted cyclohexenes, The Journal of Organic Chemistry, 34 (1969) 3112-3126.
[142] W.B. Motherwell, B.C. Ross, M.J. Tozer, Some Radical Reactions of Exocyclic Carbohydrate Difluoroenol Ethers, Synlett, 1989 (1989) 68-70.
[143] J. Yoshida, S. Nakatani, S. Isoe, Electroinitiated oxygenation of alkenyl sulfides and alkynes in the presence of thiophenol, The Journal of Organic Chemistry, 58 (1993) 4855-4865.
[144] K. Boustany, Chemistry of sulfur compounds. Selectivity of addition of thiyl radicals to terminal olefins, Journal of Chemical & Engineering Data, 17 (1972) 104-106.
[145] W. El Khatib, B. Youssef, C. Bunel, B. Mortaigne, Fireproofing of polyurethane elastomers by reactive organophosphonates, Polymer International, 52 (2003) 146-152.
[146] M.S. Kharasch, W. Nudenberg, G.J. Mantell, REACTIONS OF ATOMS AND FREE RADICALS IN SOLUTION. XXV. THE REACTIONS OF OLEFINS WITH MERCAPTANS IN THE PRESENCE OF OXYGEN1, The Journal of Organic Chemistry, 16 (1951) 524-532.
[147] J.M. Narayanam, C.R. Stephenson, Visible light photoredox catalysis: applications in organic synthesis, Chem Soc Rev, 40 (2011) 102-113.
[148] Q. Li, H. Zhou, D.A. Wicks, C.E. Hoyle, Thiourethane-based thiol-ene high Tg networks: Preparation, thermal, mechanical, and physical properties, Journal of Polymer Science Part A: Polymer Chemistry, 45 (2007) 5103-5111.
[149] B.D. Fairbanks, T.F. Scott, C.J. Kloxin, K.S. Anseth, C.N. Bowman, Thiol−Yne Photopolymerizations: Novel Mechanism, Kinetics, and Step-Growth Formation of Highly Cross-Linked Networks, Macromolecules, 42 (2008) 211-217.
[150] J.-P. Bégué, D. Bonnet-Delpon, A. Kornilov, Synthesis of 3-(Alkylthio and Phenylthio)-1,1,1-trifluoroalkan-2-ones via Ring Opening of Epoxy Ethers, Synthesis, 1996 (1996) 529-532.
[151] V. Kesavan, D. Bonnet-Delpon, J.-P. Bégué, Fluoro alcohol as reaction medium: one-pot synthesis of β-hydroxy sulfoxides from epoxides, Tetrahedron Letters, 41 (2000) 2895-2898.
[152] M. Chini, P. Crotti, L.A. Flippin, F. Macchia, Regiochemical control of the ring-opening of 1,2-epoxides by means of chelating processes. 3. Aminolysis and azidolysis of the cis- and trans-oxides derived from 4-(benzyloxy)cyclohexene, The Journal of Organic Chemistry, 56 (1991) 7043-7048.

[153] P. Wipf, P. Jeger, Y. Kim, Thiophilic ring-opening and rearrangement reactions of epoxyketone natural products, Bioorganic & Medicinal Chemistry Letters, 8 (1998) 351-356.
[154] E.J. Corey, D.A. Clark, G. Goto, A. Marfat, C. Mioskowski, B. Samuelsson, S. Hammarstroem, Stereospecific total synthesis of a "slow reacting substance" of anaphylaxis, leukotriene C-1, Journal of the American Chemical Society, 102 (1980) 1436-1439.
[155] J.A. Carioscia, J.W. Stansbury, C.N. Bowman, Evaluation and Control of Thiol-ene/Thiol-epoxy Hybrid Networks, Polymer (Guildf), 48 (2007) 1526-1532.
[156] C.L. Ventola, The Nanomedicine Revolution: Part 2: Current and Future Clinical Applications, Pharmacy and Therapeutics, 37 (2012) 582-591.
[157] S. Cohen, D. Janicki-Deverts, W.J. Doyle, G.E. Miller, E. Frank, B.S. Rabin, R.B. Turner, Chronic stress, glucocorticoid receptor resistance, inflammation, and disease risk, Proceedings of the National Academy of Sciences, 109 (2012) 5995-5999.
[158] A. Mantovani, P. Allavena, A. Sica, F. Balkwill, Cancer-related inflammation, Nature, 454 (2008) 436-444.
[159] R. Medzhitov, Origin and physiological roles of inflammation, Nature, 454 (2008) 428-435.
[160] S. Mpofu, C.M.A. Mpofu, D. Hutchinson, A.E. Maier, S.R. Dodd, R.J. Moots, Steroids, non-steroidal anti-inflammatory drugs, and sigmoid diverticular abscess perforation in rheumatic conditions, Ann Rheum Dis, 63 (2004) 588-590.
[161] F. Richy, O. Bruyere, O. Ethgen, V. Rabenda, G. Bouvenot, M. Audran, G. Herrero-Beaumont, A. Moore, R. Eliakim, M. Haim, J.-Y. Reginster, Time dependent risk of gastrointestinal complications induced by non-steroidal anti-inflammatory drug use: a consensus statement using a meta-analytic approach, Ann Rheum Dis, 63 (2004) 759-766.
[162] R.D. Mathison, J.S. Davison, A.D. Befus, D.A. Gingerich, Salivary gland derived peptides as a new class of anti-inflammatory agents: review of preclinical pharmacology of C-terminal peptides of SMR1 protein, Journal of Inflammation (London, England), 7 (2010) 49-49.
[163] J.M. Chalmers, R.J. Meier, Molecular characterization and analysis of polymers, Elsevier, Amsterdam ; London, 2008.
[164] D.J. Gardiner, P.R. Graves, H.J. Bowley, Practical Raman spectroscopy, Springer-Verlag, Berlin, 1989.
[165] H.G.M. Edwards, A.F. Johnson, I.R. Lewis, Applications of Raman spectroscopy to the study of polymers and polymerization processes, Journal of Raman Spectroscopy, 24 (1993) 475-483.
[166] T. Owen, Fundamentals of Modern UV-visible Spectroscopy: Primer, Agilent Technologies, 2000.
[167] Suppression of Multiple Scattering by Photon Cross-correlation Techniques, Journal of Modern Optics, 38 (1991) 1849.
[168] J.B. Pawley, Handbook of biological confocal microscopy, 3rd ed. ed., Springer, New York, NY, 2006.
[169] H. Fessi, F. Puisieux, J.P. Devissaguet, N. Ammoury, S. Benita, Nanocapsule formation by interfacial polymer deposition following solvent displacement, International Journal of Pharmaceutics, 55 (1989) R1-R4.
[170] J.M. Barichello, M. Morishita, K. Takayama, T. Nagai, Encapsulation of hydrophilic and lipophilic drugs in PLGA nanoparticles by the nanoprecipitation method, Drug Dev Ind Pharm, 25 (1999) 471-476.
[171] S. Schubert, J.T. Delaney, U.S. Schubert, Nanoprecipitation and nanoformulation of polymers: from history to powerful possibilities beyond poly(lactic acid), Soft Matter, 7 (2011) 1581-1588.

[172] S. Galindo-Rodriguez, E. Allemann, H. Fessi, E. Doelker, Physicochemical parameters associated with nanoparticle formation in the salting-out, emulsification-diffusion, and nanoprecipitation methods, Pharm Res, 21 (2004) 1428-1439.
[173] D. Quintanar-Guerrero, E. Allémann, H. Fessi, E. Doelker, Preparation Techniques and Mechanisms of Formation of Biodegradable Nanoparticles from Preformed Polymers, Drug Development and Industrial Pharmacy, 24 (1998) 1113-1128.
[174] J. Aubry, F. Ganachaud, J.-P. Cohen Addad, B. Cabane, Nanoprecipitation of Polymethylmethacrylate by Solvent Shifting:1. Boundaries, Langmuir, 25 (2009) 1970-1979.
[175] A.L. Le Roy Boehm, R. Zerrouk, H. Fessi, Poly epsilon-caprolactone nanoparticles containing a poorly soluble pesticide: formulation and stability study, J Microencapsul, 17 (2000) 195-205.
[176] T. Govender, S. Stolnik, M.C. Garnett, L. Illum, S.S. Davis, PLGA nanoparticles prepared by nanoprecipitation: drug loading and release studies of a water soluble drug, Journal of Controlled Release, 57 (1999) 171-185.
[177] S. Schubert, J.J.T. Delaney, U.S. Schubert, Nanoprecipitation and nanoformulation of polymers: from history to powerful possibilities beyond poly(lactic acid), Soft Matter, 7 (2011) 1581-1588.
[178] L. Mu, S.S. Feng, A novel controlled release formulation for the anticancer drug paclitaxel (Taxol®): PLGA nanoparticles containing vitamin E TPGS, Journal of Controlled Release, 86 (2003) 33-48.
[179] H. Jeffery, S.S. Davis, D.T. O'Hagan, The preparation and characterisation of poly(lactide-co-glycolide) microparticles. I: Oil-in-water emulsion solvent evaporation, International Journal of Pharmaceutics, 77 (1991) 169-175.
[180] E.A. Mahmoud, J. Sankaranarayanan, J.M. Morachis, G. Kim, A. Almutairi, Inflammation responsive logic gate nanoparticles for the delivery of proteins, Bioconjug Chem, 22 (2011) 1416-1421.
[181] M.F. Zambaux, F. Bonneaux, R. Gref, P. Maincent, E. Dellacherie, M.J. Alonso, P. Labrude, C. Vigneron, Influence of experimental parameters on the characteristics of poly(lactic acid) nanoparticles prepared by a double emulsion method, Journal of Controlled Release, 50 (1998) 31-40.
[182] Y. Ogawa, M. Yamamoto, H. Okada, T. Yashiki, T. Shimamoto, A New Technique to Efficiently Entrap Leuprolide Acetate into Microcapsules of Polylactic Acid or Copoly(Lactic Glycolic) Acid, Chem Pharm Bull, 36 (1988) 1095-1103.
[183] F.T. Meng, G.H. Ma, W. Qiu, Z.G. Su, W/O/W double emulsion technique using ethyl acetate as organic solvent: effects of its diffusion rate on the characteristics of microparticles, Journal of Controlled Release, 91 (2003) 407-416.
[184] J. Liu, Z. Qiu, S. Wang, L. Zhou, S. Zhang, A modified double-emulsion method for the preparation of daunorubicin-loaded polymeric nanoparticle with enhanced in vitro anti-tumor activity, Biomed Mater, 5 (2010) 065002.
[185] T. Delmas, A. Fraichard, P.-A. Bayle, I. Texier, M. Bardet, J. Baudry, J. Bibette, A.-C. Couffin, Encapsulation and Release Behavior from Lipid Nanoparticles: Model Study with Nile Red Fluorophore, Journal of Colloid Science and Biotechnology, 1 (2012) 16-25.
[186] P. Xu, E. Gullotti, L. Tong, C.B. Highley, D.R. Errabelli, T. Hasan, J.-X. Cheng, D.S. Kohane, Y. Yeo, Intracellular drug delivery by poly(lactic-co-glycolic acid) nanoparticles, revisited, Molecular pharmaceutics, 6 (2009) 190-201.
[187] T. Mosmann, Rapid colorimetric assay for cellular growth and survival: Application to proliferation and cytotoxicity assays, Journal of Immunological Methods, 65 (1983) 55-63.
[188] R. Qi, M. Shen, X. Cao, R. Guo, X. Tian, J. Yu, X. Shi, Exploring the dark side of MTT viability assay of cells cultured onto electrospun PLGA-based composite nanofibrous scaffolding materials, Analyst, 136 (2011) 2897-2903.

[189] I. Amjadi, M. Rabiee, M.-S. Hosseini, Anticancer Activity of Nanoparticles Based on PLGA and its Co-polymer: In-vitro Evaluation, Iranian Journal of Pharmaceutical Research : IJPR, 12 (2013) 623-634.
[190] S. Bisht, G. Feldmann, S. Soni, R. Ravi, C. Karikar, A. Maitra, A. Maitra, Polymeric nanoparticle-encapsulated curcumin ("nanocurcumin"): a novel strategy for human cancer therapy, Journal of Nanobiotechnology, 5 (2007) 3.
[191] B.D. Fairbanks, T.F. Scott, C.J. Kloxin, K.S. Anseth, C.N. Bowman, Thiol−Yne Photopolymerizations: Novel Mechanism, Kinetics, and Step-Growth Formation of Highly Cross-Linked Networks, Macromolecules, 42 (2009) 211-217.
[192] O. Turunc, M.A.R. Meier, A novel polymerization approach via thiol-yne addition (vol 50, pg 1689, 2012), J Polym Sci Pol Chem, 50 (2012) 3466-3466.
[193] Y. Cheng, J. Hao, L.A. Lee, M.C. Biewer, Q. Wang, M.C. Stefan, Thermally controlled release of anticancer drug from self-assembled gamma-substituted amphiphilic poly(epsilon-caprolactone) micellar nanoparticles, Biomacromolecules, 13 (2012) 2163-2173.
[194] M. Giorgio, M. Trinei, E. Migliaccio, P.G. Pelicci, Hydrogen peroxide: a metabolic by-product or a common mediator of ageing signals?, Nat Rev Mol Cell Biol, 8 (2007) 722-728.
[195] A. Brandle, A. Khan, Thiol-epoxy 'click' polymerization: efficient construction of reactive and functional polymers, Polym Chem-Uk, 3 (2012) 3224-3227.
[196] J. Vandenbergh, M. Peeters, T. Kretschmer, P. Wagner, T. Junkers, Cross-linked degradable poly(β-thioester) networks via amine-catalyzed thiol-ene click polymerization, Polymer, 55 (2014) 3525-3532.

Appendices

Appendix A

Appendix A (a-f) ^{1}H NMR spectrum of polysulfide's synthesized by thiol-yne reactions.

Appendix B

Appendix B (a-e) ^{1}H NMR spectrum of poly (β-hydroxy thioethers) synthesized by thiol-epoxide reactions.

Appendix C

Appendix C (a-f) ^{1}H NMR spectrum of poly (β-thioesters) synthesized by thiol-ene reactions.

Appendix D

Appendix D (a-b) Calibration curve for the determination of Nile Red encapsulation efficiency.

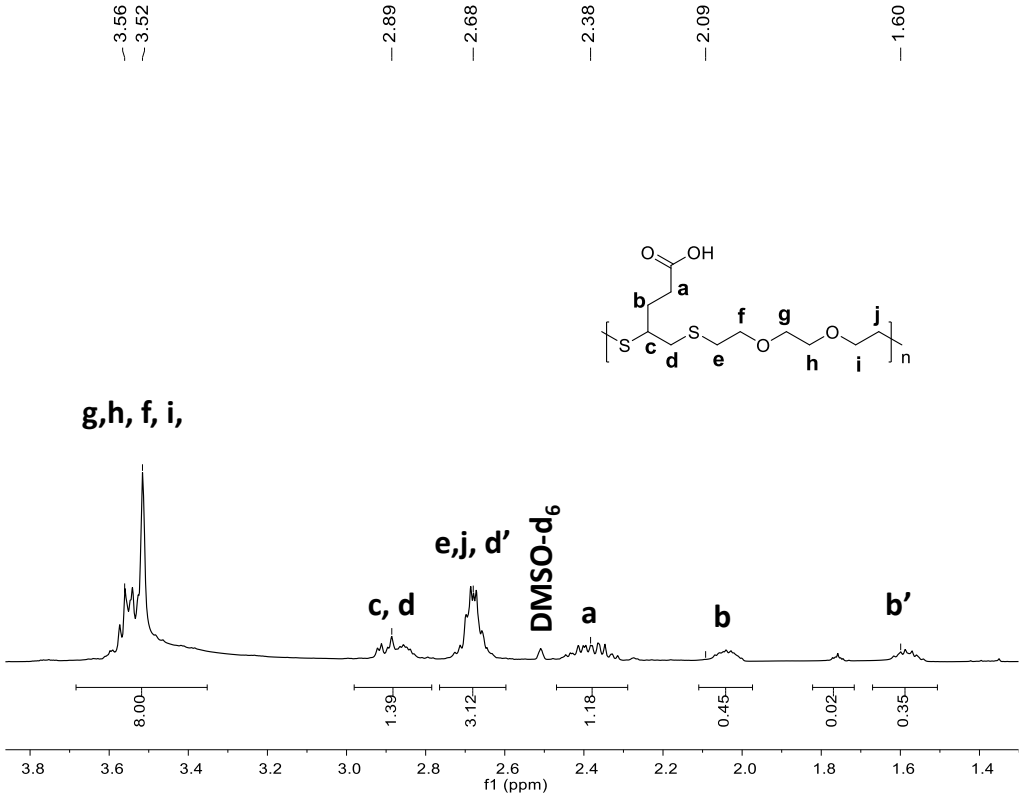

Appendix A a) *[1]H NMR spectrum of polymer AU*

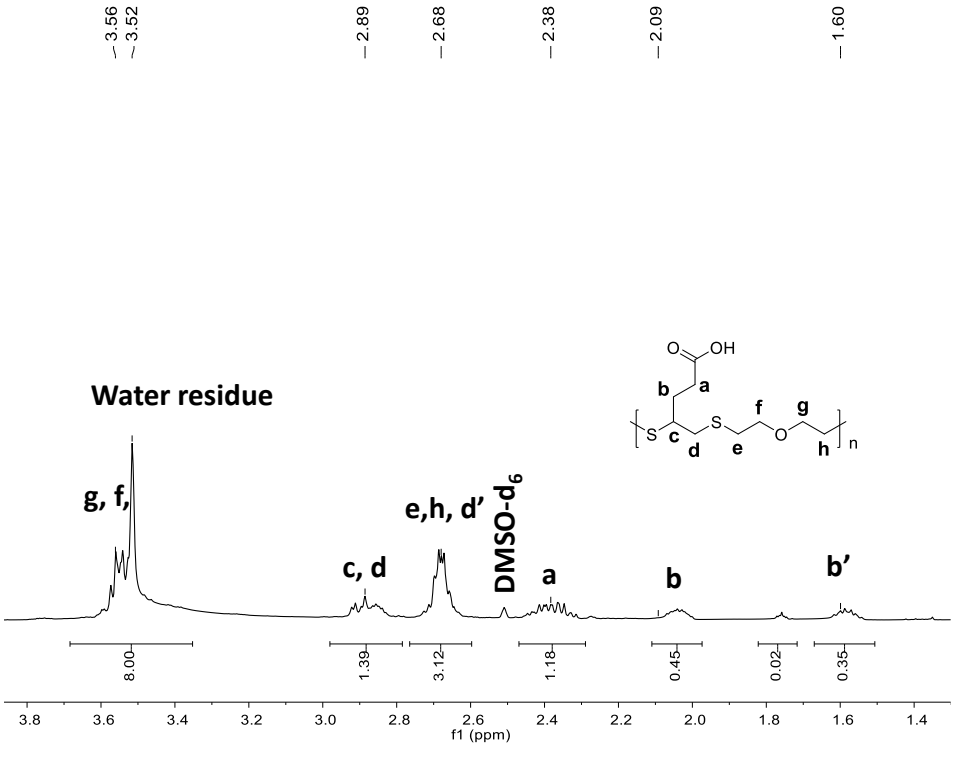

Appendix A b) *[1]H NMR spectrum of polymer AV*

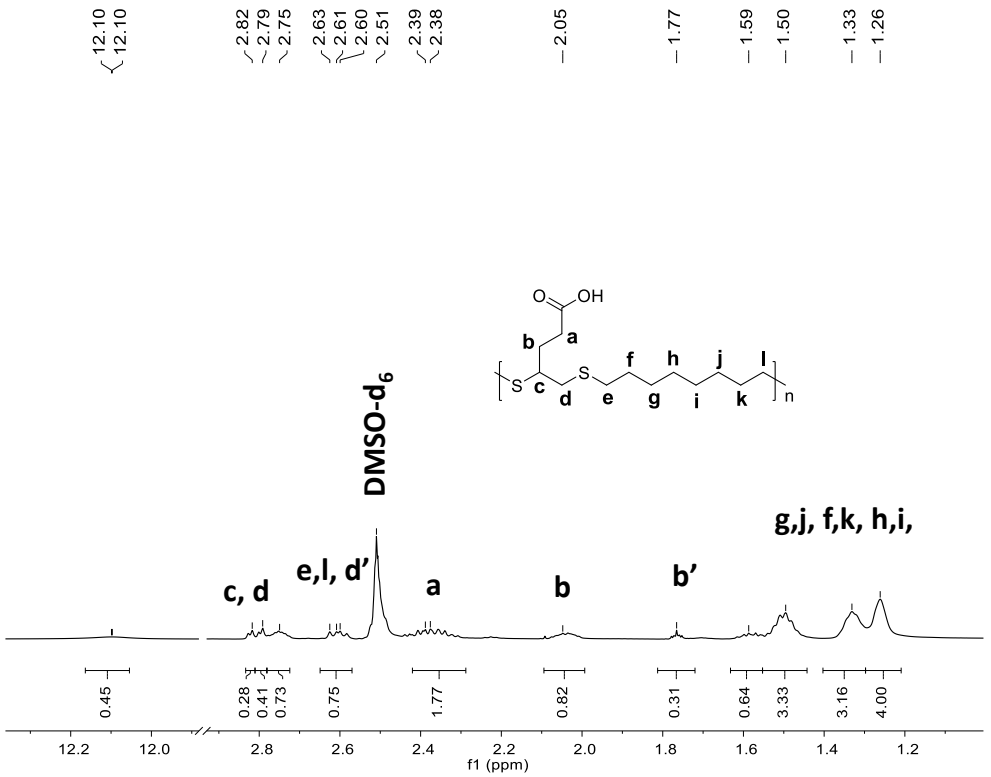

Appendix A c) *[1]H NMR spectrum of polymer AY*

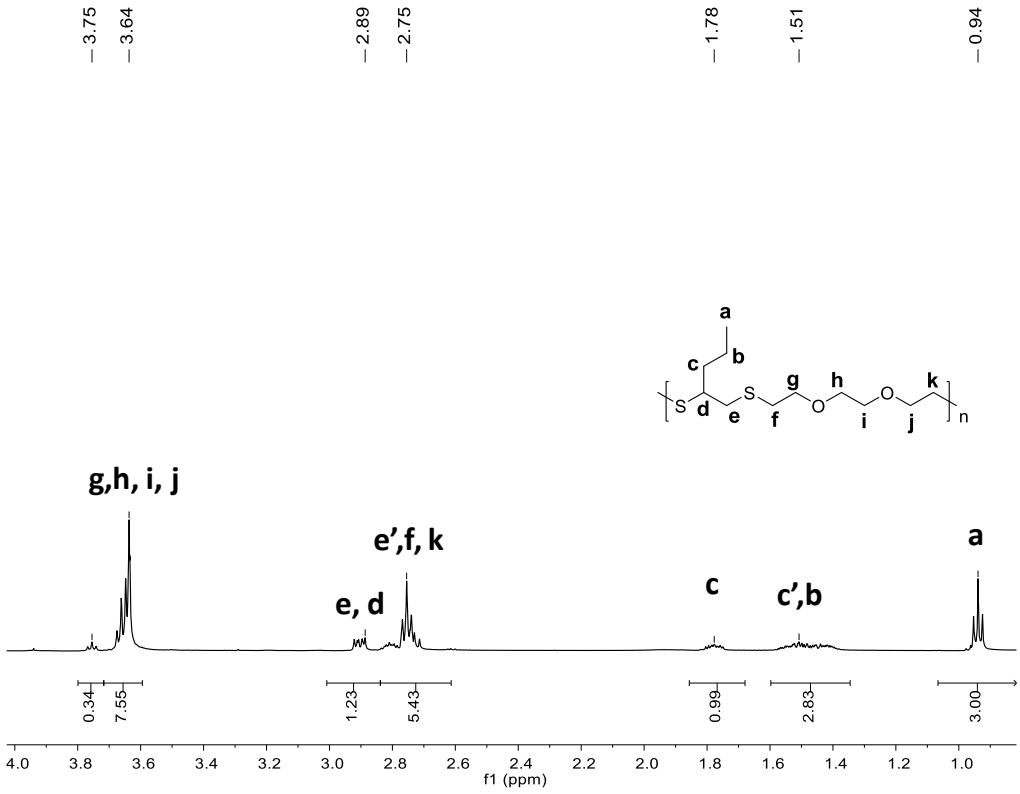

Appendix A d) *[1]H NMR spectrum of polymer EU*

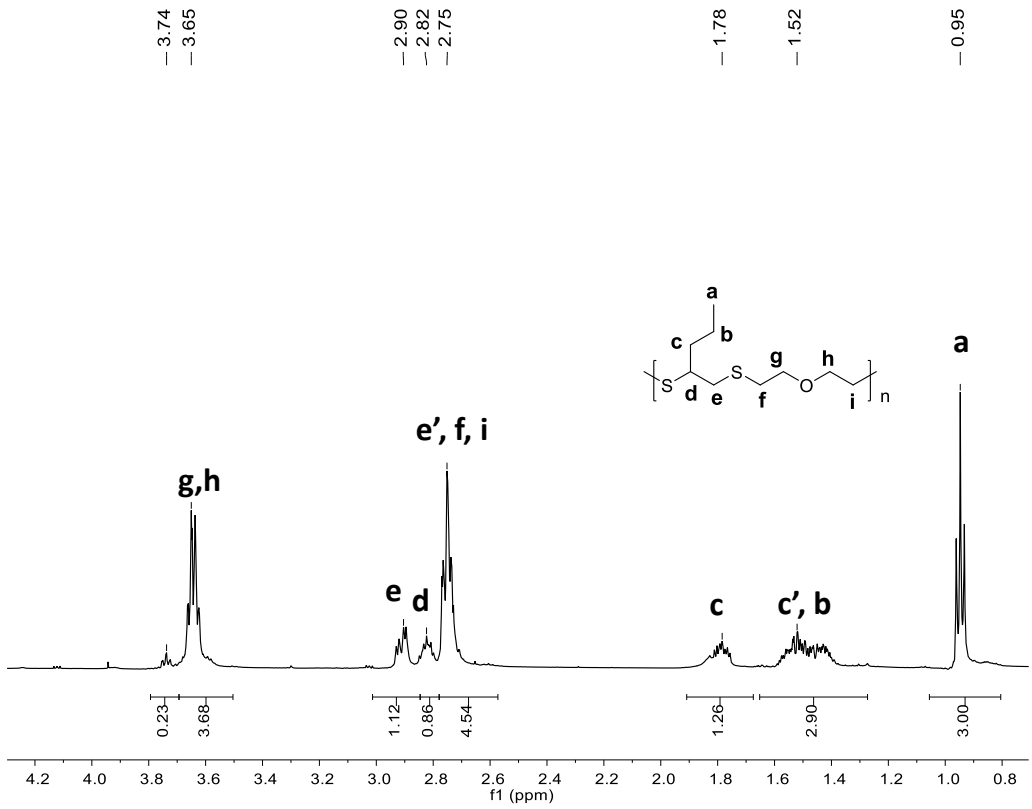

Appendix A e) *[1]H NMR spectrum of polymer EV*

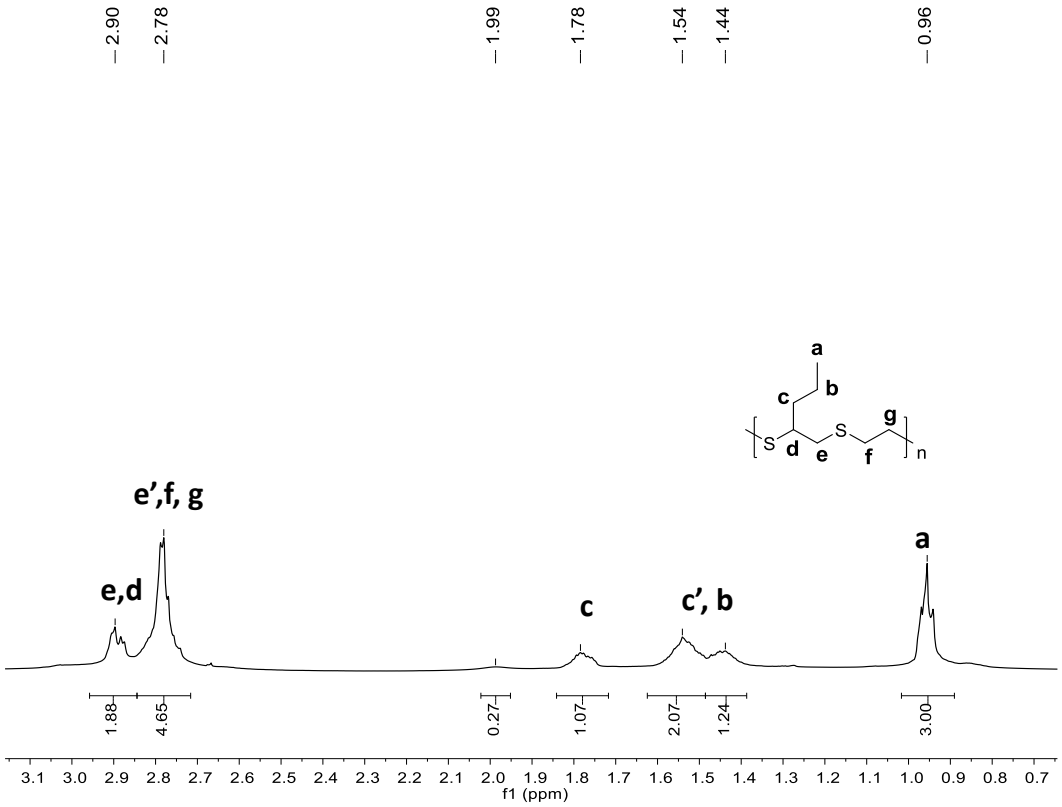

Appendix A f) *[1]H NMR spectrum of polymer ET*

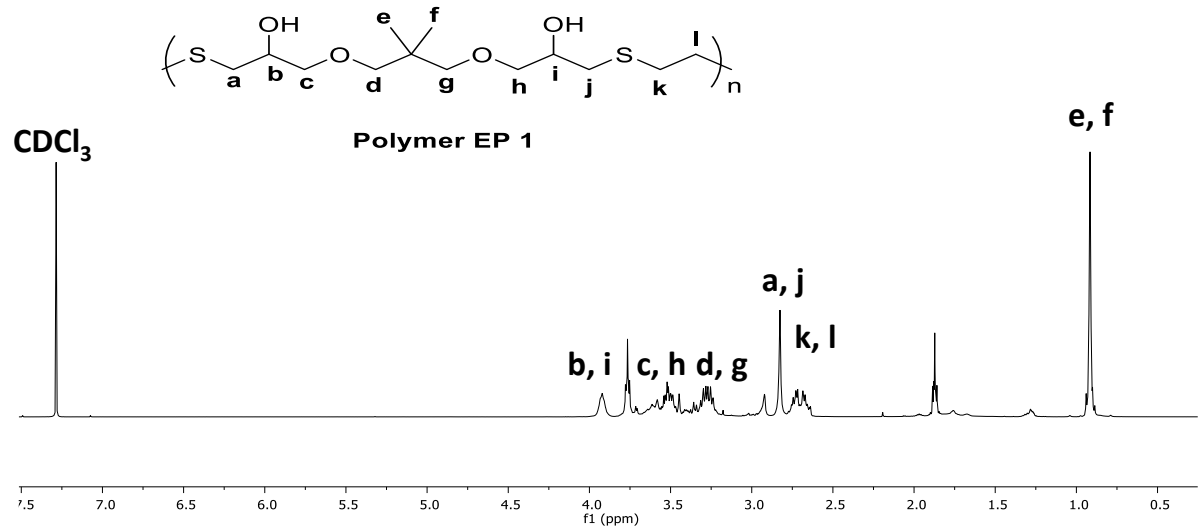

Appendix B a) *[1]H NMR spectrum of polymer EP1*

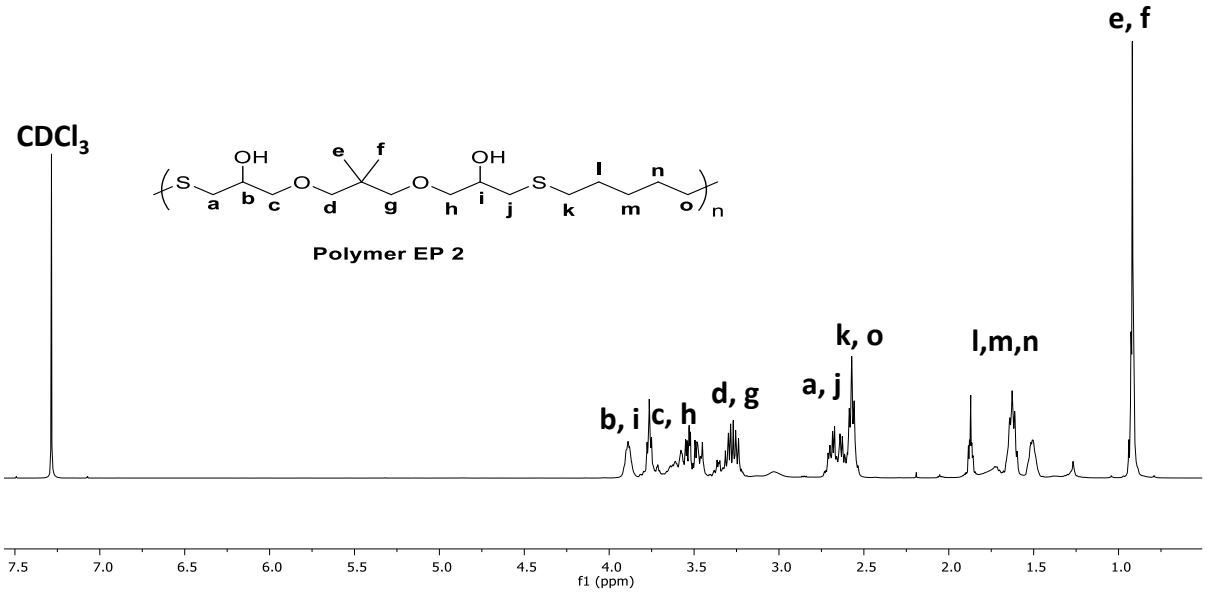

Appendix B b) *[1]H NMR spectrum of polymer EP2*

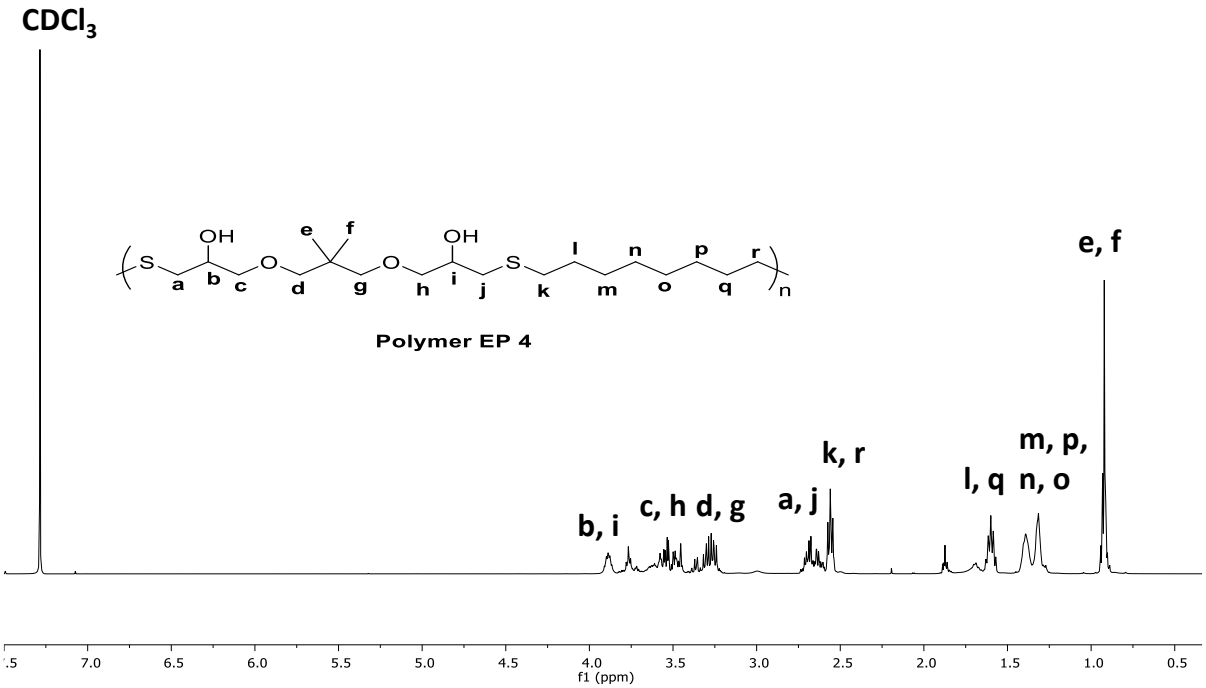

Appendix B c) *[1]H NMR spectrum of polymer EP4*

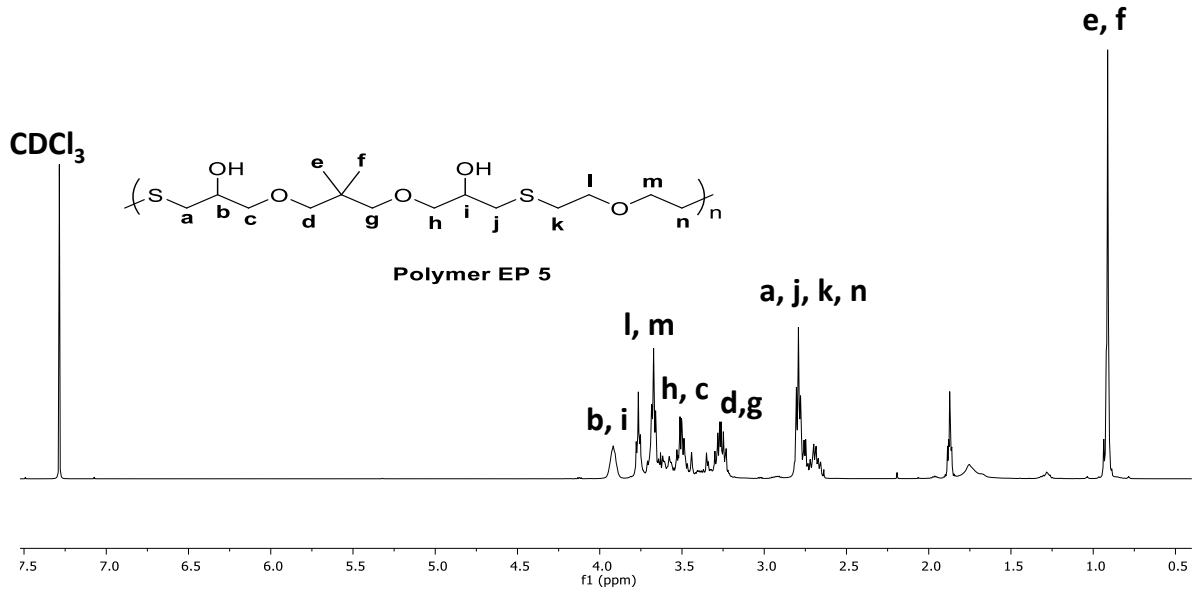

Appendix B d) *[1]H NMR spectrum of polymer EP5*

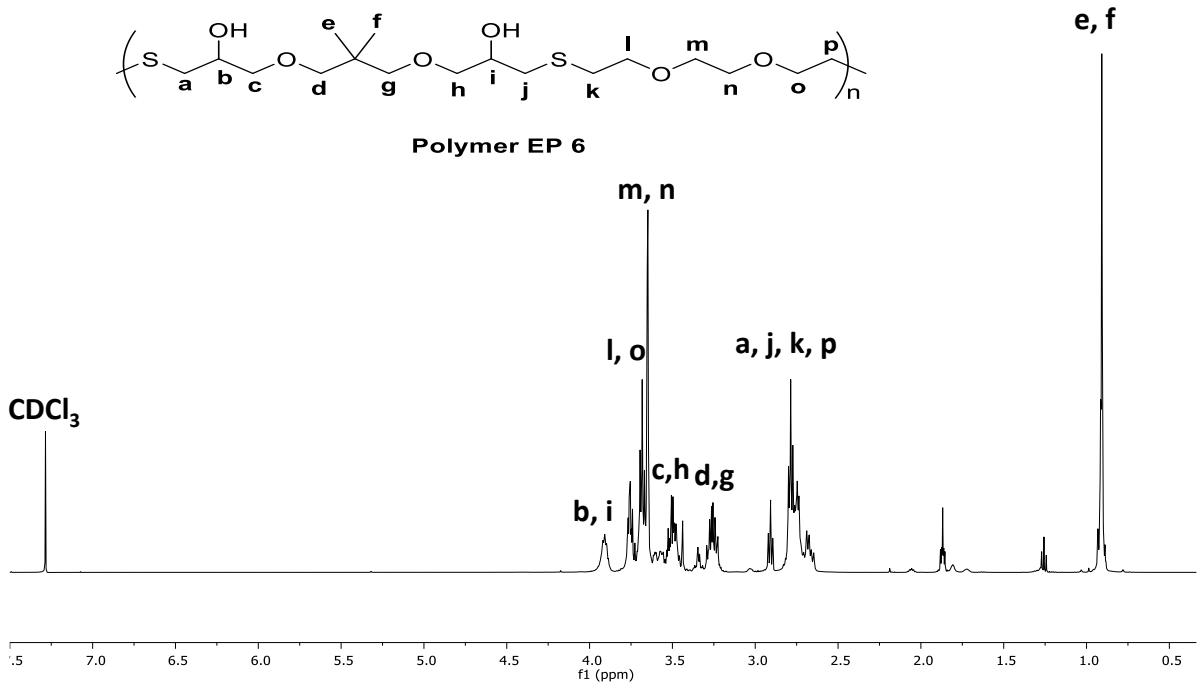

Appendix B e) *^{1}H NMR spectrum of polymer EP6*

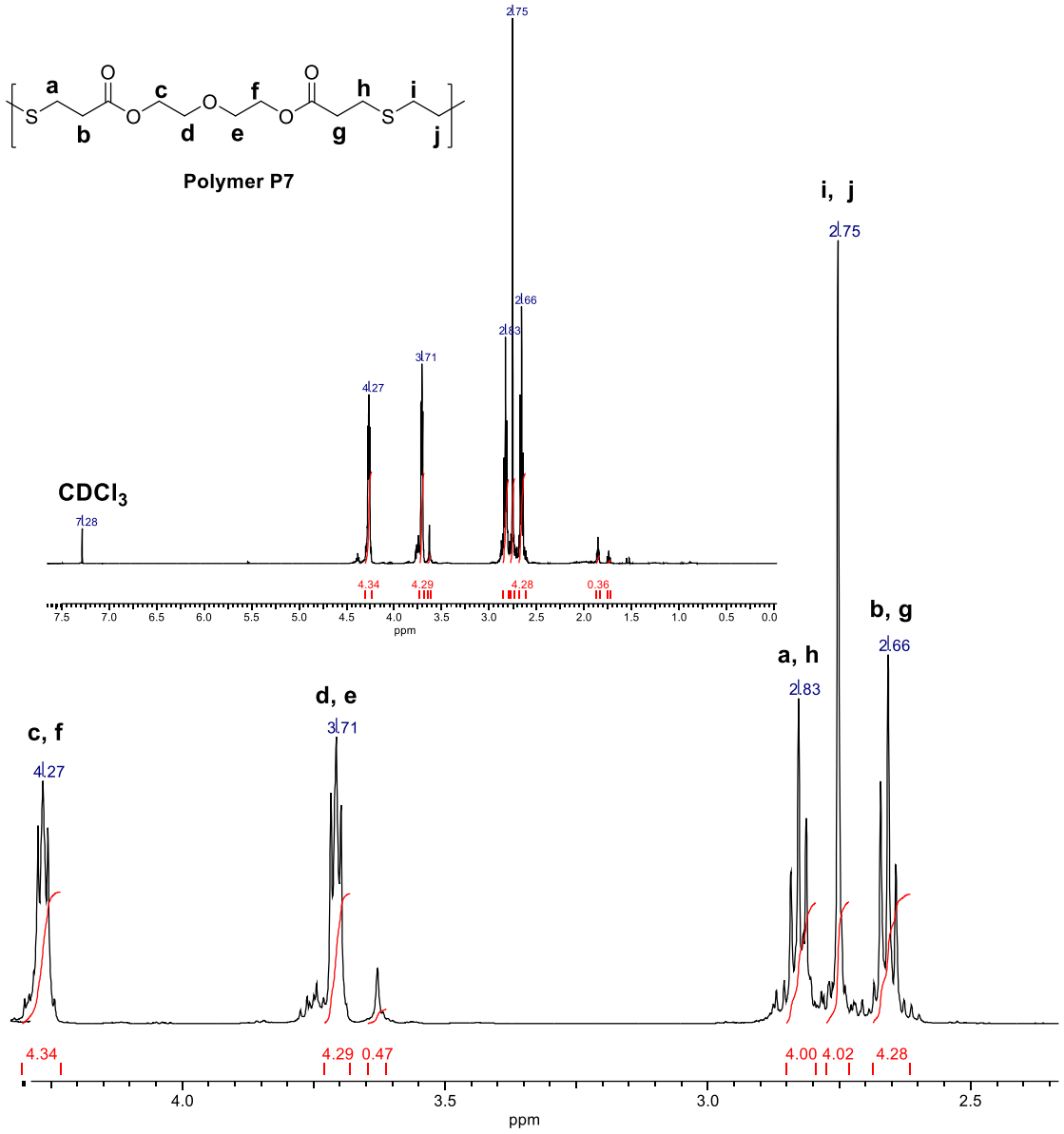

Appendix C a) *^{1}H NMR spectrum of polymer P7*

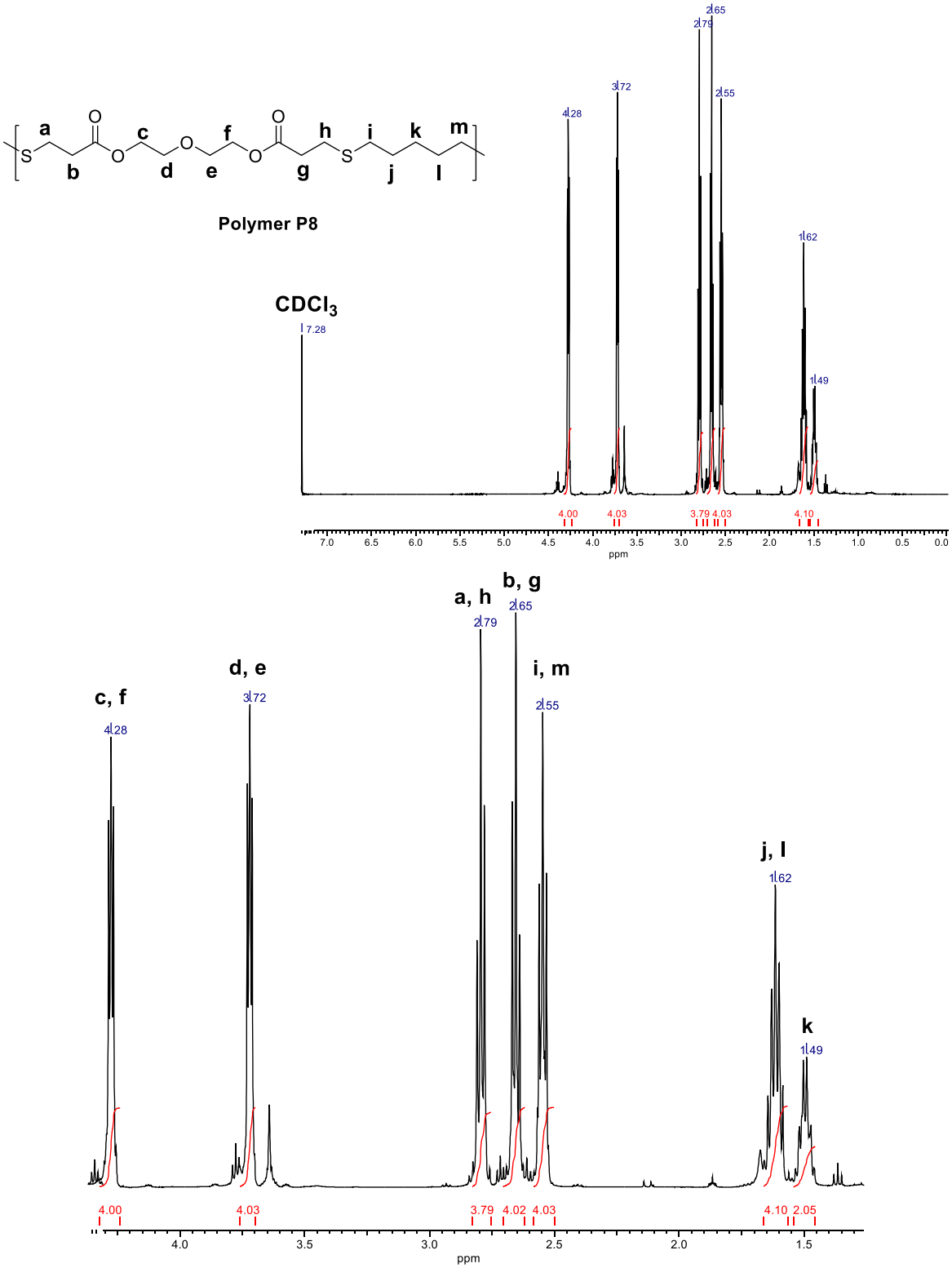

Appendix C b) *^{1}H NMR spectrum of polymer P8*

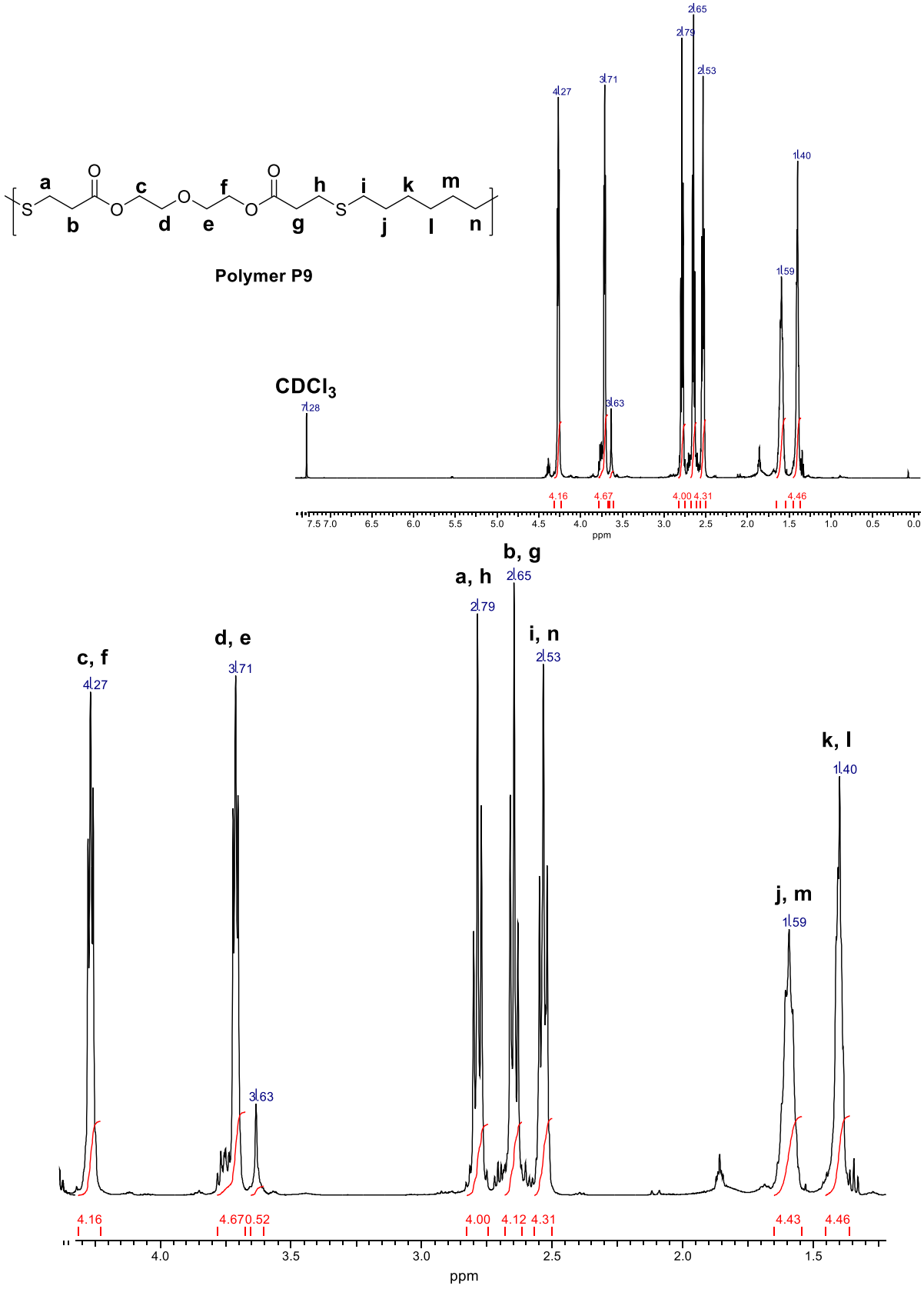

Appendix C c) *^{1}H NMR spectrum of polymer P9*

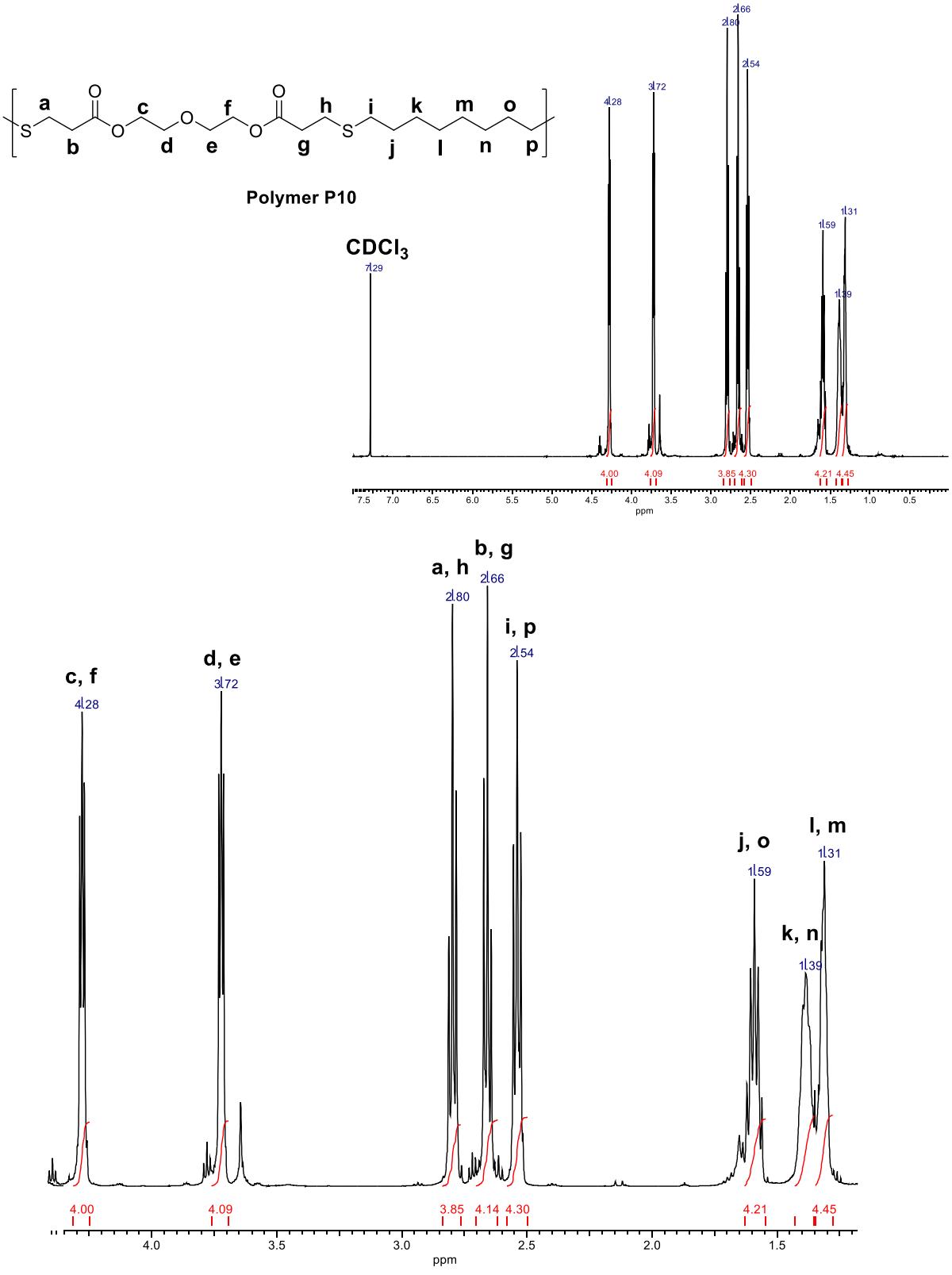

Appendix C d) *^{1}H NMR spectrum of polymer P10*

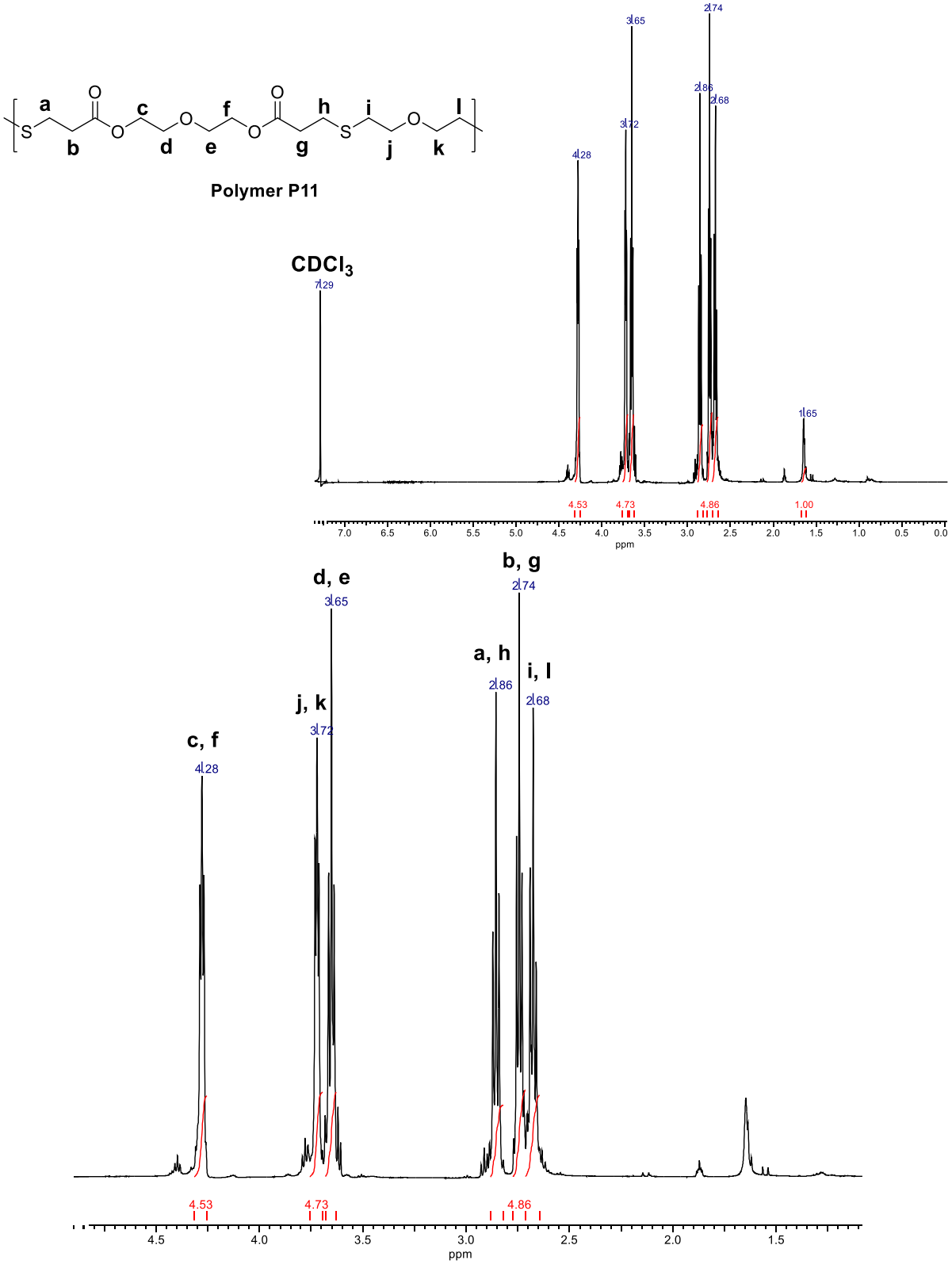

Appendix C e) *^{1}H NMR spectrum of polymer P11*

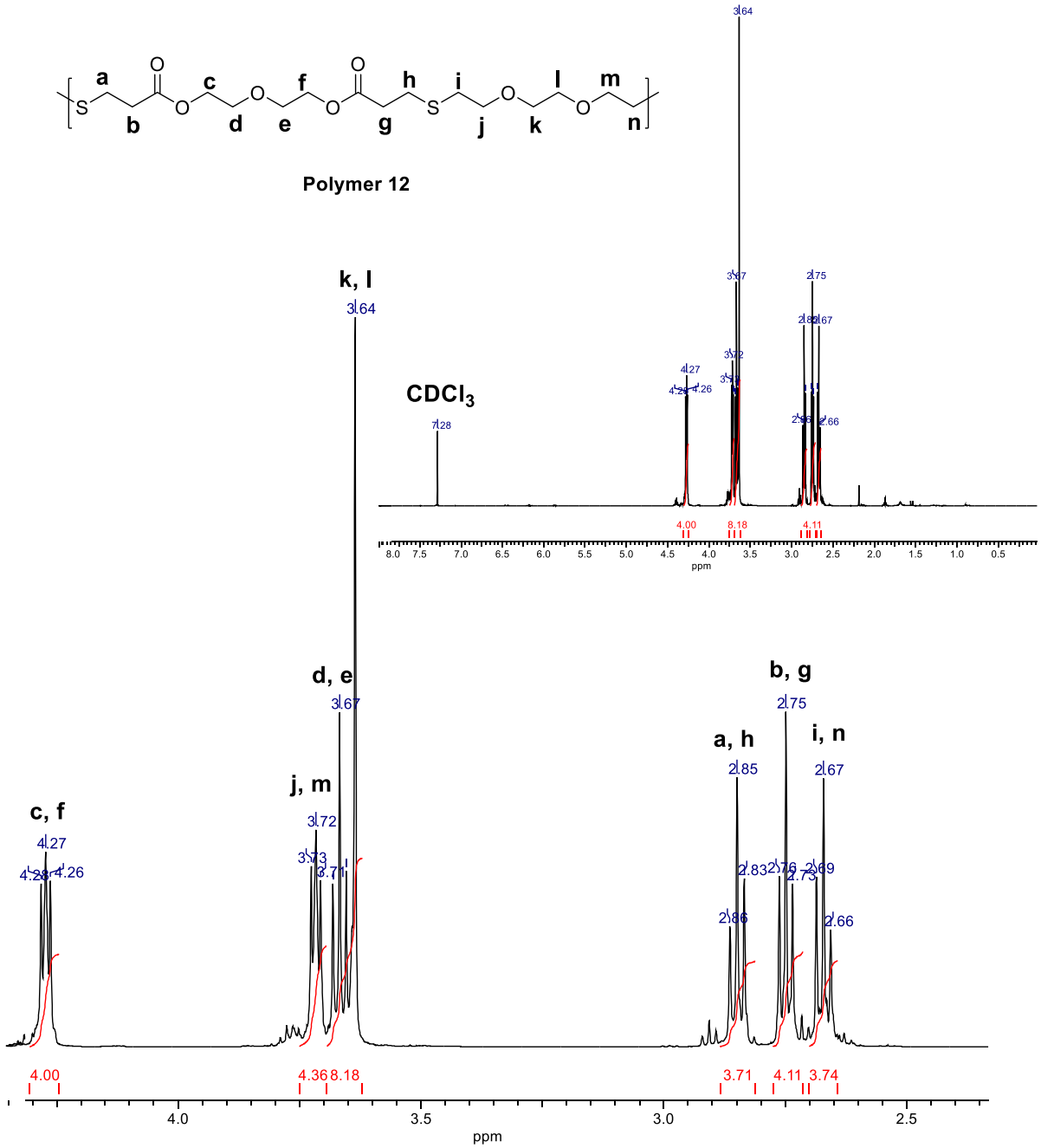

Appendix C f) *^{1}H NMR spectrum of polymer P12*

Appendix D Standard calibration curve for Nile red

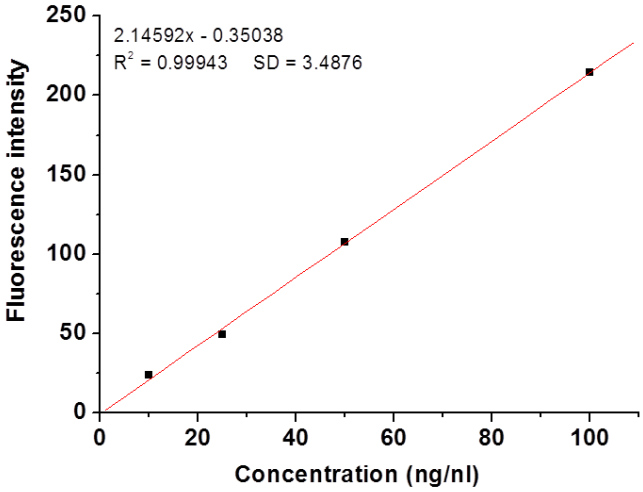

ppendix D a) *Standard calibration curve for Nile Red dissolved in THF*

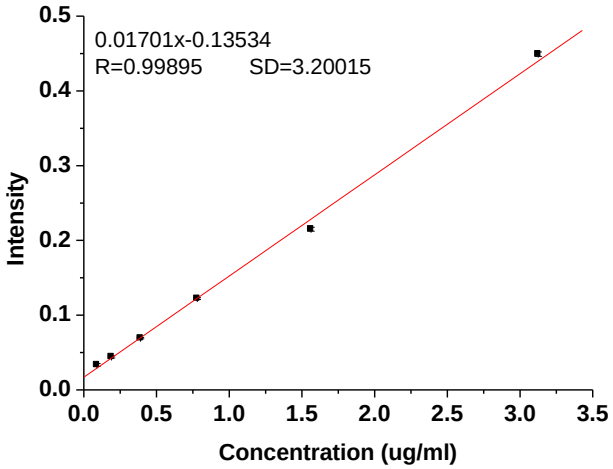

Appendix D b) *Standard calibration curve for Nile Red dissolved in acetone*

List of Publications

1. *Girish Shankara, Linxian Li, Maria Camila Blanco Jaimes, Alexander Efremov, Shubhangi Kakkar, Michael Grunze, Pavel A Levkin* Oxidation-responsive polymer nanoparticles via thiol-yne click reaction (Journal of Controlled Release, under revision).

2. *Girish Shankara, Yihang Wu, Linxian Li, Michael Grunze, Pavel A Levkin* Oxidation sensitive poly(β-hydroxy thioether) synthesized via base catalyzed thiol-epoxy ring opening polymerization. (under preparation)

3. *Girish Shankara, Yihang Wu, Linxian Li, Michael Grunze, Pavel A Levkin* Biodegradable poly(β-thioester)s nanoparticles synthesized via base-catalyzed Michael-type nucleophilic thiol-ene polyaddition. (under preparation)

Eidesstattliche Versicherung gemäß § 8 der Promotionsordnung der Naturwissenschaftlich-Mathematischen Gesamtfakultät der Universität Heidelberg

1. Bei der eingereichten Dissertation zu dem Thema

_____

_____

_____

handelt es sich um meine eigenständig erbrachte Leistung.

2. Ich habe nur die angegebenen Quellen und Hilfsmittel benutzt und mich keiner unzulässigen Hilfe Dritter bedient. Insbesondere habe ich wörtlich oder sinngemäß aus anderen Werken übernommene Inhalte als solche kenntlich gemacht.

3. Die Arbeit oder Teile davon habe ich wie folgt/bislang nicht[1)] an einer Hochschule des In- oder Auslands als Bestandteil einer Prüfungs- oder Qualifikationsleistung vorgelegt.

Titel der Arbeit:_____

_____

Hochschule und Jahr:_____

Art der Prüfungs- oder Qualifikationsleistung:_____

4. Die Richtigkeit der vorstehenden Erklärungen bestätige ich.

5. Die Bedeutung der eidesstattlichen Versicherung und die strafrechtlichen Folgen einer unrichtigen oder unvollständigen eidesstattlichen Versicherung sind mir bekannt.

Ich versichere an Eides statt, dass ich nach bestem Wissen die reine Wahrheit erklärt und nichts verschwiegen habe.

_____ _____

Ort und Datum Unterschrift

[1)] Nicht Zutreffendes streichen. Bei Bejahung sind anzugeben: der Titel der andernorts vorgelegten Arbeit, die Hochschule, das Jahr der Vorlage und die Art der Prüfungs- oder Qualifikationsleistung.